50-286

TURBINE MISSILE ANALYSIS FOR INDIAN POINT 3 NUCLEA
GENERATING STATION WITH REPLACEMENT LP-2 MOTOR
(SAIC-84/3]5] (Rev. 1))

Docket #50-286
Control #8405160209
Date 5/7/86 of Document:
REGULATORY DOCKET FILE

— NOTICE —

THE ATTACHED FILES ARE OFFICIAL RECORDS OF THE DIVISION OF DOCUMENT CONTROL. THEY HAVE BEEN CHARGED TO YOU FOR A LIMITED TIME PERIOD AND MUST BE RETURNED TO THE RECORDS FACILITY BRANCH 016. PLEASE DO NOT SEND DOCUMENTS CHARGED OUT THROUGH THE MAIL. REMOVAL OF ANY PAGE(S) FROM DOCUMENT FOR REPRODUCTION MUST BE REFERRED TO FILE PERSONNEL.

DEADLINE RETURN DATE _____

_____ _____

_____ _____

_____ _____

RECORDS FACILITY BRANCH

SAIC-84/3151 (Rev. 1)

TURBINE MISSILE ANALYSIS FOR INDIAN POINT 3 NUCLEAR GENERATING STATION WITH REPLACEMENT LP-2 ROTOR

Revision 1

Prepared by:

S. Finn
M. Jacobs
B. Johnson

Prepared for:

New York Power Authority

November 1984

TABLE OF CONTENTS

Section		Page
	EXECUTIVE SUMMARY	1
1	INTRODUCTION AND SUMMARY	3
	1.1 Report Organization	3
	1.2 Background Information	3
	1.3 Project Description	6
2	METHODS	8
	2.1 Methods Overview	8
	2.2 Initial Conditions for Turbine Missiles	9
	2.3 Plant Specification	20
	2.4 Missile Trajectories and Strike Locations	22
	2.5 Missile Interaction with Walls	22
	2.6 Strikes on Safety-Related Areas	29
	2.7 Damaging Strikes	29
3	INDIAN POINT 3 PLANT LAYOUT AND SAFETY DESIGN	32
	3.1 General Layout of Indian Point 3 Relative to Turbine Missile Hazards	32
	3.2 Redundancy of Plant Shutdown Equipment	45
4	RESULTS	50
	4.1 Probability of Safety Compromise	50
	4.2 Plant Vulnerability	60
	4.3 Hazard Due to Turbine Missiles from Unit 2	64
5	CONCLUSIONS	65
6	REFERENCES	66
	APPENDIX A - QUALITY ASSURANCE CHECKS	
	APPENDIX B - MATHEMATICAL DERIVATIONS	
	APPENDIX C - COMPUTER PRINTOUTS FOR MISIP	
	APPENDIX D - SENSITIVITY AND CONSERVATISM	
	APPENDIX E - PHOTOGRAPHIC SURVEY	

LIST OF TABLES

Table		Page
2.1	Exit Disc and Fragment Missile Properties for Each Segment for LP-1 and LP-3 (from Reference 6)	10
2.1A	Exit Disc and Fragment Missile Properties for Each Segment for LP-2 (from Reference 7)	11
2.2	Disc Dimensions (all turbines)	12
2.3	Blade Ring Fragments Dimensions for LP-1 and LP-3	13
2.3A	Blade Ring Fragments Dimensions for LP-2	14
2.4	IP-3 Turbine Disc Parameters	19
2.5	P_1 Values for IP-3 Turbine Discs	21
2.6	Maximum and Minimum Projected Areas for Turbine Missiles from LP-1 and LP-3 (in^2)	27
2.6A	Maximum and Minimum Projected Areas for Turbine Missiles from LP-2 (in^2)	28
3.1	Summary of Indian Point 3 Critical Area Modeling	46
4.1	Results for 100 Trials - Each for 90° Breakup of All Discs (A Total of 86,400 Missiles was Generated and Tracked to Produce This Table)	51
4.2	Results for 2000 Trials Each for Critical Discs, 90° Segments (24,000 Missile Traces per Disc, for a Grand Total of 432,000 Traces)	53
4.3	Results for 200 Trials Each for Critical Discs, 120° Segments (18,000 Missile Traces per Disc for a Grand Total of 324,000 Traces)	54
4.4	Safety Regions Struck by Turbine Missiles in Simulation Study	55
4.5	Number of Safety Region Penetrations per Disc for 2000 Simulated Failures at Rated Speed, 90° Segments	56
4.6	Number of Safety Region Penetrations per Disc for 2000 Simulated Failures at 132 Percent Overspeed, 90° Segments	57
4.7	Number of Safety Region Penetratons per Disc for 2000 Simulated Failures at Rated Speed, 120° Segments	58

LIST OF TABLES (CONTINUED)

Table		Page
4.8	Number of Safety Region Penetrations per Disc for 2000 Simulated Failures at 132 Percent Overspeed, 120° Segments . .	59
B2-1	Comparison of Measured and Calculated Ricochet Velocities . .	B8
C1-1	Computer Specification of the Indian Point 3 Plant	C3
C2-1	Example Computer Printout - Targets Struck During Each Trial .	C14
C2-2	Example Computer Printout - Summary of Target Results	C16

LIST OF FIGURES

Figure		Page
2.1	Physical Dimension of Disc Missiles (from Reference 1)	15
2.2	Physical Dimensions of Blade Ring Fragments (from Reference 2)	16
2.3	Starting Conditions for Turbine Missiles	18
3.1	General Layout of Indian Point 3	33
3.2	Plant Arrangements	34
3.3	Service Water System Model Overview	36
3.4	Service Water Pump Motor Enclosure	38
3.5	Service Water Strainer Pit	39
3.6	Service Water Valve Pit	41
3.7	Electrical Penetration Area (elev 36')	42
3.8	Switchgear Room	44
B2-1	Missile State at 0 Normal Velocity in the Concrete	B6
B5-1	Disc and Blade Ring Fragments for Disc 2 Shown Relative to Turbine Base for Indian Point 3	B16
C3-1	Plant Layout for Elevation = 7	C19
C3-2	Plant Layout for Elevation = 14	C20
C3-3	Plant Layout for Elevation = 18	C21
C3-4	Plant Layout for Elevation = 35	C22
C3-5	Plant Layout for Elevation = 53	C23
C3-6	Plant Layout for Elevation = 65	C24
C3-7	Plant Layout for Elevation = 80	C25
C3-8	Plant Layout for Elevation = 90	C26

LIST OF FIGURES (CONTINUED)

Figure		Page
C3-9	Plant Layout for Elevation = 100.	C27
C3-10	Plant Layout for Elevation = 200	C28
D-1	Comparison of G.E. and Westinghouse Initial Missile Velocities Compared to Their Maximum Theoretical Values . . .	D3
D-2	Vital Areas Penetrated as a Function of Initial Velocity (Westinghouse and G. E. Turbines Compared)	D4
E-1	Main Service Water Pump Motors #31, #32 (MISIP Targets 502, 500)	E2
E-2	Main Service Water Pump Motors #31, #32, #33 (MISIP Targets 502, 500, 497).	E2
E-3	Main Service Water Pump Motors #35, #36 (MISIP Targets 504, 501).	E3
E-4	Main Service Water Pump Motor #36 (MISIP Target 504)	E3
E-5	Service Water Strainer	E4
E-6	Service Water Strainers #31, #32 (MISIP Targets 510, 509) . .	E4
E-7	View of Service Water Piping Path from Pump Motor Enclosure. Pipes are under the Road (MISIP Target 516) and the Concrete Bunker (MISIP Target 517)	E5
E-8	View of Service Water Pump Motor Enclosure From the Service Water Valve Pit	E5
E-9	Inside Service Water Valve Pit Showing Adjacent Essential and Non-Essential Service Water Components (MISIP Target 526)	E6
E-10	Backup Service Water Pump Yard (MISIP Target 197)	E6
E-11	Top of Backup Service Water Valve Pit (MISIP Target 198) . .	E7
E-12	Upper Electrical Penetration Area Showing Common Area Where Lower Cables Join (MISIP Target 226)	E7
E-13	Upper Electrical Penetration Area Showing Common Area Where Lower Cables Join (MISIP Target 226)	E8

LIST OF FIGURES (CONTINUED)

Figure		Page
E-14	Area of Cable Spreading Room Common to Both Trains	E8
E-15	Area of Cable Spreading Room Common to Both Trains (MISAP Target 529)	E9
E-16	Cable Spreading Room Showing All Cables Entering the Electrical Tunnels (MISIP Target 529)	E9
E-17	Start of Electrical Tunnels Showing All Cables Together (Upper Area is MISIP Target 490, Lower Area is MISIP Target 489). . . .	E10
E-18	Start of Electrical Tunnesl Showing All Cables Together (Upper Area is MISIP Target 490, Lower Area is MISIP 489)	E10
E-19	Auxiliary Feedwater Piping	E11
E-20	Auxiliary Feedwater Piping	E12

EXECUTIVE SUMMARY

This report describes the methodology and results of a simulation study of the turbine missile hazard to the Indian Point 3 Nuclear Generating Station, operated by the New York Power Authority (NYPA). A previous study (1) of the turbine missile hazard to the plant had indicated an unacceptably high risk. Much of the risk was attributable to a high probability of failure for the LP-2 rotor. Subsequently, the LP-2 rotor has been replaced by one with a lower probability of failure. The current analysis was performed with the new rotor, and with a more accurate model of the plant. The improved plant model provides a more accurate representation of redundant equipment in the systems which had been found to be most vulnerable to damage from turbine missiles.

The major conclusion is that the plant, as presently configured, provides adequate protection against turbine missile hazards. Numerical predictions are:

1. Probability of a turbine failure which produces external missiles: 1.07×10^{-4}/year.

2. Probability of turbine missile damage to safety-related equipment in the plant: 4.09×10^{-7}/year.

3. Probability of damaging by turbine missiles a function required for safe shutdown of the plant: 1.70×10^{-8}/year.

4. Probability that turbine missiles will produce an offsite release of radioactive material: 7.47×10^{-9}/year.

Item 1, above, is derived from data supplied by Westinghouse (the turbine manufacturer) and based on a 5-year inspection interval for failure of the low-pressure turbine motors at rated speed. (Failure of high-pressure turbine rotors in such a manner as to produce external missiles is

considered incredible.) Items 2 and 3 are calculated by the simulation methods described in this report and are based on simulated disc breakup at rated speed into four 90° segments. Breakup into three 120° segments was also examined and found to result in fewer compromises of the plant's ability to achieve safe shutdown. Item 4, the most important probability from a safety and licensing standpoint, is determined by considering those individual turbine missile strike combinations which compromise a function required for safe shutdown and accounting for in-place procedures which allow a safe shutdown without relying on that particular function which has been compromised by these missiles. That is, if there are in-place procedures for achieving safe shutdown when the plant equipment required for a particular function has been compromised, then such missile strikes are not considered to compromise plant safety. For example, damage to the main service water system can be overcome by using the backup service water system.

It is possible for offsite releases to be generated by missile strikes on the spent fuel storage. However, the spent fuel storage at Indian Point 3 is sufficiently protected that those missiles which can strike it have a negligible probability of producing an offsite release.

The current risk from turbine missiles is mainly due to strikes on components of the main service water system. As mentioned previously, the risk is reduced by using the backup service water system. Other areas of concern include the electrical penetration area, the switchgear room, and cable spreading room. Added shielding in these locations can further reduce the risk.

However, no risk reduction is required for protection against offsite consequences. The probability that turbine missiles would cause an offsite release of radioactive material calculated in this study is within the acceptance criteria of 10^{-7} per year as stated in Regulatory Guide 1.115, Rev. 1, "Protection Against Low-Trajectory Turbine Missiles." The methodology used in this study is considered sufficiently accurate and the required assumptions considered sufficiently conservative that risk reduction below what is predicted herein is not warranted.

1. INTRODUCTION AND SUMMARY

1.1 REPORT ORGANIZATION

Section 1 of this report is a brief overview of the background, methods, and results of the turbine missile analysis of the Indian Point 3 nuclear generating station, operated by the New York Power Authority (NYPA). Section 2 contains the methods used in narrative form, with detailed mathematical backup contained in Appendix B. Section 3 is a description of plant layout and modeling of the Indian Point 3 Plant. Section 4 discusses the results of the study. Section 5 contains the conclusions and recommendations of the authors.

The Appendices are as follows: A describes the Quality Assurance Procedures, B contains details and justifications for the methods used, C shows computer specifications of the plant and sample output, including computer drawn sections of the plant, D summarizes sensitivity and conservatism of the analysis, and E contains photographs taken during the physical on-site survey of the plant.

1.2 BACKGROUND INFORMATION

The safety assessment of any nuclear plant requires prediction of the probability of damage due to missiles resulting from steam turbine failure. As with any other occurrence of a potential hazard the major concern is the specific accident which may lead to a release of radioactive contaminants violating the limits specified in 10CFR100*. This report describes a simulation study which predicts an upper limit to the probability of exceeding the 10CFR100 limits. The analysis of the turbine missile hazard is based on assumed turbine disc failure in a low pressure turbine at

*Title 10, Code of Federal Regulations, Part 100 "Reactor Site Criteria"(2).

both rated speed and at 132 percent of rated speed (overspeed). The analysis considered disc breakup into four 90° segments and disc breakup into three 120° segments. As will be discussed in Section 4, disc breakup at rated speed into 90° segments results in the highest probability of compromising plant safety.

Failure produces missiles from the breakup of a turbine disc and other secondary internal impacts from the disc sectors (Section 2.1). Missiles of various sizes, shapes, and velocities result which, after leaving the turbine casing, become projectile hazards to the remainder of the plant.

Typically, the overall probability of producing a compromise of plant safety, P_4, is factored into the following separate probabilities:

P_1 = probability of turbine failure;

P_2 = conditional probability given a turbine failure that missiles from a failed turbine strike each redundant component in a system required for safe shutdown;

P_3 = conditional probability given a missile strike that the function of the struck component is critically impaired.

so that:

$$P_4 = P_1 \times P_2 \times P_3 \qquad (1.2\text{-}1)$$

P_1 is a function of crack initiation, subsequent crack growth with time, and critical crack depth. P_1 is not specifically addressed in this analysis. The Westinghouse determination[3] of P_1 is utilized in this analysis for each disc of the low pressure system for determining P_4. Actual P_1 values for the Indian Point 3 turbines were supplied by NYPA. The high pressure turbine is assumed to have a negligibly low probability of failure of the type which produces external missiles.

The other two component probabilities are addressed by the analysis described herein. P_2 is directly calculated by the analysis

described in this document. P_3 is addressed indirectly in that the energy range of missiles which strike critical components is computed. P_3 is difficult to assess precisely because of the many variables involved. The energy of striking missiles, however, is probably the most important of these variables and an estimate of it is provided by this analysis. For turbine missiles, P_3 is typically considered to be unity since these very heavy missiles are rather damaging. Furthermore, such an assumption is conservative.

Simulated turbine failures that result in strikes on a sufficient number of components of a critical system are considered to compromise the safety of the plant. The quantity P_2 as calculated in this study accounts for all redundant equipment, and is, therefore, the probability given a turbine failure that missiles cause in a safety compromise of the plant.

In determining violation of the conditions of 10CFR100 (i.e., an offsite release) it is necessary to go beyond P_4 as defined above. In plants such as Indian Point 3 with a protected spent fuel storage, damage to the reactor core is the only mechanism which can produce an offsite release. Core damage comes from compromise of functions which are required to achieve and maintain a safe-shutdown condition.

Neither an offsite release nor damage to the core is an automatic consequence of damage to equipment which must ultimately function in order to achieve and maintain a safe shutdown. Generally there is a significant length of time between damage to such equipment and the requirement that it function in the capacity required for achieving or maintaining a safe shutdown. Repairs can be made or alternative actions taken before such equipment is actually needed.

In fact, for most safety related equipment, there is already in place a procedure for achieving a safe shutdown when the normal function provided by the equipment has been compromised. Those functions which are predicted by this study to be compromised by turbine missiles are considered to have a negligible probability of resulting in an offsite release if there is already in place at Indian Point 3 an established procedure for achieving a safe shutdown when plant equipment that normally performs that function has been lost.

1.3 PROJECT DESCRIPTION

This study includes new calculations of the risk to Indian Point 3 due to turbine missiles to account for the installation of a new LP-2 rotor. In the previous study much of the risk had been due to the old LP-2 rotor. New calculations were performed with new P1 values and new weights, dimensions, and impact areas of turbine missiles supplied by NYPA for all discs.

In addition, the calculations utilized an improved geometric model of the plant. Areas of the plant where most of the safety compromises are expected to occur, namely the service water system, switchgear room, cable spreading room, and electrical penetration area, were remodelled based on an examination of plant drawings and a physical on-site survey of the plant, including a photographic record. The purpose of the improved model is to more accurately represent the respective positions of redundant equipment in the critical locations. For example, in the previous study the service water pump motor enclosure was divided into two cells, one for each safety train, containing three motors each. The improved model separates each pump motor into separate cells. In order to damage one train it is now necessary to have missile strikes in at least 2 of the 3 cells for that train, instead of just one strike in the one large cell. This improved model was expected to reduce the number of calculated safety compromises due to strikes on the service water system.

In some cases, the updated plant model is more conservative. For example, the on-site survey discovered an area of the upper electrical penetration area in which cables from the lower electrical tunnel rise and join cables from the upper tunnel in a common penetration area. This had not been modeled previously. In the updated model this area is considered a source of common mode failure, and any missile strikes in this area will result in a safety compromise.

In this project, particular attention was paid to the service water system, which is a common target for turbine missiles. The plant has a backup service water system which can be used when the main service water system is unavailable. In order to be conservative, P_4 values were first calculated without taking credit for the backup system. Then P_4 values were re-calculated assuming the backup system could be used in an emergency. This is an example of an emergency procedure which allows the plant to

achieve a safe shutdown despite the loss of a critical system. Results for each of these cases are discussed in Section 4.

The possibility of simultaneous missile strikes on components of the main and backup service water systems was investigated. (Each disc breakup generates at least 9 missiles allowing the possibility of simultaneous strikes in more than one location). Because the backup system is in such a location as to make simultaneous strikes unlikely, the new plant model contains only a rough representation of the backup system. If it was found that there were a large number of simulated turbine failures that resulted in simultaneous hits on both systems a more detailed model of the backup system would have been developed. However, only one case out of 144,000 resulted in simultaneous hits, so a more detailed model was deemed unnecessary.

2. METHODS

2.1 METHODS OVERVIEW

SAIC's general category of turbine missile codes are designated MIS (Missile Impact Simulation). The analysis is an extension of the work embodied in the code MIDAS[4] written for Offshore Power Systems and the code MISPGE written for Portland General Electric[5]. A number of improvements in the options and calculational procedures have been incorporated for this study.

For designation convenience, the code used in this study is called MISIP (Missile Impact Simulation of Indian Point). It differs from the other codes primarily in the incorporation of the Indian Point 3 plant model.

The basic procedure involves the tracing of individual missile trajectories by the following sequence:

- determination by Monte Carlo methods of the initial missile velocity and direction from the respective ranges given;
- calculation by equations of free-flight ballistics of the missile strike locations on the walls of the plant;
- determination by Monte Carlo methods of the projected area with which the missile impacts the wall;
- calculation by empirical relations of the missile-barrier interaction effects;
- calculation by energy balance and Monte Carlo means (for missile direction) of the missile state following the interaction;

- termination of the missile trace if the missile ricochets more than three times consecutively in the same room* or exits the plant in a direction which precludes its return or its striking an adjacent plant.

All safety related component rooms (targets) penetrated during the flight of the missile are recorded. Computer output normally lists the number of discs allowed to break up, the number of times each target is struck and penetrated by each breakup, and the characteristics (type and final energy) of the missiles which hit the targets. Detailed traces of each missile flight may be printed out, and any desired interim data are available. From the code output the probability of safety compromise is determined. The specific combination of failures which result in safety compromises are examined and compromises of those functions which are covered by procedures for achieving and maintaining a safe shutdown without the given function are considered to have a negligible probability of occurrence.

2.2 INITIAL CONDITIONS FOR TURBINE MISSILES

Starting conditions required for turbine missile calculations are:

- missile mass,
- starting coordinates,
- initial direction, and
- initial magnitude of velocity.

Missile mass and energy are provided by the Westinghouse Electric Products Division[6,7]. Tables 2.1 and 2.1A shows a summary of the weights and initial energies of the missiles which emerge from the various turbine discs. Figures 2.1 and 2.2 show the missile shapes and Tables 2.2, 2.3, and 2.3A give their dimensions. These tables and figures are excerpted from References 6 and 7.

---

*This procedure is equivalent to a low-energy termination, but is more convenient as it obviates the need for keeping track of a potential energy reference frame.

Table 2.1. Exit Disc and Fragment Missile Properties for Each Segment for LP-1 and LP-3 (From Reference 6).

	Missile	Disc or Fragment Weight (lbs)	100 Percent Rated Speed		132 Percent Overspeed	
			Exit Velocity (ft/sec)	Exit Kinetic Energy ($x10^6$ ft-lb)	Exit Velocity (ft/sec)	Exit Kinetic Energy ($x10^6$ ft-lb)
90° Segments	Disc No 1	2570	Contained	Contained	Contained	Contained
	Fragment 1	2550				
	Fragment 2	2065				
	Fragment 3	245				
	Disc No 2	2705	156	1.02	238	2.38
	Fragment 1[a]	2825	155	1.05	236	2.44
	Fragment 2[a]	350	172	0.16	251	0.34
	Fragment 1[b]	2745	158	1.07	240	2.45
	Fragment 2[b]	340	175	0.16	254	0.34
	Disc No 3	3725	217	2.72	311	5.59
	Fragment 1	2955	217	2.14	311	4.43
	Fragment 2	390	206	0.26	--	--
	Fragment 2	145	--	--	489	0.54
	Disc No 4	3040	330	5.15	471	10.47
	Fragment 1	310	330	0.52	471	1.07
	Fragment 2	705	240	0.63	342	1.28
	Disc No 5	3315	379	7.38	523	14.06
	Fragment 1	345	379	0.77	523	1.46
	(No Number 2)	--	--	--	--	--
	Disc No 6	3905	412	10.30	560	19.00
	Fragment 1	375	412	0.99	560	1.82
	Fragment 2	1065	167	0.46	227	0.85
120° Segments	Disc No 1	3425	Contained	Contained	Contained	Contained
	Fragment 1	3400				
	Fragment 2	2755				
	Fragment 3	330				
	Disc No 2	3605	122	0.83	195	2.13
	Fragment 1[a]	3825	121	0.87	193	2.21
	Fragment 2[a]	470	142	0.15	211	0.32
	Fragment 1[b]	3720	123	0.88	196	2.23
	Fragment 2[b]	455	144	0.15	214	0.32
	Disc No 3	4970	176	2.39	260	5.21
	Fragment 1	3970	176	1.91	260	4.16
	Fragment 2	520	*	*	--	--
	Fragment 2	195	--	--	*	*
	Disc No 4	4055	256	4.12	368	8.55
	Fragment 1	410	256	0.42	368	0.86
	Fragment 2	940	202	0.59	291	1.24
	Disc No 5	4415	313	6.71	430	12.66
	Fragment 1	460	313	0.70	430	1.32
	(No Number 2)	--	--	--	--	--
	Disc No 6	5210	356	10.25	479	18.59
	Fragment 1	500	356	0.98	479	1.79
	Fragment 2	1425	178	0.70	240	1.27

[a]LP-1

[b]LP-3

*Exit missile energies of less than 100,000 ft-lb are not reported.

Table 2.1A. - Exit Disc and Fragment Missile Properties for Each Segment for LP-2 (from Reference 7).

	Missile	Disc or Fragment Weight (lbs)	100 Percent Rated Speed		132 Percent Overspeed	
			Exit Velocity (ft/sec)	Exit Kinetic Energy ($x10^6$ ft-lb)	Exit Velocity (ft/sec)	Exit Kinetic Energy ($x10^6$ ft-lb)
90° Segments	Disc No 1 Fragment 1 Fragment 2 Fragment 3	2570 2550 2065 245	Contained	Contained	Contained	Contained
	Disc No 2 Fragment 1 Fragment 2	2705 2825 350	155 155 172	1.01 1.05 0.16	236 236 251	2.33 2.44 0.34
	Disc No 3 Fragment 1 Fragment 2 Fragment 2	3725 2955 390 145	217 217 205 --	2.71 2.15 0.25 --	311 311 -- 290	5.60 4.44 -- 0.19
	Disc No 4 Fragment 1 Fragment 2	3040 310 705	330 330 240	5.15 0.52 0.63	471 471 342	10.47 1.07 1.28
	Disc No 5 Fragment 1 (No Number 2)	3310 345 --	379 379 --	7.39 0.77 --	523 523 --	14.07 1.47 --
	Disc No 6 Fragment 1 Fragment 2	3880 375 1065	413 413 168	10.28 0.99 0.47	561 561 228	18.96 1.83 0.86
120° Segments	Disc No 1 Fragment 1 Fragment 2 Fragment 3	3425 3400 2755 330	Contained	Contained	Contained	Contained
	Disc No 2 Fragment 1 Fragment 2	3605 3825 470	121 121 142	0.82 0.87 0.15	193 193 211	2.08 2.21 0.32
	Disc No 3 Fragment 1 Fragment 2 Fragment 2	4970 3975 520 195	175 175 * --	2.37 1.90 * --	260 260 -- *	5.22 4.17 -- *
	Disc No 4 Fragment 1 Fragment 2	4055 410 940	256 256 202	4.12 0.42 0.59	368 368 291	8.55 0.86 1.24
	Disc No 5 Fragment 1 (No Number 2)	4410 460 --	313 313 --	6.73 0.70 --	431 431 --	12.69 1.32 --
	Disc No 6 Fragment 1 Fragment 2	5170 500 1425	357 357 178	10.22 0.99 0.70	481 481 240	18.55 1.79 1.28

*Exit missile energies of less than 100,000 ft-lb are not reported.

Table 2.2.* Disc Dimensions (all turbines).

90° Segments

Disc No.	1	2	3	4	5	6
W (ft.)	6.08	6.08	6.08	6.08	5.88	5.32
L (ft.)	2.63	2.71	2.80	2.88	2.83	2.51

120° Segments

Disc No.	1	2	3	4	5	6
W (ft.)	7.44	7.44	7.45	7.44	7.20	6.52
L (ft.)	2.63	2.71	2.80	2.88	2.83	2.51

*From these dimensions, impact areas have been developed and are presented in Tables 2.6 and 2.6A.

Table 2.3.* Blade Ring Fragments Dimensions for LP-1 and LP-3.

Disc No.	Missile	L (in.)		B (in.)	H (in.)	Notes
		90° Segment	120° Segment			
1**	Bld. Ring No 1 Fragment	89.8	119.8	8.8	11.4	
	Bld. Ring No 2 Fragment	109.5	146.1	9.0	7.4	
	Bld. Ring No 3 Fragment	50.5	67.5	3.9	4.4	
2	Bld. Ring No 1 Fragment	99.8	133.8	10.1	9.9	LP-1
	Bld. Ring No 1 Fragment	100.0	134.2	9.6	10.2	LP-3
	Bld. Ring No 2 Fragment	50.6	68.0	3.7	6.6	LP-1
	Bld. Ring No 2 Fragment	50.6	67.7	3.6	6.6	LP-3
3	Bld. Ring No 1 Fragment	90.8	122.2	12.1	9.5	LP-1
	Bld. Ring No 1 Fragment	91.6	121.9	12.1	9.5	LP-3
	Bld. Ring No 2 Fragment	53.6	71.5	9.5	2.7	100% Speed
	Bld. Ring No 2 Fragment	53.9	72.5	3.8	2.5	132% Speed
4	Bld. Ring No 1 Fragment	84.9	112.3	4.3	3.0	
	Bld. Ring No 2 Fragment	85.5	114.0	9.4	3.1	
5	Bld. Ring No 1 Fragment	80.1	106.9	3.9	3.9	
6	Bld. Ring No 1 Fragment	73.6	98.2	3.0	6.0	
	Bld. Ring No 2 Fragment	74.5	99.6	13.3	3.8	

*From these dimensions, impact areas have been developed and are presented in Table 2.6.

**Disc 1 produces a third blade ring fragment, but it never escapes the turbine casing.

Table 2.3A.* Blade Ring Fragments Dimensions for LP-2.

Disc No.	Missile	L (in.)		B (in.)	H (in.)
		90° Segment	120° Segment		
1**	Bld. Ring No 1 Fragment	89.9	119.8	8.8	11.4
	Bld. Ring No 2 Fragment	109.5	146.1	9.0	7.4
	Bld. Ring No 3 Fragment	39.2	52.3	3.9	4.4
2	Bld. Ring No 1 Fragment	99.8	133.8	10.1	10.0
	Bld. Ring No 2 Fragment	38.3	51.4	3.7	6.6
3	Bld. Ring No 1 Fragment	90.8	122.2	12.1	9.5
	Bld. Ring No 2 Fragment	35.8	47.5	9.5	2.7
4	Bld. Ring No 1 Fragment	84.9	112.3	4.3	3.0
	Bld. Ring No 2 Fragment	85.5	114.0	9.4	3.1
5	Bld. Ring No 1 Fragment	80.1	106.9	3.9	3.9
6	Bld. Ring No 1 Fragment	73.6	98.2	3.0	6.0
	Bld. Ring No 2 Fragment	74.5	99.6	13.3	3.8

*From these dimensions, impact areas have been developed and are presented in Table 2.6A.

**Disc 1 produces a third blade ring fragment, but it never escapes the turbine casing.

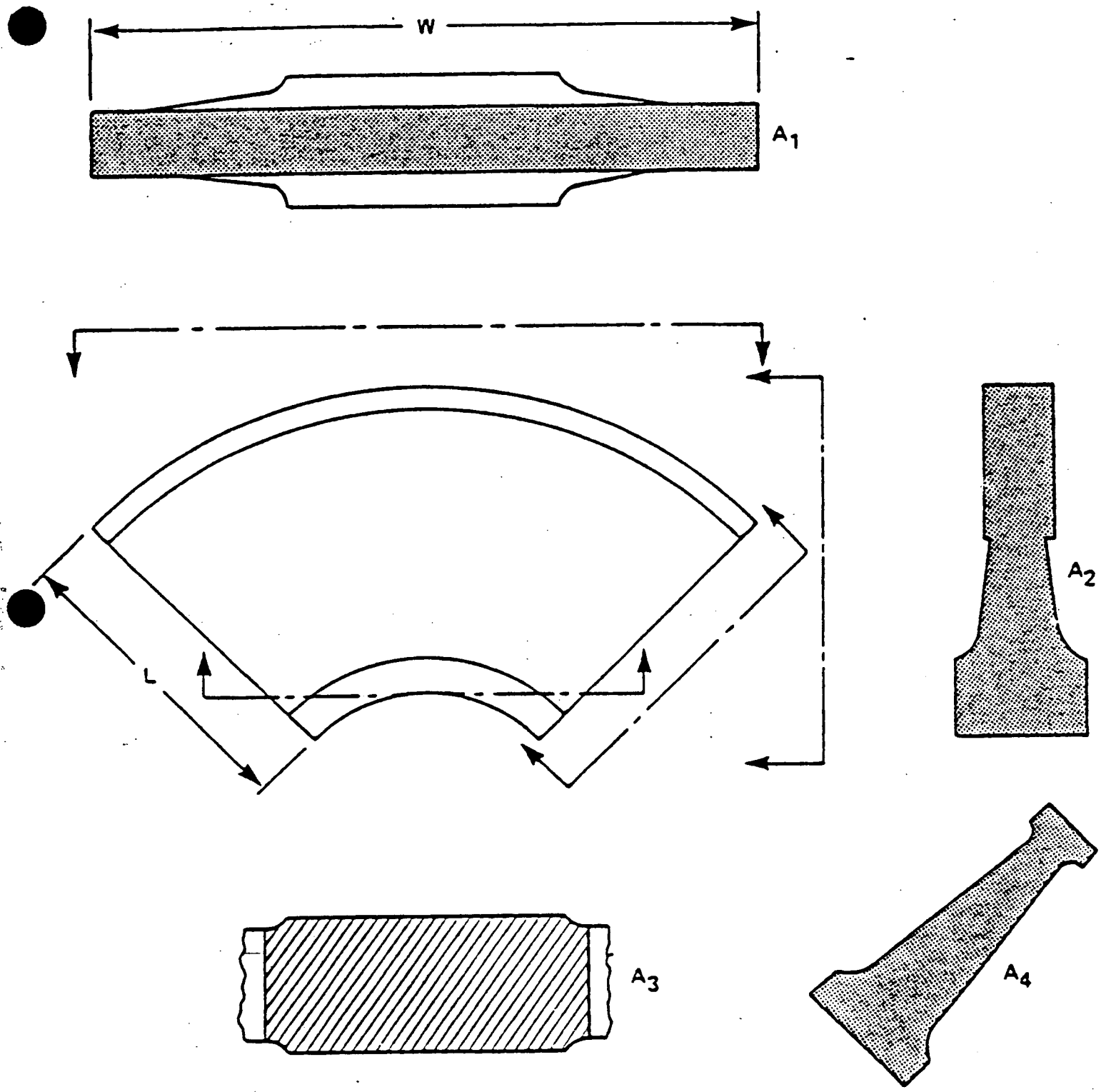

Figure 2.1. Physical Dimensions of Disc Materials (from References 6 and 7).

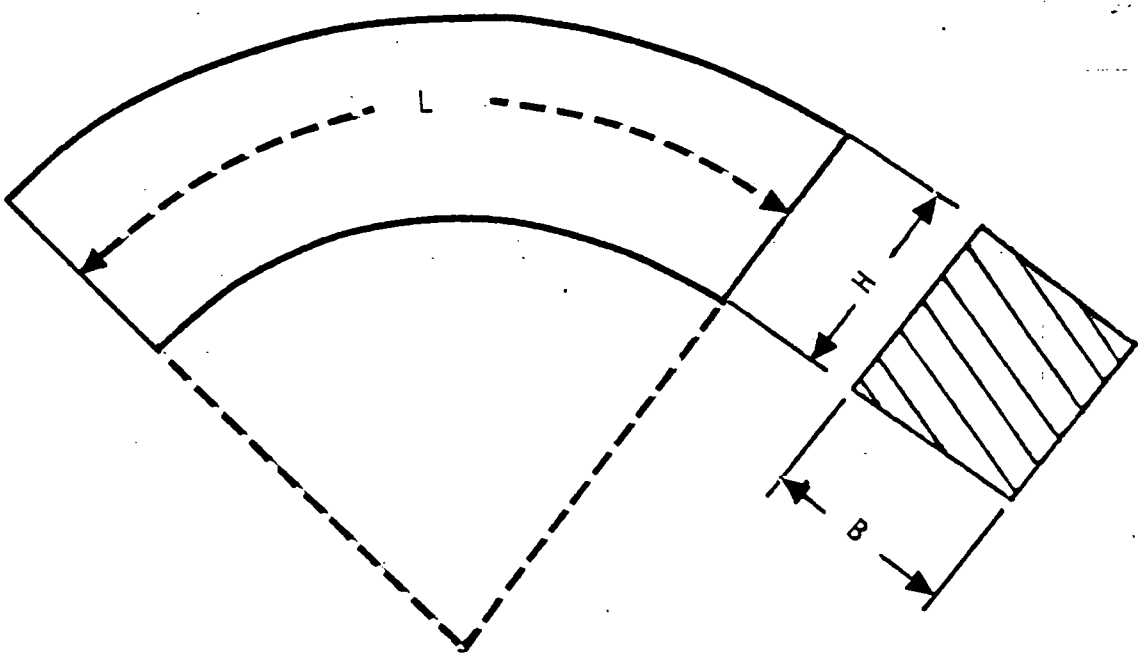

Figure 2.2. Physical Dimensions of Blade Ring Fragments (from References 6 and 7).

The figures show missile shapes for 90° segments, but the shapes for 120° segments are similar. Figure 2.3 indicates the coordinate system utilized in the calculations and the relationship between the turbine missile initial velocity, the position vector and its components parallel to each of the plant Cartesian coordinates. References 6 and 7 give the azimuthal (ϕ) range and rotational (θ) range of turbine missiles. Inner discs emerge with a ϕ range uniformly distributed between -5° and $+5^o$. End discs (two per turbine) emerge uniformly between 5° and 25° measured outward from the center of each turbine. $\phi = 0$ corresponds to missile emergence perpendicular to the turbine axis. The rotational range is from 0 to 360 degrees, but the turbine pedestal and condenser stop any missiles emerging in a downward direction. The turbine base prevents missile emergence at angles requiring penetration of this region. Details of this determination are contained in Appendix B.

Since there are two additional fragments ejected per disc section, a total of 12 missiles per disc failure with 90° segments and 9 with 120° segments are produced. All missiles are considered to emerge tangentially at a radius, r_o, equal to the average radial center-of-mass distance of the disc segments. The mass center varies somewhat according to the size and shape of the segment as well as its angular dimension. Interaction of the missiles with other turbine internals and also the casing could alter the effective radius of emergence. All are assumed to emerge at 1.4 feet for this study. The initial x value for each fragment is listed in Table 2.4. Initial y and z values are determined by

$$y = y_o + r_o \sin \theta$$
$$z = z_o + r_o \cos \theta$$

where y_o and z_o are the y and z coordinates of the turbine shaft and r_o is the radial distance to the center of mass of the segments. Initial components of velocity in the Cartesian system are

$$\dot{X}_o = V_o \sin \phi$$
$$\dot{Y}_o = V_o \cos \phi \sin (\theta - \tfrac{\pi}{2})$$
$$\dot{Z}_o = V_o \cos \phi \cos (\theta - \tfrac{\pi}{2})$$

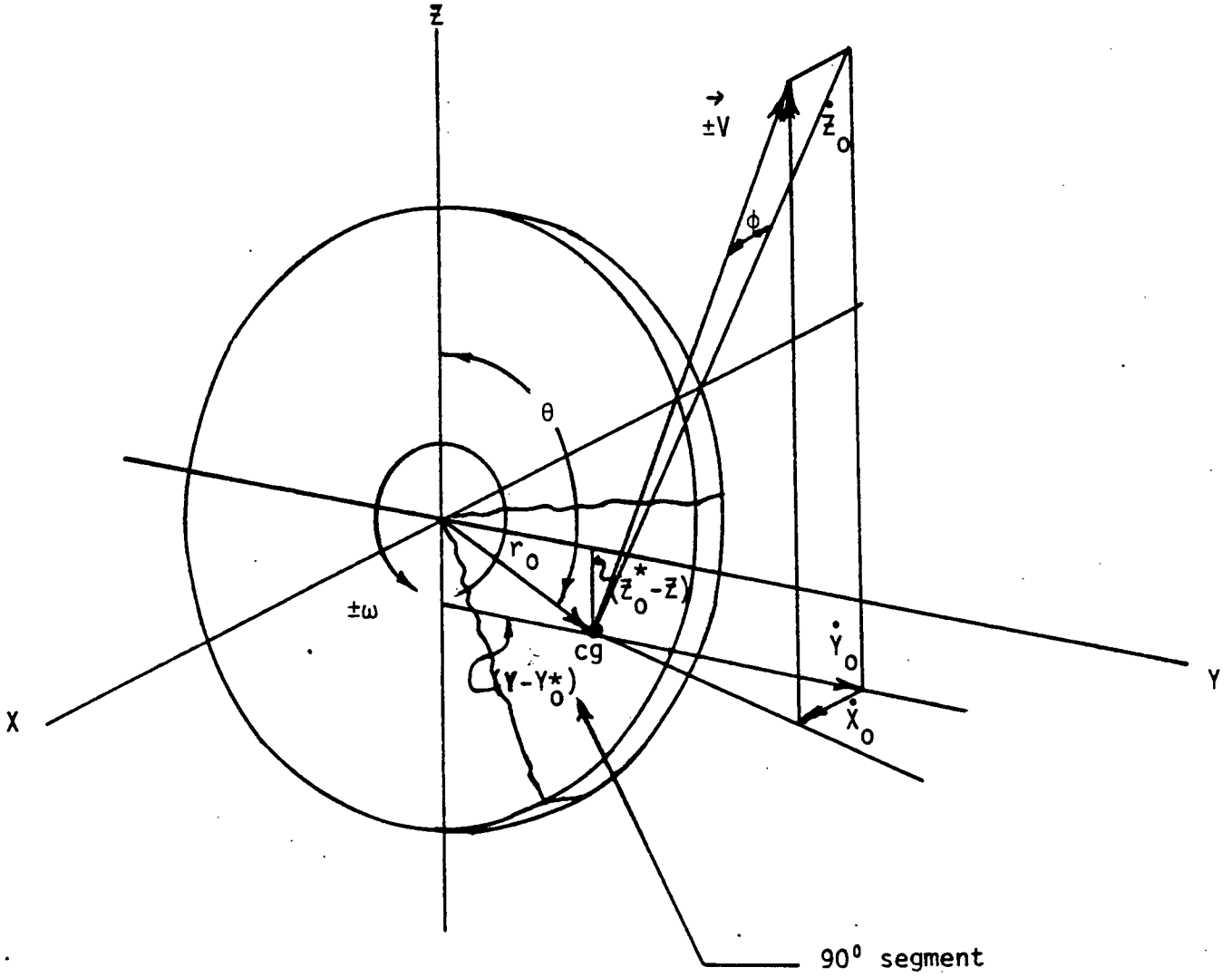

* Y_o and Z_o are coordinates of turbine axis

Figure 2.3. Starting Conditions for Turbine Missiles.

Table 2.4. IP-3 Turbine Disc Parameters.

IP-3 Number	Westinghouse Number	Axial Distance[a] (ft)	Missile Aximuthal Range (ϕ) (degrees)	
1	6	272.0	-25	-5
2	5	273.0	-5	5
3	4	274.0	-5	5
4	3	275.6	-5	5
5	2	276.7	-5	5
6	1	277.6	-5	5
7	1	279.4	-5	5
8	2	280.3	-5	5
9	3	281.4	-5	5
10	4	282.5	-5	5
11	5	283.7	-5	5
12	6	285.0	5	25
13	6	309.5	-25	-5
14	5	310.8	-5	5
15	4	312.0	-5	5
16	3	313.1	-5	5
17	2	314.2	-5	5
18	1	315.1	-5	5
19	1	316.9	-5	5
20	2	317.8	-5	5
21	3	318.9	-5	5
22	4	320.0	-5	5
23	5	321.2	-5	5
24	6	322.5	5	25
25	6	347.0	-25	-5
26	5	348.3	-5	5
27	4	349.5	-5	5
28	3	350.6	-5	5
29	2	351.7	-5	5
30	1	352.6	-5	5
31	1	354.4	-5	5
32	2	355.3	-5	5
33	3	356.4	-5	5
34	4	357.5	-5	5
35	5	358.7	-5	5
36	6	360.0	5	25

[a]Distance from the X = 0 coordinate of the plant. See Appendix C.

where ϕ and θ are indicated on Figure 2.3 and V_0 is selected from Table 2.1. Theta is selected to exclude the turbine base and all emergent angles below horizontal. Missiles emerging at angles below horizontal are stopped by the turbine pedestal and condenser. Justification for exclusion of the turbine base is contained in Appendix B-5.

Table 2.4 lists starting axial coordinates and azimuthal ranges according to the numerical disc designation. Table 2.5 lists the P_1 numbers used in this analysis. The values for 132 percent overspeed are lower than those for rated speed because they include the probability of achieving overspeed conditions.

The θ range which excludes the turbine base and the flight paths below horizontal is from 100° to 285°.

2.3 PLANT SPECIFICATION

The plant is modeled in a Cartesian coordinate system with the exception of the reactor containment and the moisture separator reheaters which are modeled (as they truly are) as concrete and steel cylinders, respectively. The code accepts as plant input one line of data for each room of the plant. The line contains the location, thickness and material specifications of each of the six walls. An additional designator for exterior plant walls indicates the potential fates of missiles which exit these walls. These fates are designated

R - Exit through the roof (roof exits include those missiles which may fall back on plant),

G - Exit through a floor slab,

E - Exit through an exterior wall below grade level,

L - Exit through X_{min} side of plant,

W - Exit through X_{max} side of plant,

D - Exit through Y_{min} side of plant, and

Table 2.5. P_1 Values for IP-3 Turbine Discs.

Disc Number	100 Percent Rated Speed			132 Percent Overspeed		
	18-month*	3-year	5-year	18-month	3-year	5-year
1	5.65E-10	4.60E-9	2.69E-7	1.19E-11	9.20E-10	1.47E-8
2	2.14E-14	3.58E-12	5.08E-10	1.02E-14	9.42E-13	6.48E-11
3	1.05E-13	1.43E-11	1.58E-9	1.27E-14	1.13E-12	7.38E-11
4	1.35E-8	4.84E-7	1.03E-5	4.43E-10	1.07E-8	1.41E-7
5	1.77E-8	6.15E-7	1.27E-5	3.76E-10	9.39E-9	1.29E-9
6	0	0	0	0	0	0
7	0	0	0	0	0	0
8	2.22E-9	2.25E-7	5.61E-6	1.28E-10	3.74E-9	6.21E-8
9	2.39E-8	7.92E-7	1.54E-5	7.30E-10	1.64E-8	1.97E-7
10	4.36E-12	4.06E-10	2.78E-8	3.83E-13	2.33E-11	9.46E-10
11	7.85E-12	6.78E-10	4.31E-8	5.00E-12	1.98E-10	4.97E-9
12	3.80E-13	5.32E-11	6.04E-9	1.02E-13	8.21E-12	4.79E-10
13	2.91E-13	4.24E-11	5.07E-9	6.50E-14	5.66E-12	3.59E-10
14	2.75E-16	6.77E-14	1.55E-11	3.07E-16	3.93E-14	4.04E-12
15	1.22E-14	2.05E-12	2.93E-10	1.95E-15	2.12E-13	1.76E-11
16	2.19E-12	2.38E-10	1.99E-8	1.51E-13	1.02E-11	4.78E-10
17	5.20E-11	4.22E-9	2.41E-7	1.26E-12	6.74E-11	2.36E-9
18	0	0	0	0	0	0
19	0	0	0	0	0	0
20	1.01E-10	7.79E-9	4.14E-7	1.79E-12	9.27E-11	3.12E-9
21	6.70E-12	6.61E-10	4.84E-8	3.79E-13	2.32E-11	9.49E-10
22	3.12E-12	3.00E-10	2.15E-8	2.81E-13	1.77E-11	7.52E-10
23	1.27E-13	1.75E-11	1.96E-9	7.35E-14	5.22E-12	2.62E-10
24	6.65E-11	5.42E-9	3.17E-7	9.65E-11	4.57E-10	1.40E-8
25	1.17E-12	1.46E-10	1.44E-8	2.67E-13	1.94E-11	9.94E-10
26	4.24E-14	6.53E-12	8.39E-10	2.59E-14	2.08E-12	1.21E-10
27	6.30E-15	1.14E-12	1.78E-10	9.75E-16	1.14E-13	1.04E-11
28	2.16E-8	7.26E-7	1.43E-5	6.40E-10	1.46E-8	1.80E-7
29	3.00E-8	9.75E-7	1.84E-5	6.05E-10	1.41E-8	1.78E-7
30	0	0	0	0	0	0
31	0	0	0	0	0	0
32	3.60E-8	1.14E-6	2.09E-5	6.85E-10	1.57E-8	1.93E-7
33	8.75E-9	3.33E-7	7.59E-6	2.98E-10	7.62E-9	1.08E-7
34	2.35E-15	4.66E-13	8.19E-11	3.97E-16	5.09E-14	5.18E-12
35	2.63E-13	3.36E-11	3.42E-9	1.51E-13	9.78E-12	4.40E-10
36	8.90E-11	8.91E-10	6.72E-8	2.10E-12	1.16E-10	4.32E-9
Total	1.55E-7	5.16E-6	1.07E-4	4.02E-9	8.55E-8	1.01E-6

*Length of turbine inspection interval.

U - Exit through Y_{max} side of plant.

Rectangular parallelepipeds enclose the cylindrical containment vessel and the moisture separator reheaters. These are fictitious cells which serve as a convenient artifice to facilitate calculating missile interactions with a cylindrical surface in an otherwise all-Cartesian system. More details are contained in Appendix C, which includes the total computer specification of the plant, and a mapping at each elevation of the safety-related areas designated as "targets" by the code.

2.4 MISSILE TRAJECTORIES AND STRIKE LOCATIONS

The equations of free-flight ballistics (neglecting air resistance) are used to determine trajectories and strike locations on given plant walls. Exact details are contained in Reference 8. In brief, the code keeps track of each cell, or room, in which the given missile is located and determines the next wall struck by solving the velocity equations (in component form) for the minimum time to strike one of the enclosing walls. This minimum time replaced in the original equations locates the strike point. Special routines are called if the missile enters "cells" which contain either the containment or the moisture separator reheaters. Details of these routines are described in Appendix B.

2.5 MISSILE INTERACTION WITH WALLS

2.5.1 Concrete Wall Interactions

In the Indian Point 3 Plant the only walls which offer significant resistance to the missiles are concrete walls. The effect of walls such as office room partitions and corrugated metal is neglected.

This study used a formula for concrete penetration which was derived on the basis of tests performed by the Commissariat a' l'Energie Atomique-Electricite de France (CEA-EDF)[9]. The Electric Power Research Institute recommends this formula as providing the best match to experimental data over a full range of missile velocities [10]. It's form is

$$T_p = 0.765\ \sigma_c^{-3/8}\left(\frac{W}{D}\right)^{1/2} V_i^{3/4} \qquad (2.5\text{-}1)$$

where

T_p = thickness of wall that is penetrated 50 percent of the time for the given missile (in)

σ_c = concrete compression strength (psi)

W = missile weight (lb)

D = effective diameter (in)

D = $2\sqrt{A/\pi}$ where A represents an effective impact area

V_i = incident velocity (ft/sec)

The combination of impact area and velocity obviously governs barrier penetration for a given missile. In the MIS code the actual thickness (T) of the barrier is compared with T_p to determine whether or not the barrier is penetrated.

(a) Missile state following penetration.

If T_p (as calculated by Equation 2.5-1) exceeds T, the velocity (V_p) required to penetrate the barrier is calculated by a rearrangement of Equation 2.5-1, as follows:

$$V_p = T_p^{4/3}\,\sigma_c^{1/2}\left(\frac{D}{W}\right)^{1/3} \Big/ 0.765 \qquad (2.5\text{-}2)$$

The residual velocity (V_r) following penetration[12] is

$$V_r = \sqrt{\frac{W}{W+W_w}\,(V_i^2 - V_p^2)} \qquad (2.5\text{-}3)$$

where

W_w = weight of wall plug removed (lb) = $\pi \frac{(1.4D)^2}{4} \rho_c T$

ρ_c = density of concrete = 0.086 lb/in^3

The wall thickness used in Equations 2.5-1, 2.5-2, and 2.5-3 is that parallel to the velocity vector (actual thickness divided by the cosine of the obliquity angle). If the missile penetrates the wall, it is assumed to continue without alteration of its original direction. The containment is a special case, in that the trace is terminated if the containment is penetrated, and the possibility of safety compromise examined separately from the program. (Containment penetrations are not observed with simulated missile traces for Indian Point 3.)

(b) Missile state following ricochet.

Following ricochet, the MIS code calculates the missile velocity and angle of obliquity (with the normal to the surface at the point of contact). The ricochet model (Reference 11) is based on converting only the elastic strain energy stored locally in the concrete wall and in the missile, when the normal velocity becomes 0, to kinetic energy of the rebounding missile*. The elastic energy available (ξ) is estimated as

$$\xi = \frac{2V\sigma_c^{\,2}}{6\,E_s} + \frac{2LA\sigma_c^{\,2}}{6\,E_c} \qquad (2.5\text{-}4)$$

where

V	= missile volume (in^3)
σ_c	= compressive strength of concrete
E_s, E_c	= modulus of elasticity in steel and in concrete, respectively
L	= thickness of concrete barrier (in)
A	= impact area (in^2)

*The overall structural response of the wall is ignored. The rebound contribution from the overall structural response of the wall is assumed to be manifest later in time than the local response. Derivation of Equation 2.5-4 and comparison with experimental results is contained in Appendix B-2.

In experimental work at Calspan (Reference 12), the rebound velocities of steel missiles ricocheting from concrete walls were measured. The Calspan measured rebound velocities are compared in Appendix B-2 with those calculated with the rebound energy predicted by Equation 2.5-4. The rebound velocity is

$$V_{rebound} = \sqrt{\frac{2\xi}{M}} \qquad (2.5\text{-}5)$$

where ξ is given by Equation 2.5-4 and M is the missile mass. The value of $\sigma_c]_{dynamic}$ used for concrete is the concrete static compressive strength augmented by 55 percent. This value is typical of impact strengths of concrete (Reference 13). The value of $\sigma_c]_{dynamic} = 2\sigma_c]_{static}$ was used in the code to ensure conservatism, and compensate for considering only local wall response in contributing to rebound energy.

Offshore Power Systems (OPS) has formulated the model that is used in this study to determine direction following ricochet. It describes exit angle of obliquity as a function of the incident angle of obliquity. (Reference 14).

$$\theta_e]_{min} = \theta_i \qquad (2.5\text{-}6)$$

$$\theta_e]_{max} = \theta_i + \frac{2\theta_i}{\pi}\left(\frac{\pi}{2} - \theta_i\right) \qquad (2.5\text{-}7)$$

where

θ_i, θ_e = incident, exit angles of obliquity, respectively.

Exit angle, θ_e, is randomly selected from a uniform distribution between $\theta_{e/min}$ and $\theta_{e/max}$. The OPS model produces missile traces which appear realistic.

In the Cartesian system, one of the three basic velocity components is always the normal component. Coplanarity of the incident and exit velocities with the surface normal is then assured by maintaining the other (non-normal) velocity components in the same ratio before and after ricochet, which is valid for plane or cylindrical surfaces. (see Appendix B).

From the penetration equations (2.5-1 and 2.5-2) it is obvious that a significant parameter is the projected area of the missile (that projected area perpendicular to the velocity vector). These area values are picked at random from a uniform distribution between an assumed maximum and minimum calculated from the data of Tables 2.6 and 2.6A where both a rim maximum and a global maximum* are listed for all disc-sector missiles. The area range for all impacts is chosen between the minimum and the maximum rim areas rather than the global maximum. This choice is equivalent to the assumption that the missile maintains its initial orientation relative to its original place of rotation.

2.5.2 Steel Wall Interactions

The moisture separator reheaters (MSR's) interact significantly with the missiles because they are located adjacent to the turbines at the same elevation. The MSR's are steel. Steel wall interactions differ significantly from concrete and their specification is somewhat complicated. Calculation of steel wall interactions are described and derived in Appendix B-3. Briefly, the steel interactions are based on a method derived from experiment by Hagg and Sankey[15] who show that steel perforations can occur in one of two stages. In the first stage, or phase, the resistance of the barrier to perforation is provided only by local compression and shear in the wall because there has been no time for a tensile wave to propagate in the plane of the barrier at significant distances from the interaction point. In the second stage, the barrier "stretches" in its plane perpendicular to the direction of missile penetration and tensile strength contributes significantly to perforation resistance. Perforation can occur in either stage. The perforation conditions and expressions for residual velocity and the ricochet conditions are somewhat unwieldy and hence are

*See footnotes on Table 2.6.

Table 2.6. Maximum and Minimum Projected Areas for Turbine Missiles from LP-1 and LP-3 (in^2)[a].

	Westinghouse Disc Number	Fragment Number	Minimum Area	Rim Maximum Area	Global Maximum Area[b]	Notes
90° Segments	1	--	183	478	1775	
		1	100	1024	1024	
		2	67	986	986	
	2	--	193	425	1805	
		1	100	1008	1008	LP-1
		1	98	1020	1020	LP-3
		2	24	334	334	LP-1
		2	24	334	334	LP-3
	3	--	253	579	1836	
		1	112	1099	1099	LP-1
		1	112	1108	1108	LP-3
		2	26	509	509	100% Speed
		2	26	205	205	132% Speed
	4	--	209	426	1863	
		1	13	365	365	
		2	29	804	804	
	5	--	226	452	1756	
		1	15	312	312	
	6	--	278	566	1423	
		1	18	442	442	
		2	51	991	991	
120° Segments	1	--	183	608	2364	
		1	100	1366	1366	
		2	67	1315	1315	
	2	--	193	628	2403	
		1	100	1351	1351	LP-1
		1	98	1369	1369	LP-3
		2	24	449	449	LP-1
		2	24	447	447	LP-3
	3	--	253	710	2450	
		1	112	1479	1479	LP-1
		1	112	1475	1475	LP-3
		2	26	679	679	100% Speed
		2	26	276	276	132% Speed
	4	--	209	616	2480	
		1	13	483	483	
		2	29	1072	1072	
	5	--	226	649	2340	
		1	15	417	417	
	6	--	278	828	1900	
		1	18	589	589	
		2	51	1325	1325	

[a]Calculated from data of Reference 6 (Figure 3).

[b]Global maximum is the maximum of the rim area (projection on a plane parallel to the disc axis) or the "flat" area (projection in a plane perpendicular to the disc axis). Note that the true maximum area projection is somewhat larger than the global maximum listed here, because neither the rim nor the flat corresponds exactly to the maximum projection. Reference 4 contains examples. The maximum used is, therefore, smaller than true maximum in all cases, which is a conservative approach.

Table 2.6A. Maximum and Minimum Projected Areas for Turbine Missiles from LP-2 (in^2)*.

	Westinghouse Disc Number	Fragment Number	Minimum Area	Rim Maximum Area	Global Maximum Area**
90° Segments	1	--	183	478	1775
		1	100	1025	1025
		2	67	986	986
	2	--	193	425	1805
		1	100	1008	1008
		2	24	334	334
	3	--	253	579	1835
		1	115	1099	1099
		2[a]	26	509	509
		2[b]	10	205	205
	4	--	209	426	1863
		1	13	365	365
		2	29	804	804
	5	--	225	451	1756
		1	15	312	312
	6	--	275	554	1423
		1	18	442	442
		2	51	991	991
120° Segments	1	--	183	608	3130
		1	100	1366	1366
		2	67	1315	1351
	2	--	193	628	3192
		1	100	1351	1351
		2	24	449	449
	3	--	253	710	3266
		1	115	1479	1479
		2[a]	26	679	679
		2[b]	10	276	276
	4	--	209	616	3319
		1	13	483	483
		2	29	1072	1072
	5	--	225	648	3138
		1	15	462	462
	6	--	275	811	2540
		1	18	589	589
		2	51	1325	1325

* Calculated from data of Reference 7 (Figure 3).

**Global maximum is the maximum of the rim area (projection on a plane parallel to the disc axis) or the "flat" area (projection in a plane perpendicular to the disc axis). Note that the true maximum area projection is somewhat larger than the global maximum listed here, because neither the rim nor the flat corresponds exactly to the maximum projection. Reference 4 contains examples. The maximum used is, therefore, smaller than true maximum in all cases, which is a conservative approach.

[a] Rated Speed [b] 132% overspeed

listed only in Appendix B-3. The ricochet velocity for steel interactions was derived specifically for the turbine missile study for Offshore Power Systems, and the derivation is shown in Appendix B-3.

2.6 STRIKES ON SAFETY-RELATED AREAS

Rooms of the plant are designated as safety-related areas if they contain equipment used for safe shutdown of the reactor or if missile strikes on equipment in that room could potentially cause a release of radioactivity in excess of that specified in 10CFR100[2]. These rooms are called "targets" in the computer printout. Any number of targets may be used. The missile trace continues until the missile either has ricocheted more than three times in the same room, penetrates the containment, or has left the "plant". All targets struck by the missile are recorded and summed. Strikes on redundant components are appropriately accounted for to determine safety compromises. A safety compromise is produced by a damaging strike on all redundant components of a given system required for safe shutdown. These systems are discussed in Section 3.2.

2.7 DAMAGING STRIKES

Potential damage mechanisms for safety-related plant equipment are: (1) direct strikes by missiles, (2) strikes by secondary missiles, such as spallation fragments, and (3) structural damage (i.e., wall displacement of sufficient magnitude to damage the equipment in any room or cell having an exterior wall subject to such damage). In the following subsections, these mechanisms are discussed relative to the Indian Point 3 analysis.

2.7.1 Direct Missile Strikes

In this analysis, any missile entering into a cell (room) containing critical (safety-related) equipment is assumed to damage the equipment sufficiently to compromise the function of the equipment. This procedure represents an obvious upper-bound to the probability of engendering strikes since it is possible that the missile might miss the critical components of the cell. For this reason, however, the plant was modelled so that cells containing critical equipment were as small as practicable to reduce the chance that missiles entering cells would hit the equipment. Further, upon entering a cell, the missile brings with it

pieces of the wall whose overall dimensions transverse to the wall are at least as large as those of the missile, itself. These generally spread out from the direction of missile travel to increase the areal coverage by potentially damaging missiles. Missiles which do not exit the cell once they enter (i.e., those trapped in the cell) are subject to multiple wall ricochets, thereby, increasing further the chances of equipment damage.

In summary, the assumption is an upper-bound, but the modeling techniques employed make it as reasonable an approximation to the true value as is practicable, given the constraints of the computer model.

2.7.2 Spallation Fragments

Recent EPRI tests[10] indicate that not only are the values of spall threshhold velocities for missiles much larger than previously assumed, but they also have shown that spall fragments tend to be small and have a large spread in direction and velocity from a parabolic zone on the back face. Further, the presence of the reinforcing bars tends to inhibit the expulsion of spallation fragments.

It has been concluded, therefore, that pipes, valves, large equipment such as motors, and even insulated electrical cabling would have a very low probability of damage by spall fragments. An examination was made of the nature and location of critical equipment relative to the walls struck by missiles in the Indian Point 3 plant. It was concluded that probability of spallation damage was so small that it could be ignored.

The EPRI study showed steel liners to be completely effective in preventing spall fragments. Therefore, those non-penetrating strikes on the containment cannot produce a spallation hazard.

Only the control room has a significant amount of equipment potentially damagable by spallation fragments, but the inner walls of the control room are a composite type material which does not spall. Therefore, this mechanism can be ignored for this study without introducing significant error.

2.7.3 Structural Damage

Again, reference is made to the EPRI tests[10]. Gross movement of the panels struck by full scale missiles (or scale models) was miniscule. An examination was made of the Indian Point 3 plant design to check for the

potential compromises of safety equipment due to structural damage of the wall surrounding it. No cases were found where safety-related equipment was mounted so close to such a wall (or ceiling) to be a potential hazard.

2.7.4 Summary of Damaging Strike Modeling

Since the probability of a damaging strike by missiles entering a cell is an upper-bound, and since our algorithm overestimates perforation compared to EPRI tests (Appendix D), it is felt that this overestimation more than compensates for neglect of the very small probabilities of either spall fragment damage or structural damage.

It is concluded that the probability of damaging strikes has been appropriately bounded in this analysis.

3. INDIAN POINT 3 PLANT LAYOUT AND SAFETY DESIGN

3.1 GENERAL LAYOUT OF INDIAN POINT 3 RELATIVE TO TURBINE MISSILE HAZARDS

Figure 3.1 is an overall layout of Indian Point 3. The plant belongs to the general category designated as an "in-line" plant (Figure 3.2) wherein the turbine orientation allows direct hits from low trajecting missiles (LTM's) on vital plant components in case of turbine failure. LTM's (Low Trajectory Missiles) are those whose incident velocity vector is less than 45° with the horizontal. HTM's (High Trajectory Missiles) emerge at angles greater than 45° with the horizontal. Any given point whose vector from the turbine axis is less than 45° with the horizontal and which is within the azimuthal and distance range of the missile can be struck by either an LTM or HTM. Protection against LTM strikes on critical components can be afforded by geometric arrangement as in the "peninsula" arrangement shown in Figure 3.2, and this is, indeed the motivation for such plant arrangements. However, for HTM's any point within the distance range is potentially vulnerable to a missile strike.

Generally, the higher velocity LTM's present the greater risks for this category of missiles because of their greater penetration capacity, but for HTM's, the lower velocity missiles may present the greater risks because their limited distance range produces a greater number of strikes per unit area.

Indian Point 3 is unusual among in-line plants in that it is also less vulnerable to the highest velocity LTM's. This effect is caused by the separation between the turbine and the major safety areas which can be struck by LTM's (the primary auxiliary building and the water intake regions). LTM's must have an initial trajectory above horizontal to clear the turbine pedestal and turbine base. Those with higher velocities also clear the critical safety regions, but the lower velocity ones do not. For typical plants, whose safety regions directly abut the turbine hall, essentially all LTM trajectories intersect these regions and the higher-velocity missiles, of course, cause more damage.

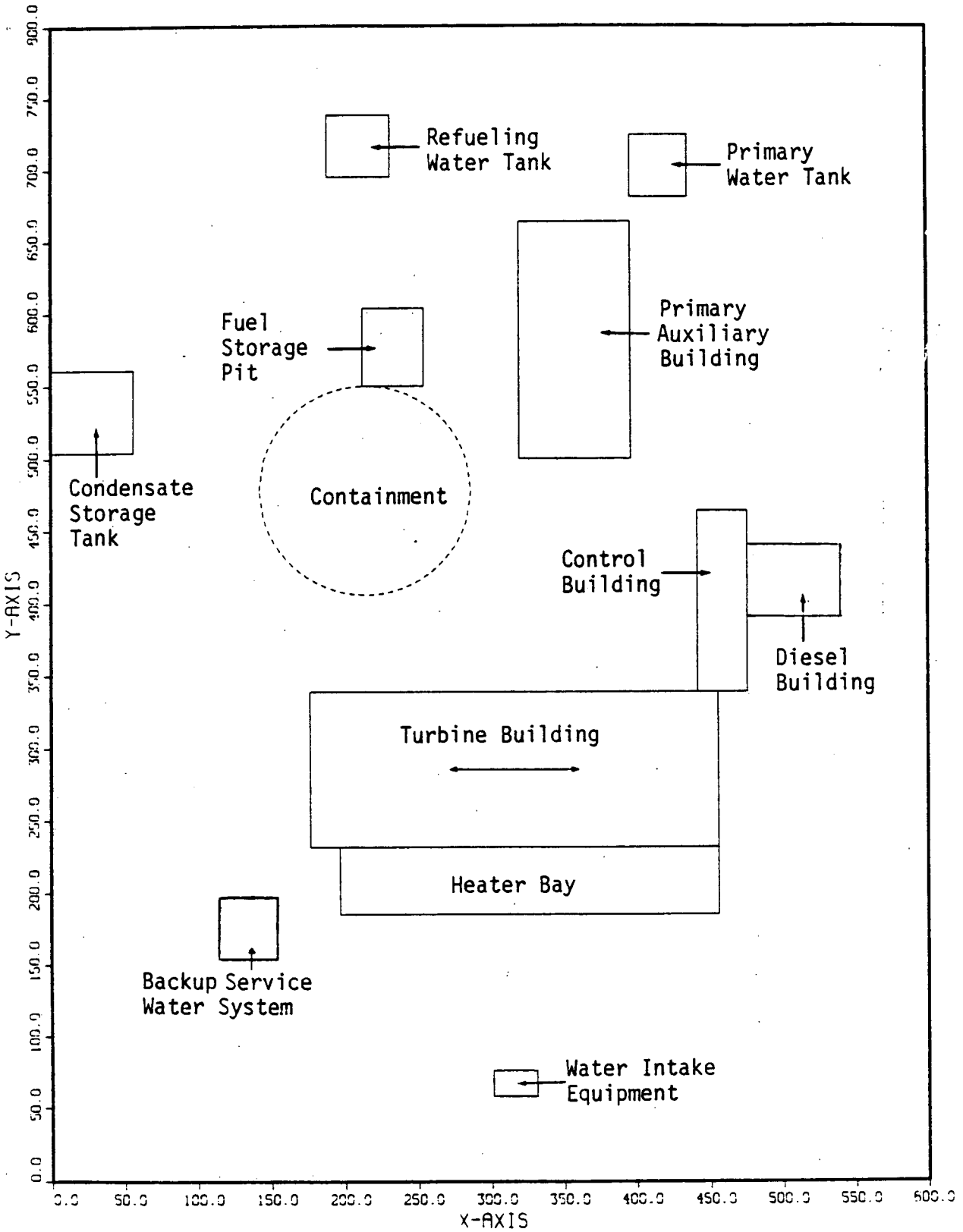

Figure 3.1. General Layout of Indian Point 3.

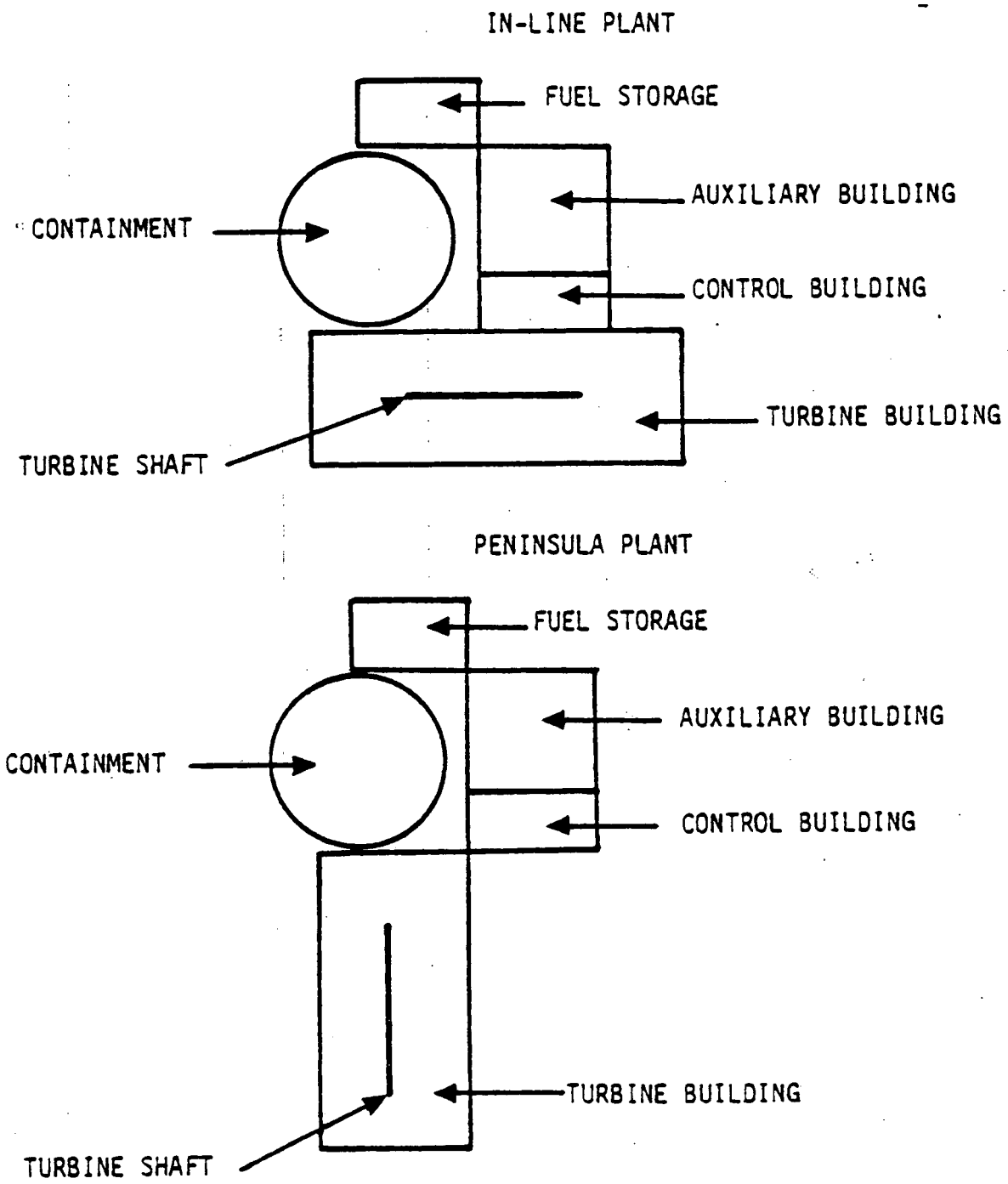

Figure 3.2. Plant Arrangements.

The general model of the Indian Point 3 plant was divided into several rooms or compartments to form the input for the MISIP code. All actual walls were modeled as is. Additionally, many large rooms were divided by imaginary "air" walls into smaller compartments. An example is a large room with a pump on one side. In the model such a room was divided into two compartments, one containing the pump and the other containing essentially empty space. Thus, if a simulated turbine missile entered this pump room, a determination could be made as to whether the pump itself would have been struck, or if the missile landed harmlessly in the empty part of the room. Also, rooms with redundant equipment were compartmentalized in order to determine whether all or part of the equipment in the room would be struck by missiles.

For the current study, an improved plant model has been developed through the examination of plant drawings and a physical on-site survey, in an attempt to reconstruct the layout of components where safety compromises occurred. In many instances, several components from one large room were separated into smaller compartments for each component. Thus, if a simulated missile entered one compartment, depending upon its velocity and energy, it may not continue through into other compartments causing the entire system to fail. Plant areas that were examined were the main and backup service water systems, switchgear room, cable spreading room, electrical tunnels, electrical penetration area, piping penetration area, and auxiliary feedwater system, A photographic record of these areas can be found in Appendix E.

The previous model treated the service water system as consisting of two rooms containing service water pump motors and two rooms containing service water strainers. Two rooms were used for each type of component in order to separate the two safety trains. Figure 3.3 is an overview of the service water system, showing the general layout of the pump motors, strainer pit, piping as it goes under the roadway and concrete bunker, and the valve pit. In the previous turbine missile analysis, missile breakups which resulted in strikes on either both pump motor rooms, or both strainer rooms, or a pump and strainer room from different safety trains were considered safety compromises. In the updated model, each service water pump motor and each strainer were self-contained in separate rooms. This provides a more accurate representation of the areas of the service water

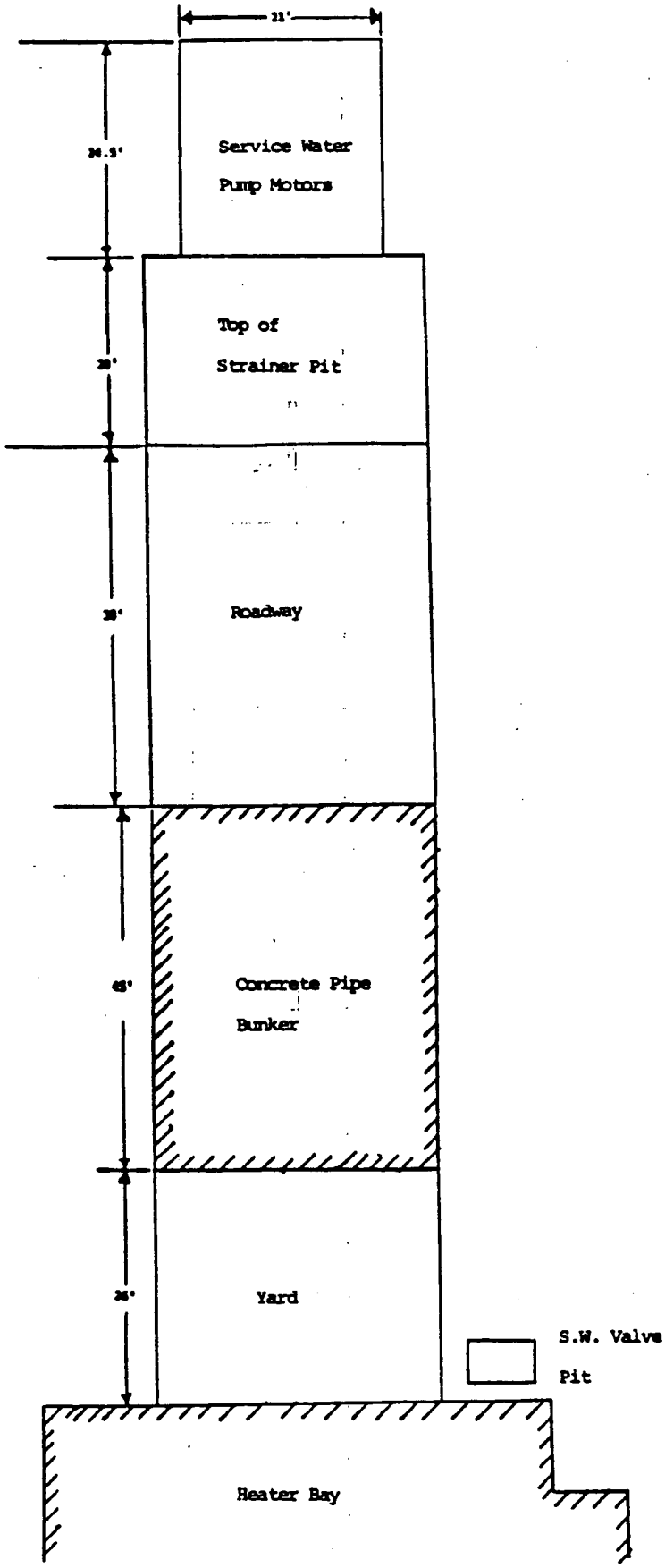

Figure 3.3. Service Water System Model Overview.

system that are affected by missile strikes. In order to maintain an operable service water system, 2 of 3 pumps, and their associated strainers, from either safety train are required. Missile penetrations of the service water areas that do not preclude meeting this requirement are not considered safety compromises.

Figure 3.4 shows the room configuration for the service water pump motors, which was arrived at based on the on-site survey. In Appendix E, Figures E.1 through E.4 are photographs of the service water pump motors. Figures E.1 and E.2 show the relative orientation of motors #31, #32, and #33, which are designated in the model as rooms 502, 500, and 497, respectively. Figure E.3 provides a similar layout for motors #35 and #36, which are designated in the model as rooms 501 and 504, respectively. Figure E.4 shows a measurement of motor #36, which helped establish the dimensions of room 504.

Figure 3.5 shows the room configuration for the service water valve pit. Figure E.5 indicates the size of a strainer, thus providing the dimensions of each individual strainer compartment. Figure E.6 provides the layout configuration of strainers #31 and #32 which are designated in the model as rooms 510 and 509, respectively.

The service water pipes and service water valve pit were remodelled after a careful inspection was performed during the on-site physical survey and discussions with the key NYPA official were held. The service water pipes were modelled as two rooms, where one room was developed for all the pipes passing under the roadway and the other room was structured for all the pipes passing through the concrete bunker. The pipes passing under the roadway were modelled as room 516 which was assumed to have eight feet of dirt between the pipes and the top surface of the roadway. The pipes passing through the concrete bunker were modelled as room 517.

In Appendix E, Figures E.7 and E.8 show two photographs of the roadway and concrete bunker. The top photograph was taken in front of the service water pump motor enclosure to illustrate that the service water pipes travel under the road in the foreground and through the concrete bunker which can be seen in the background behind the fence. In the background on the left, the top of the valve pit can be seen. The lower photograph is a view of the service water pump motor enclosure which was

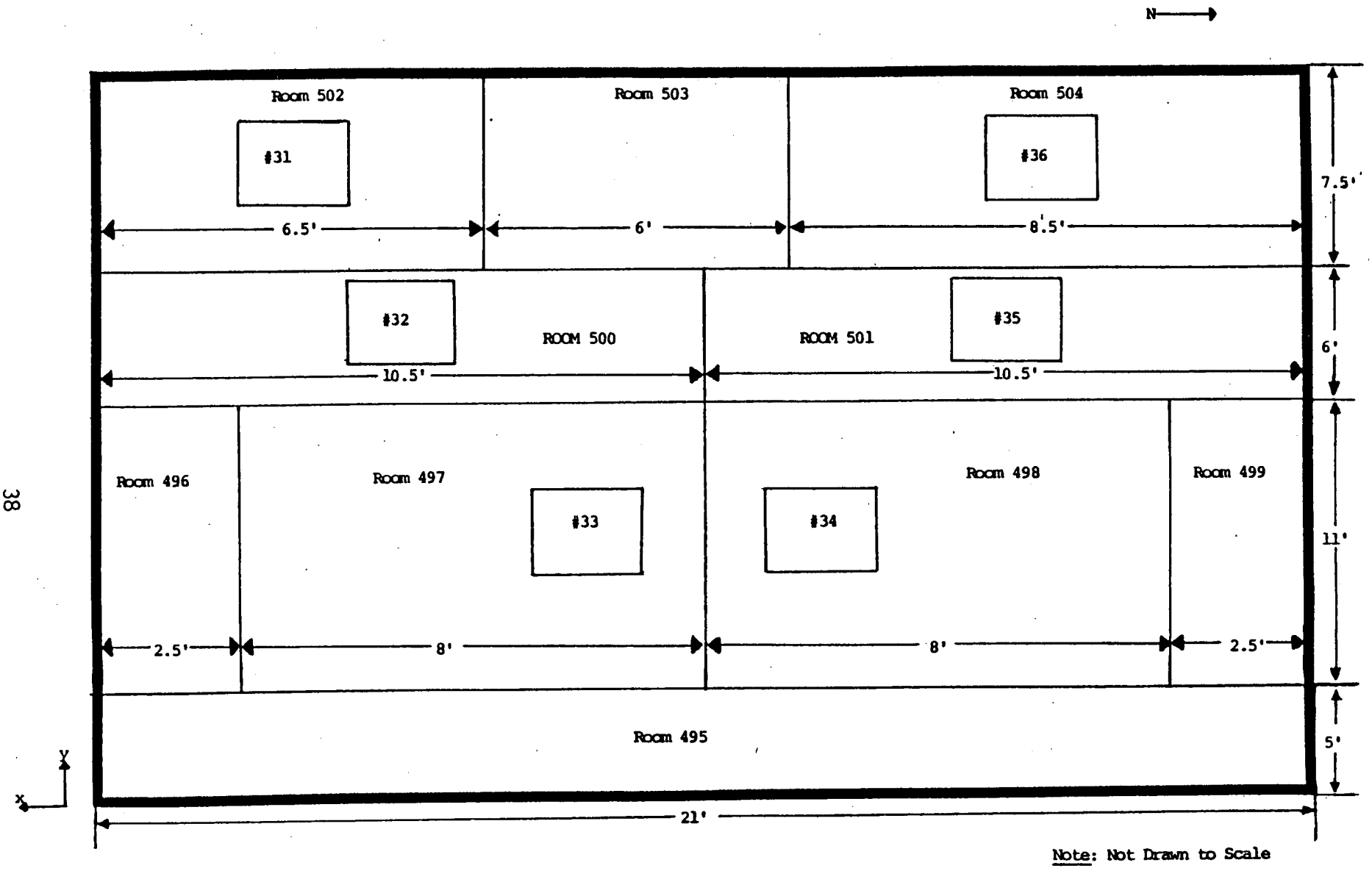

Figure 3.4. Service Water Pump Motor Enclosure.

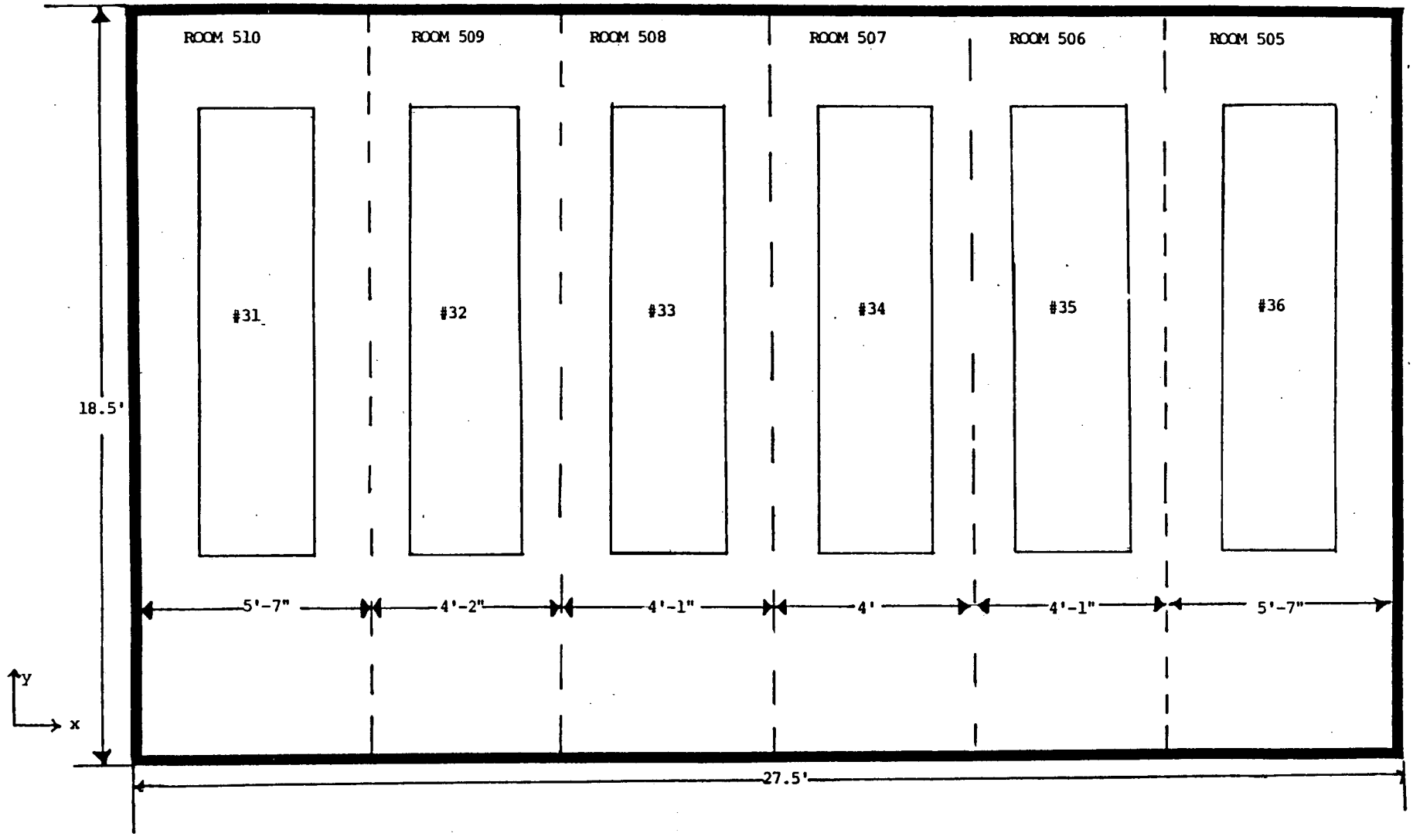

Figure 3.5. Service Water Strainer Pit.

taken near the service water valve pit. The concrete bunker and roadway can be viewed clearly in this photograph.

The service water valve pit was divided into four separate rooms, which included two rooms 524 and 525 for the essential service water, room 526 for the overlap of the essential and non-essential service water and room 527 for the non-essential service water, as shown in Figure 3.6. Figure E.9 provides a view within the main service water valve pit illustrating the proximity of components of the essential and non-essential service water systems. This region of overlap was modelled as room 526.

The backup service water pump motors and the backup service water valve pit were each modelled as only one room because the backup system is redundant with the main service water system. The reason for simplifying the modelling of the backup service water pump motors and valve pit was based upon an assumption that a simulated disc breakup would not result in missile strikes on both the main service water and the backup service water systems. During the analysis, there was only one case which resulted in strikes on both systems, so a more detailed model of the backup system was deemed unnecessary. In Appendix E, Figure E.10 is a photograph of the backup service water pump yard which was modelled as room 197, and Figure E. 11 is a photograph of the top of the backup service water valve pit. This area next to the heater bay was modelled as room 198.

While reviewing the previous model for the electrical penetration area, it was decided that a better model could be developed for the area. During the on-site physical survey, SAIC visited the electrical penetration area to decide how the model could be improved. After a physical inspection of the electrical penetration area and a careful review of the drawings, another room was constructed which modelled the area where the cables from the lower tunnel rise and join the cables from the upper tunnel. In this analysis, room 226 was modelled as the common area where the cables from the lower and upper electrical penetration areas come together. Figures E.12 and E.13 provide two photographs of this area. The lower electrical penetration area and the upper electrical penetration are redundant, but a strike in this common region can produce a safety compromise. Figure 3.7 shows a comparison of the previous and updated models of the electrical penetration area.

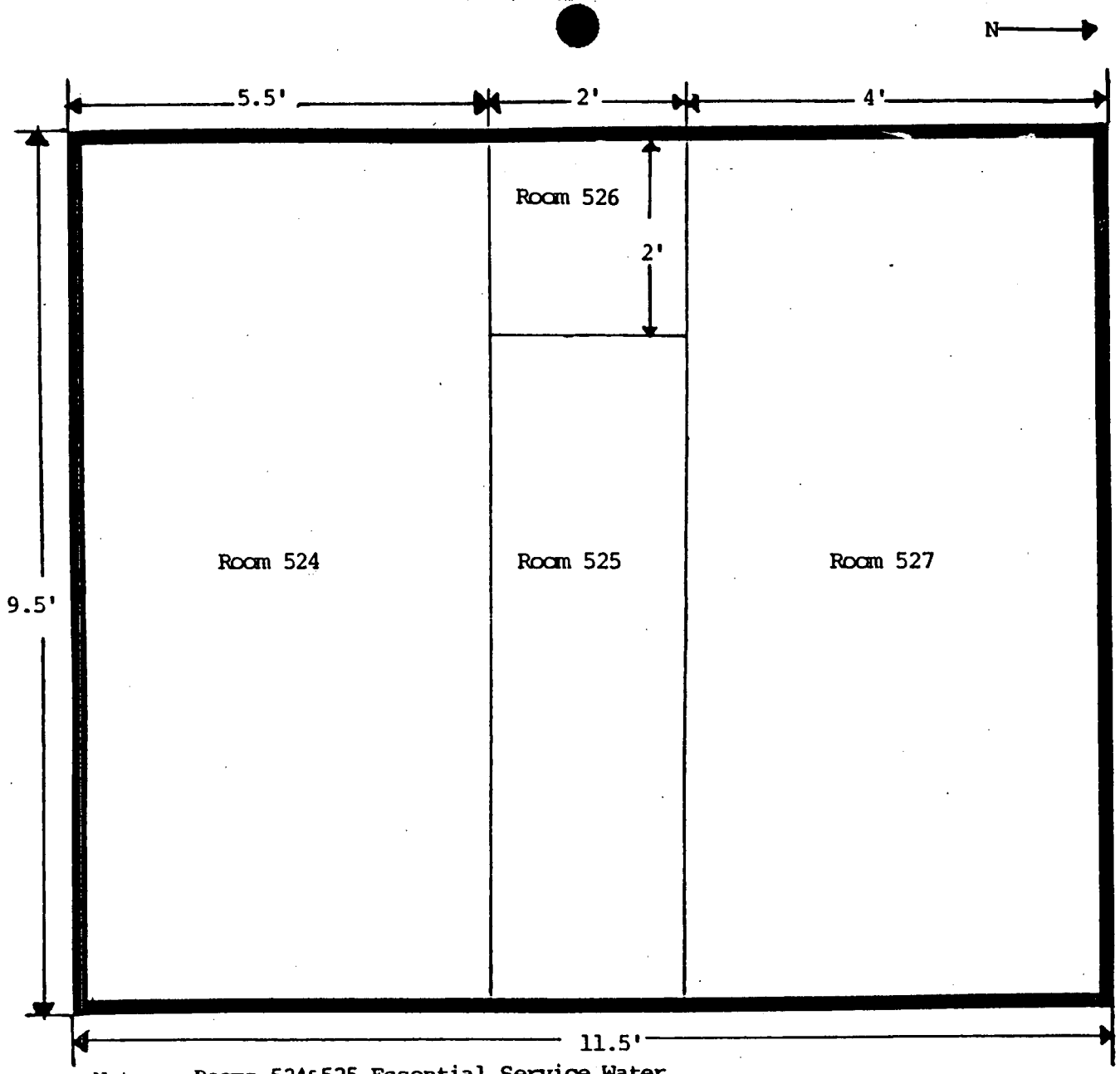

Notes: Rooms 524&525-Essential Service Water
Room 526-Essential & Non-essential Overlap
Room 527- Non-essential Service Water

Figure 3.6. Service Water Valve Pit.

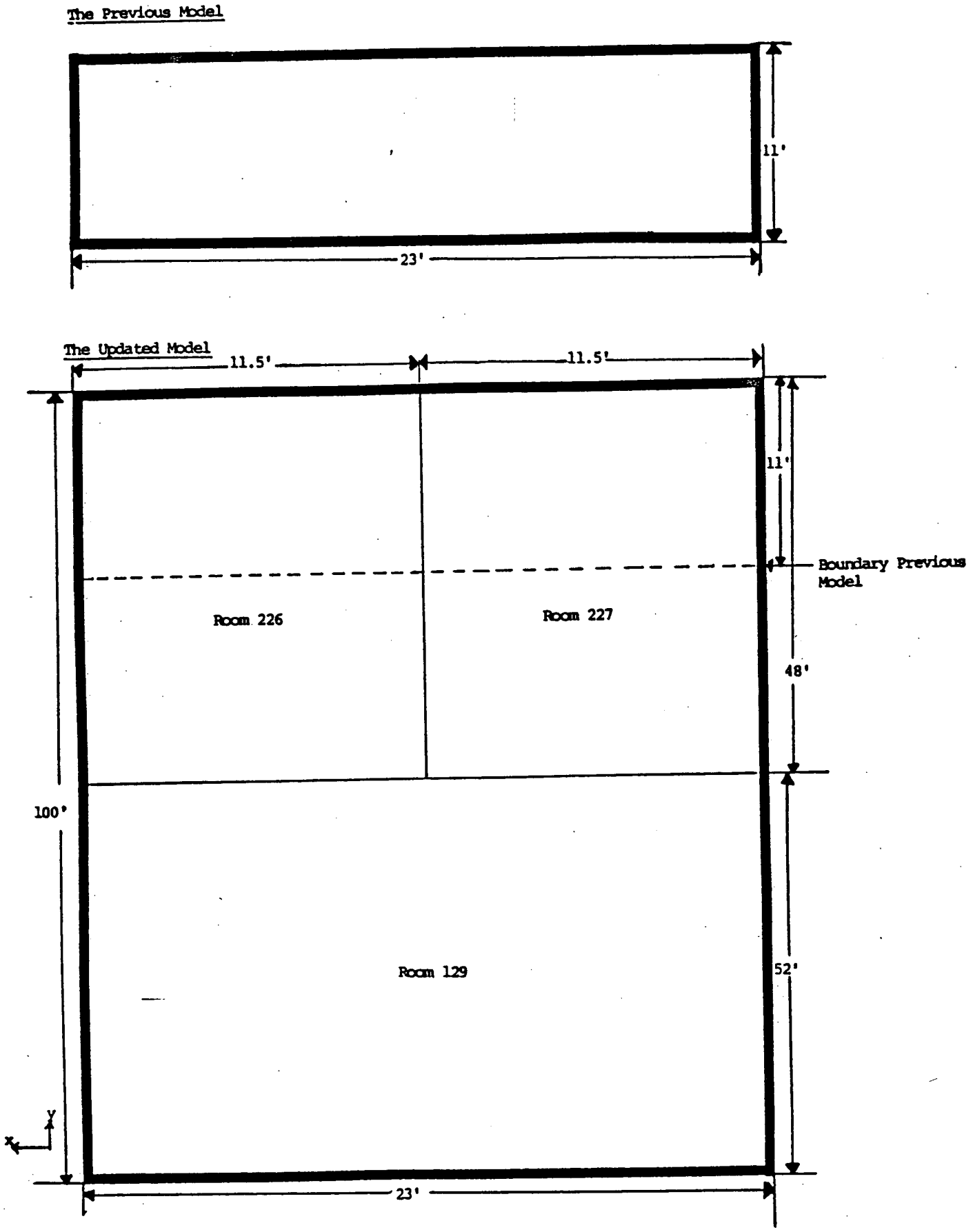

Figure 3.7. Electrical Penetration Area (elev 36').

The cable spreading room was also remodelled to account for a common area where all the cables join before entering the electrical tunnels. In the analysis, this area was designated as room 529 and its dimensions assimilated into the code to calculate safety compromises for strikes in this area. A missile strike to this area would cause extensive damage to all the cables creating substantial problems for plant operations. Figures E.14 and E.15 provide two photographs of this area, while Figure E. 16 shows the cables leaving the cable spreading room and entering the electrical tunnels.

Before the on-site physical survey, an improved model for the switchgear room was determined to be needed. The survey indicated that the switchgear rooms should be divided into nine compartments, where four separate compartments were structured for bus 3A, bus 6A, bus 2A, and bus 5A. An additional four rooms were constructed to represent areas where a missile could be assumed to affect two buses simultaneously, such as, bus 3A and bus 6A, bus 3A and bus 2A, bus 6A and bus 5A and, bus 2A and bus 5A. A final compartment was created for the common area where all the buses would be affected. The size of the regions where more than one bus would be affected is based on the relative positions of the buses and the dimensions of the simulated turbine missiles. For the analysis phase, it was decided by the SAIC staff and NYPA officials that a safety compromise would occur only if a simulated missile strike affected at least two buses. Figure 3.8 shows the updated model of the switchgear room.

Other areas of the plant that were examined during the physical survey were the piping penetration area, the electrical tunnels, and the auxiliary feedwater system. In each case, it was determined that no changes to the existing model were warranted. Figures E.17 and E.18 show the start of the electrical tunnels where the cables have just left the cable spreading room. There is an area in which there is no separation between the two trains, until the concrete separation at the top of the stairs. This area has been modelled as rooms 489 (lower cables) and 490 (upper cables). The auxiliary feedwater pumps are behind a shield wall and are therefore protected from missile strikes. Auxiliary feedwater piping splits into four paths, each of which has been modelled as a separate compartment, rooms 99, 102, 232, and 233. Figures E.19 and E.20 are photographs of

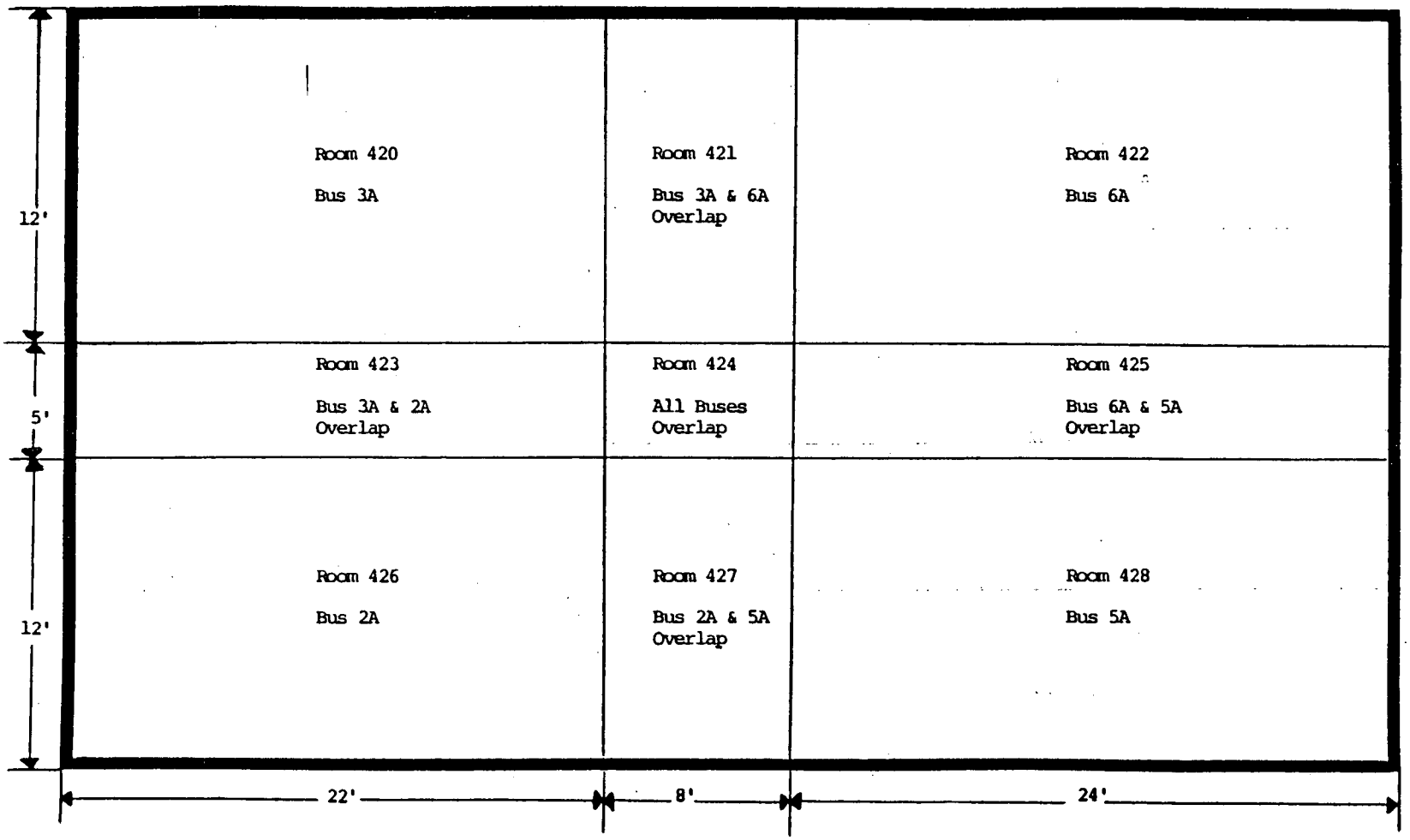

Figure 3.8. Switchgear Room.

auxiliary feedwater piping. Photographs are not permitted in the piping penetration area.

The resulting model contained 152 compartments designed as targets or safety regions, and 377 non-safety regions.* Table 3.1 describes each of the safety regions. This table relates each region to regions of the plant fire protection system. Redundancy considerations, as discussed in the next section, are also listed.

Appendix C contains plant layouts at various elevations to illustrate the location of critical plant areas. Safety regions are hashed.

3.2 REDUNDANCY OF PLANT SHUTDOWN EQUIPMENT

The safety of the plant following a turbine missile event is dependent upon the ability to safely shut down and maintain the core in a coolable configuration. In this analysis it is assumed that the cold or hot shut-down options are to be maintained. For this requirement, the following systems, along with their power sources and power and control activities must be maintained:

1. Reactor Control System (including control room, associated equipment and cabling);

2. Primary Cooling Systems (including boron control and makeup water);

3. Secondary Cooling Systems (following a turbine missile event, either the auxiliary feed system or the turbine by-pass systems must be available and for the long term, the residual heat removal system must be available);

4. Component Cooling Systems.

*This determination was made by SAIC based on appropriate documentation supplied by NYPA and in consultation with NYPA personnel.

Table 3.1. Summary of Indian Point 3 Critical Area Modeling.

Fire Protection Area Designation	Missile Code Designation (System No.)*	Remarks
1 Component Cooling Pumps & Cabling	293, 294, 485 (1,4)	Each pump is redundant.
2 Containment Spray Pumps #31, 32	312, 482 (4)	Each pump is redundant.
2A Primary Make-up Water System	298, 299, 309 (2)	Protected from missile strikes.
3 RHR Pump #31	250 (2)	Redundant with other RHR pumps.
4 RHR Pump #32	252 (2)	Redundant with other RHR pumps.
9A RHR Pump	249 (2)	Redundant with other RHR pumps.
69A RHR Piping and Valves	251 (2)	
12A Valve Corrodor	259, 260 (2)	
3A Piping Tunnel	295, 296 (2,3,4)	Protected from missile strikes.
5A, 58A Piping Tunnels	263, 264, 265, 275, 279, 280, 281, 283, 284, 285, 286, 287, 288, 289 (2,3,4)	Protected from missile strikes.
6A Valve Room	272 (2)	
7A Lower Electrical Tunnel	64, 67, 262, 267, 417, 489 (1)	Redundant with upper electrical tunnel.
74A Lower Electrical Penetration Area	90 (1)	Redundant with upper electrical penetration area.
60A Upper Electrical Tunnel	184, 185, 391, 418, 488, 490 (1)	Redundant with lower electrical tunnel.
73A Upper Electrical Penetration Area	129, 226, 227 (1)	Redundant with lower electrical penetration area.
73A Common Elec. Pen Area	226 (1)	Cables from lower tunnel rise and join cables from upper tunnel
8 Boric Acid Transfer Pumps	350 (2)	
8A RHR HXs	235 (2)	Protected from missile strike.
9 Safety Injection Pumps # 31, 32, 33	266, 483, 484 (2)	Protected from missile strike.
10A Valve Corridor	236 (2)	Protected from missile strike.
10 Diesel Generator #31 and FO Tank	448, 451 (1)	Redundant with other power supplies.
101A D/G #32 and FO Tank	449, 452 (1)	Redundant with other power supplies.
102A D/G #33 and FO Tank	450, 453 (1)	Redundant with other power supplies.
11 Cable Spreading Room	429, 430, 432, 434, 435, 436, 439, 442, 443, 444, 445 (1)	Redundant with diesels - plant can isolate one diesel.
11 Cable Spreading Room Common Area	529 (1)	All cables join before entering electrical tunnels.
11 MG Sets #31, 32	431, 433 (1)	Redundant with other power supplies.
11 Reactor Trip Breakers	440, 441 (1)	Redundant with control room.
12, 13 Battery Rooms	437, 438 (1)	Redundant with other power supplies.

*1 is control system
2 is primary cooling system
3 is secondary cooling system
4 is component cooling system

Table 3.1. - Summary of Indian Point 3 Critical Area Modeling (Continued).

Fire Protection Area Designation	Missile Code Designation (System No.)*	Remarks
14 Switchgear Room, Bus 3A	420 (1)	Redundant with other buses.
14 Swtichgear Room, Buses 3A, 6A	421 (1)	Region overlaps the two buses.
14 Switchgear Room, Bus 6A	422 (1)	Redundant with other buses.
14 Switchgear Room, Buses 3A, 2A	423 (1)	Region overlaps the two buses.
14 Switchgear Room, All Buses	424 (1)	Region overlaps all buses.
14 Switchgear Room, Buses 6A, 5A	425 (1)	Region overlaps the two buses.
14 Switchgear Room, Bus 2A	426 (1)	Redundant with other buses.
14 Switchgear Room, Bus 2A, 5A	427 (1)	Region overlaps the two buses.
14 Switchgear Room, Bus 5A	428 (1)	Redundant with other buses.
15 Control Room	446 (1)	Safe shutdown capability from local control stations.
17A Large PAB Area:		
Motor Control Centers	314 (1)	
Air Receivers	357 (1)	Control valves fail in safe position.
N_2 Storage	359 (1)	Redundant with air system.
Component Cooling Hxs	346, 352 (4)	Each redundant.
27A Large PAB Area:		
Top of Comp. Cooling HXs	479, 480 (4)	Each redundant.
Comp. Cooling Surge Tanks	378, 478 (4)	Each redundant.
Boric Acid Tanks	386, 481 (2)	Each redundant.
20A Pipe Chase	319 (2)	
23A Pipe Chase	338, 382 (2)	
25A Seal Water HX	373 (2)	
28A Valve Corridor	365, 366 (2)	
29A Volume Control Tank	363 (2)	
32A Non-regenerative HX	377 (2)	
23 Aux. Feedwater Pumps	100 (3)	Protected from missile strikes.
52A Aux. Feedwater Piping, Cables	101 (3)	Protected from missile strikes.
57A Feedwater Stop & Check Valves	99, 102, 232, 233 (3)	All redundant
55A Service Water Pump Motor #33	497 (4)	Two of three pumps in either train required.
55A Service Water Pump Motor #34	498 (4)	Two of three pumps in either train required.
55A Service Water Pump Motor #32	500 (4)	Two of three pumps in either train required.
55A Service Water Pump Motor #35	501 (4)	Two of three pumps in either train required.
55A Service Water Pump Motor #31	502 (4)	Two of three pumps in either train required.
55A Service Water Pump Motor #36	504 (4)	Two of three pumps in either train required.
55A Service Water Strainer #36	505 (4)	Two of three strainers in either train required.
55A Service Water Strainer #35	506 (4)	Two of three strainers in either train required.

*1 is control system
2 is primary cooling system
3 is secondary cooling system
4 is component cooling system

Table 3.1. Summary of Indian Point 3 Critical Area Modeling (Continued).

Fire Protection Area Designation	Missile Code Designation (System No.)*	Remarks
55A Service Water Strainer #34	507 (4)	Two of three strainers in either train required.
55A Service Water Strainer #33	508 (4)	Two of three strainers in either train required.
55A Service Water Strainer #32	509 (4)	Two of three strainers in either train required.
55A Service Water Strainer #31	510 (4)	Two of three strainers in either train required.
55A Service Water Pipes	516, 517	All pipes passing under road and through concrete bunker.
55A Service Water Valve Pit	524, 525	Essential service water.
55A Service Water Valve Pit	526	Overlap of essential and non-essential service water.
55A Service Water Valve Pit	527	Non-essential service water.
Backup Service Water Pump Yard	197 (4)	Redundant with main service water.
Backup Service Water Valve Pit Area	198 (4)	Redundant with main service water.
59A Piping Penetration Area	127, 130, 135 (2,3,4)	Region 127 is empty space - missile strikes do not cause safety compromise.
105A Primary Water Storage Tank	156 (2)	Redundant with RWST.
106A Refueling Water Storage Tank	471 (2)	
552, 553 Condensate Storage Tank	491 (2)	
Offsite Feeder	85 (1)	Redundant with other power supplies.
90A, 91A Spent Fuel Storage	176	Can be struck by HTMs only, but strikes cannot cause offsite release.
Additional control cabling between control room and containment	200, 201, 202, 203, 204, 205 (1)	Redundant with additional control cabling between turbine building and containment.
Additional control cabling between turbine building and containment	213, 216, 218, 220 (1)	Redundant with additional control cabling between control room and containment.

*1 is control system
2 is primary cooling system
3 is secondary cooling system
4 is component cooling system

All of these systems have redundant components, controls, and power circuitry so that no failure of a single item will compromise the ability to maintain a safe shutdown condition. These components and their redundancies are described in Table 3.1. Some areas, such as the piping penetration area (fire protection region 59A), contain equipment too close together to model redundancy. In this analysis, strikes on such areas were considered to compromise plant safety.

4. RESULTS

4.1 PROBABILITY OF SAFETY COMPROMISE

Using the MISIP code, a series of computer simulations were performed on the generation of turbine missiles at the Indian Point 3 plant. As discussed earlier, 36 turbine discs were analyzed under various conditions. A set of calculations was performed for the breakup of all discs at both rated speed and at 132 percent overspeed. Disc breakup into 90° segments was considered, and 100 trial breakups per disc were analyzed. The results of these calculations are reported in Table 4.1.

The model of the plant contains 152 targets, or safety regions, and 377 non-safety regions. Each trial on a disc generated 12 missiles as discussed in Section 2. Each missile was tracked and any penetrations of safety regions were recorded. P_2 was then determined on the basis of these 100 trials. The probability of disc failure for a 5-year inspection interval, P_1 (see Table 2.5), was then multiplied by P_2 to give the probability of safety region penetration for each disc as shown in Table 4.1. The summation of the 36 probabilities represents the overall probability of safety region penetration. Then the redundancy considerations discussed in Section 3.2 were accounted for, resulting in a smaller number of simulated safety compromises. Redundancy was considered in two ways. First, credit was not taken for the backup service water system, so that missile strikes which eliminated the main service water system were considered safety compromises. Then the backup service water system was included, resulting in fewer safety compromises. The outcome of 100 trials on all 36 discs resulted in five simulated safety compromises at rated speed and eight safety compromises <u>at</u> 132 percent overspeed. With only two exceptions, all of these safety compromises result from missile strikes on the service water system piping under the roadway, and thus would be eliminated if credit is taken for the backup service water system. The two exceptions, both occurred at 132 percent overspeed. Failure of disc 3 resulted in a strike on room 226, the section of the electrical penetration area which is common to both the lower and upper electrical tunnels. Failure of disc 4 resulted in strikes on both the upper (room 488) and lower (room 64) electrical tunnels.

Table 4.1. Results for 100 Trials - Each for 90° Breakup of All Discs (A Total of 86,400 Missiles was Generated and Tracked to Produce this Table).

Disc Number	100 Percent Rated Speed		132 Percent Overspeed	
	Number of Missile Penetrations of Safety Regions	Probability* Per Year of Penetration	Number of Missile Penetrations of Safety Regions	Probability* Per Year of Penetration
1	8	4.3E-9	9	2.7E-10
2	2	2.0E-12	3	3.9E-13
3	2	6.3E-12	2	3.0E-13
4	4	8.2E-8	3	8.5E-10
5	2	5.1E-8	2	5.2E-12
6	0	0	0	0
7	0	0	0	0
8	4	4.5E-8	1	1.2E-10
9	6	1.85E-7	1	4.0E-10
10	1	5.6E-11	3	5.7E-12
11	0	0	0	0
12	3	3.6E-11	3	2.9E-12
13	4	4.1E-11	0	0
14	3	9.3E-14	3	2.4E-14
15	10	5.9E-12	5	1.8E-13
16	6	2.4E-10	7	6.7E-12
17	5	2.1E-9	12	5.7E-11
18	0	0	0	0
19	0	0	0	0
20	7	5.8E-9	6	3.7E-11
21	7	6.8E-10	2	3.8E-12
22	7	3.0E-10	4	6.0E-12
23	1	3.9E-12	4	2.1E-12
24	0	0	1	2.8E-11
25	4	1.2E-10	3	6.0E-12
26	2	3.4E-12	1	2.4E-13
27	3	1.1E-12	4	8.3E-14
28	0	0	1	3.6E-10
29	2	7.4E-8	2	7.1E-10
30	0	0	0	0
31	0	0	0	0
32	2	8.4E-8	2	7.7E-10
33	1	1.5E-8	0	0
34	1	1.6E-8	0	0
35	1	6.8E-12	1	8.8E-13
36	1	1.3E-10	1	8.6E-12
Total	99	5.5E-7	86	3.7E-9

*Based on 5 year inspection interval.

Using P1 values for a five-year inspection interval, the overall probabilities of safety compromise are:

P_4 Values with 100 Trials for Five-Year Inspection Intervals

	No Credit for Backup SW	Credit Taken for Backup SW
90° segments, rated speed	2.69E-10/yr	0/yr
90° segments, 132 percent overspeed	3.06E-10/yr	2.82E-10/yr

However, 100 trials per disc do not provide adequate statistics for precise probability determinations. Therefore, new calculations were performed with 2000 trials per disc, but only the 18 discs which dominate the missile risk because of their high P_1 values were considered. Other discs were eliminated from consideration because an examination of their P_1 values and the results for 100 trials indicated that they would not make a significant contribution to P_4.

Tables 4.2 and 4.3 summarize probabilities of penetration and safety compromise for these discs. Table 4.2 summarizes the results for the 90° breakup case and Table 4.3 showns the results for 120° breakup. The probabilities were calculated using P_1 values from Table 2.5 for a 5-year inspection interval. Table 4.4 summarizes the locations of strikes on safety regions according to their designation in the MISIP code and their physical description in the plant. Tables 4.5 through 4.8 show the number of times each safety region was struck by the failure of each disc.

The overall results of the simulation are given below for 90° and 120° segments, and for failure at rated speed and at 132 percent overspeed. The P_4 values are the probabilities of safety compromise, and utilize the redundancy considerations discussed in Section 3.2. The greatest concern for the Indian Point 3 plant is disc failure at rated speed into 90° segments. The probability of compromising plant safety by this mechanism is 1.70×10^{-8}/year, if no credit is taken for the backup service water system.

Table 4.2. Results for 2000 Trials Each for Critical Discs, 90° Segments (24,000 Missile Traces per Disc, for a Grand Total of 432,000 Traces).

Disc Failure at Rated Speed

Disc Number	Number of Missile Penetrations of Safety Regions	Probability Per Year of Penetration	Number of Safety Compromises (No Credit for Backup SW)	Probability of Safety Compromise	Number of Safety Compromises (Credit Taken For Backup SW)	Probability of Safety Compromise
1	107	2.88E-9	0	0	0	0
4	46	4.74E-8	0	0	0	0
5	44	5.59E-8	0	0	0	0
8	47	2.64E-8	5	2.81E-9	5	2.81E-9
9	59	9.09E-8	4	6.16E-9	3	4.62E-9
10	50	1.39E-10	3	8.34E-12	2	5.56E-12
16	138	2.75E-10	13	2.59E-11	1	1.99E-12
17	137	2.93E-9	20	4.28E-10	1	2.14E-11
20	129	5.34E-9	22	9.11E-10	0	0
21	128	6.20E-10	10	4.84E-11	1	4.84E-12
22	109	2.34E-10	14	3.01E-11	2	4.30E-12
24	14	4.44E-10	0	0	0	0
25	112	1.61E-10	17	2.45E-11	2	2.88E-12
28	19	2.72E-8	1	1.43E-9	0	0
29	35	6.44E-8	2	3.68E-9	0	0
32	27	5.64E-8	1	2.09E-9	0	0
33	36	2.73E-8	0	0	0	0
36	10	6.72E-11	1	6.72E-12	1	6.72E-12
Total	1247	4.09E-7	113	1.70E-8	18	7.47E-9

Disc Failure at 132 Percent Overspeed

Disc Number	Number of Missile Penetrations of Safety Regions	Probability Per Year of Penetration	Number of Safety Compromises (No Credit for Backup SW)	Probability of Safety Compromise	Number of Safety Compromises (Credit Taken For Backup SW)	Probability of Safety Compromise
1	100	1.47E-10	0	0	0	0
4	39	5.50E-10	1	1.41E-11	1	1.41E-11
5	53	6.84E-12	1	1.29E-13	0	0
8	59	3.66E-10	0	0	0	0
9	41	8.08E-10	1	1.97E-11	1	1.97E-11
10	46	4.35E-12	4	3.78E-13	4	3.78E-13
16	128	6.12E-12	17	8.13E-13	2	9.56E-14
17	137	3.23E-11	16	3.78E-12	2	4.72E-13
20	156	4.87E-11	27	8.42E-12	2	6.24E-13
21	124	1.18E-11	22	2.09E-12	0	0
22	104	7.82E-12	16	1.20E-12	1	7.52E-14
24	9	1.27E-11	0	0	0	0
25	82	8.15E-12	13	1.29E-12	1	9.94E-14
28	23	4.14E-10	0	0	0	0
29	36	6.41E-10	1	1.78E-11	0	0
32	31	5.98E-10	0	0	0	0
33	20	2.16E-10	1	1.08E-11	1	1.08E-11
36	12	5.18E-9	2	8.64E-13	2	8.64E-13
Total	1200	3.88E-9	122	8.14E-11	17	4.73E-11

Table 4.3. Results for 2000 Trials Each for Critical Discs, 120° Segments (18,000 Missile Traces per Disc for a Grand Total 324,000 Traces).

Disc Failure at Rated Speed

Disc Number	Number of Missile Penetrations of Safety Regions	Probability Per Year of Penetration	Number of Safety Compromises (No Credit for Backup SW)	Probability of Safety Compromise	Number of Safety Compromises (Credit Taken For Backup SW)	Probability of Safety Compromise
1	77	2.07E-9	0	0	0	0
4	27	2.78E-8	0	0	0	0
5	22	2.79E-8	2	2.54E-9	1	1.27E-9
8	25	1.40E-8	0	0	0	0
9	38	5.85E-8	0	0	0	0
10	39	1.08E-10	2	5.56E-12	2	5.56E-12
16	77	1.53E-10	14	2.79E-11	0	0
17	102	2.18E-9	14	3.00E-10	2	4.28E-11
20	86	3.56E-9	13	5.38E-10	0	0
21	61	2.95E-10	3	1.45E-11	0	0
22	93	2.00E-10	9	1.94E-11	0	0
24	4	1.26E-10	0	0	0	0
25	54	7.78E-11	4	5.76E-12	0	0
28	11	1.57E-8	0	0	0	0
29	18	3.31E-8	0	0	0	0
32	27	5.64E-8	2	4.18E-9	0	0
33	16	1.21E-8	1	7.58E-10	0	0
36	12	8.06E-11	2	1.34E-11	2	1.34E-11
Total	789	2.54E-7	66	8.40E-9	7	1.33E-9

Disc Failure at 132 Percent Overspeed

Disc Number	Number of Missile Penetrations of Safety Regions	Probability Per Year of Penetration	Number of Safety Compromises (No Credit for Backup SW)	Probability of Safety Compromise	Number of Safety Compromises (Credit Taken For Backup SW)	Probability of Safety Compromise
1	65	9.56E-11	0	0	0	0
4	26	3.67E-10	0	0	0	0
5	40	5.16E-12	2	2.58E-13	2	2.58E-13
8	38	2.36E-10	3	1.86E-11	3	1.86E-11
9	24	4.73E-10	0	0	0	0
10	46	3.97E-12	2	1.89E-13	2	1.89E-13
16	67	3.20E-12	9	4.30E-13	0	0
17	100	2.36E-11	11	2.60E-12	1	2.36E-13
20	101	3.15E-11	10	3.12E-12	1	3.12E-13
21	66	6.26E-12	6	5.69E-13	0	0
22	80	6.07E-12	6	4.51E-13	0	0
24	9	1.27E-11	0	0	0	0
25	46	4.57E-12	8	4.95E-13	4	3.98E-13
28	18	3.24E-10	0	0	0	0
29	28	4.98E-10	1	1.78E-11	0	0
32	25	4.82E-10	0	0	0	0
33	15	1.62E-10	0	0	0	0
36	7	3.02E-12	2	8.64E-13	2	8.64E-13
Total	811	2.74E-9	60	4.57E-11	15	2.09E-11

Table 4.4. Safety Regions Struck by Turbine Missiles in Simulation Study.*

Target	Description
64, 267	Lower electrical tunnel
85	Offsite power feeder
99, 102, 232, 233	Feedwater stop and check valves
127, 135	Piping penetration area
129, 226, 227	Upper electrical penetration area
156	Primary water storage tank
176	Spent fuel storage
184, 488	Upper electrical tunnel
197	Backup service water pump yard
198	Backup service water valve pit area
213, 216, 218, 200	Cabling (turbine bldg to containment)
420, 421, 422	Control building switchgear room
429, 430, 434, 435, 436, 442, 443, 444, 445, 529	Cable spreading room
446	Control room
497, 498, 500, 501, 502, 504	Service water pump motors
505, 506, 507, 508, 509, 510	Service water strainer pit
516, 517	Service water piping

*Dimensions and locations of each target is given in Table C1-1. Layout of each target is indicated on one of Figures C3-1 through C3-12.

Table 4.5. Number of Safety Region Penetrations per Disc for 2000 Simulated Failures at Rated Speed, 90° Segments.

	SAFETY REGION NUMBER																								
DISC	64	65	99	102	127	129	135	156	176	184	197	198	213	216	218	220	226	227	232	233	267	420	421	422	429
1			17	3							44	30		5	2	3			14	1					
4			4	7	2	4			1		1	1		1					10	6					
5			4	8		3					2	1		3	2			1	15						
8			4	4		7					5	2					5		9	1					
9			6	3	1	4		1	1		6	4	1	1		4	2		6	1	1				
10			1	9		11			1		7	1					2	1	6	1					
16			2	3	2	2			1		1	2				1	1		5	1					
17			6	3		3					1				1	2	1	1	3						
20			1	2	1									1	1	1		1	1						
21			2	4	1	3						3					1	1	2	1		1			1
22			2	1		1					1	2							2						
24								2													4				3
25			1	5	1	5					24	19		1		1	2		5	4					
28				1				1			2	3							1						
29			2	1		1													2						1
32				1		2													1	2					
33			1	1		1		1	1		2	1							2		2				
36								1		1													1		
TOTAL	0	0	53	56	8	47	0	6	5	1	96	69	1	12	6	12	14	5	84	18	7	1	1	0	5

	SAFETY REGION NUMBER																								
DISC	430	434	435	436	442	443	444	445	446	488	487	498	500	501	502	504	505	506	507	508	509	510	516	517	529
1																									
4												1		4		3	2	1		2	1	1			
5												3	2	4	2	2	2	2	2	2	1	1			
8										1			3	6	4	3		1	1		1	1			
9										1			1	5	3	5	1	1	1	4	2	1	1		
10										5		1	4	2	4	3				1				1	
16										2	12	13	38	36	41	32	4	3	2	3	1	2	9	2	
17											14	21	27	38	26	40	6	6	1	3	4		17	1	
20										2	15	13	33	30	26	27	5	6	4	5	3	3	20		
21											12	17	26	45	30	40	4	2	2	1	2	5	9		
22										2	18	18	29	37	25	43		2	1	3	1	1	12	1	1
24	1		1				1		2	4															
25											8	13	13	21	10	21	1	2	1			1	15		
28										3	1		4		2	2	1						1		
29										3	1	3	5	5	3	6	5	2	2	1	1		2		
32									1	5			2	2	6	3	3	1	1			1	1		
33									2	7	1	1	2	4	1	4	2	3	1	2					
36									6	2															
TOTAL	1	0	1	0	0	0	1	0	11	37	82	104	189	239	183	234	35	32	19	26	17	17	87	5	1

Table 4.7. Number of Safety Region Penetrations per Disc for 2000 Simulated Failures at Rated Speed, 120° Segments.

	SAFETY REGION NUMBER																								
DISC	84	85	99	102	127	129	135	156	176	184	197	198	213	216	218	220	226	227	232	233	267	420	421	422	429
1			7	8							44	19		1	1	1			5	5					
4			1	2							1	3		2					6	2					
5			5	1		2							1	2		1	1		2						
8			2	1		2						1							3	1					
9			4	4	1	1			2		2	1	1						5	3					
10			5	4	1	4				1	2	2		2		1	1	1	6	1			1	1	
16			2	3		2													1						
17			2			2										1	2	2	1						
20			1			3												1	2						
21			1			3						1						1	2						
22			3			3		2	1		2							2	3						1
24									1																
25			9	4		1					18	10		1		3			3	4					
28				1		1																			
29																									
32						1															1				
33						1						1													1
36																					3			2	1
TOTAL	0	0	42	28	2	26	0	2	4	1	69	38	2	8	1	7	4	7	39	16	4	0	1	3	3

	SAFETY REGION NUMBER																								
DISC	430	434	435	436	442	443	444	445	446	488	497	498	500	501	502	504	505	506	507	508	509	510	516	517	529
1																									
4													3	2	4	2			1			3			
5												2		6		3					1		1		
8											1	1	1	4		5	1	2	1	1	1	4			
9												1		5	1	5	1		1		1	2			
10										4				3		3	1	2	1			1			
16										1	6	8	14	18	12	18	4	1	3	1	1	6	14		
17											14	15	29	27	26	21	2	5		4	5	2	11	1	
20											8	10	23	25	25	23	4		2	1	2	1	13		
21										1	5	10	8	17	10	15	1	2	1	1	3	6	3		
22											13	10	23	22	19	26	2	1	1	2	1	6	9		
24										3															
25																						1	4		
28											2	1	4	2	3	1	1	1							
29											2	1	7	4	7	2	3	2	1	1					
32									1		3	1	6	2	11	1	1	1	1	2	1	2	2		
33										3				1	1	1	4	1	1			1	1		
36		2		1	1	1		2	4																2
TOTAL	0	2	0	1	1	1	0	2	5	12	54	60	118	138	119	126	25	18	15	13	16	32	58	1	2

Table 4.8. Number of Safety Region Penetrations per Disc for 2000 Simulated Failures at 132 Percent Overspeed, 120° Segments.

	SAFETY REGION NUMBER																								
DISC	84	85	98	102	127	129	135	156	176	184	197	198	213	216	218	220	226	227	232	233	267	420	421	422	429
1			5	3							36	20		3	1	3			4						
4			1	3		1			1		5	2		1			1		2	1	1				1
5			5	4		3					3	5		3			2		5						
8	1		3	8	1	6	1		1		3	2					2		4		1				
9			3	2		1		1	1		2					1			1						
10	1		4	6	1	8		1	1		6	9					2	4	1	2		1			
16			1	1		2		1			2								3						
17			1	1		7	1		2		2					1		3							
20		1	1	2		5	1		2		1							3	2						
21			2	5		2			1		2	1						1	5	1					
22			1			3		1	3		7							1							
24										1											1				
25			2	4		5				1	20	6					4	1	3	2					
28				1					1		2									1	2				
29		2		2		1					1	1			1				1		1				
32			1	1					1					1							1				
33				2						1									2						
36		1																						3	1
TOTAL	2	4	30	45	2	44	3	4	14	3	92	46	0	8	2	5	11	13	33	7	7	1	0	3	2

	SAFETY REGION NUMBER																								
DISC	430	434	435	436	442	443	444	445	446	488	497	498	500	501	502	504	505	506	507	508	509	510	516	517	529
1																									
4									1			1		1		3						2			
5										2		2		2		4		2	1			1			
8												2		2		3	2	1	1	1	1	1			
9										1	1	1	1	3	1	2			3	3		2			
10												1		3		2				1	2	1			
16										1	5	6	14	18	13	20	2		1	5		2	9		
17											11	15	16	30	18	30	2	1	4	5	2	3	10		
20										2	14	12	23	26	23	19	1	3	7	3		7	8		
21											5	7	10	17	11	16	3		2	1	3	2	6		
22										1	12	11	22	29	19	24			1		1	1	5	1	
24									3	5															
25										2				1								2	4		
28										2		1	2		4		1		3	1					
29									3	5	2	2	2	6	1	3		1		1	1		1		
32									1	3	1	1	4	1	7	1	1	1	1	1	1	2			
33									1	7			2	2						1	1	1			
36		2			1	1		2	1																2
TOTAL	0	2	0	0	1	1	0	2	10	31	51	62	96	141	97	127	12	9	24	23	12	27	43	1	2

P_4 Values with 2000 Trials for Five-Year Inspection Intervals

	No Credit for Backup SW	Credit Taken for Backup SW
90° segments, rated speed	1.70E-8/yr	7.47E-9/yr
90° segments, 132 percent overspeed	8.14E-11/yr	4.17E-11/yr
120° segments, rated speed	8.40E-9/yr	1.33E-9/yr
120° segments, 132 percent overspeed	4.57E-11/yr	2.09E-11/yr

4.2 PLANT VULNERABILITY

As noted previously, not all penetrations of safety regions result in compromising the ability of the plant to achieve safe shutdown. The specific strike combinations which produce the safety compromise probability are summarized below for the various cases. In this summary, credit is taken for the backup service water system.

90° segments, rated speed

- Strikes on the common electrical penetration area (MISIP target 226):

  Disc 8 - 5 strikes
  Disc 9 - 2 strikes
  Disc 10 - 2 strikes
  Disc 16 - 1 strike
  Disc 17 - 1 strike
  Disc 21 - 1 strike
  Disc 25 - 2 strikes

- Strikes on the common cable spreading room area (MISIP target 529):

  Disc 22 - 1 strike

- Strikes on the switchgear room, buses 3A, 6A:

  Disc 36 - 1 strike

- Strikes on both the main service water pipes under the road and the backup service water valve pit area (MISIP targets 516 and 198):

  Disc 22 - 1 strike

<u>90° segments, 132 percent overspeed</u>

- Strikes on the common electrical penetration area (MISIP target 226):

  Disc 9 - 1 strike
  Disc 10 - 4 strikes
  Disc 16 - 1 strike
  Disc 17 - 1 strike
  Disc 25 - 1 strike

- Strikes on the common cable spreading room area (MISIP target 529):

  Disc 33 - 1 strike
  Disc 36 - 2 strikes

- Strikes on the piping penetration area (MISIP target 135):

  Disc 16 - 1 strike
  Disc 17 - 1 strike
  Disc 20 - 2 strikes
  Disc 22 - 1 strike

- Strikes on both the lower and upper electrical tunnels (MISIP targets 64 and 488):

  Disc 4 - 1 strike

120° segments, rated speed

- Strikes on the common electrical penetration area (MISIP target 226):

  Disc 5 - 1 strike
  Disc 10 - 1 strike
  Disc 17 - 2 strikes

- Strikes on the common cable spreading room area (MISIP target 529):

  Disc 36 - 2 strikes

- Strikes on the switchgear room, buses 3A, 6A

  Disc 10 - 1 strike

120° segments, 132 percent overspeed

- Strikes on the common electrical penetration area (MISIP target 226):

  Disc 5 - 2 strikes
  Disc 8 - 1 strike
  Disc 10 - 2 strikes
  Disc 25 - 4 strikes

- Strikes on the common cable spreading room area (MISIP target 529):

  Disc 36 - 2 strikes

- Strikes on the piping penetration area (MISIP target 135):

  Disc 17 - 1 strike
  Disc 20 - 1 strike

As previously noted, there are several addtional safety compromises if credit is not taken for the backup service water system. The vast majority of the cases involve strikes on the service water system piping under the road (MISIP target 516). For all discs there were 87 such

strikes for 90° segments at rated speed, 99 strikes for 90° segments at overspeed, 58 strikes for 120° segments at rated speed, and 43 strikes for 120° segments at overspeed. (The number of strikes for each individual disc can be obtained from Tables 4.5-4.8). Since these pipes are under approximately eight feet of dirt, the number of penetrations of target room 516 was somewhat surprising. However, further study showed that the number of missiles which bounced off the road without penetrating to the pipes below was much larger than the number of missiles which penetrated to the piping. For the 90° segments, rated speed case, there were only 87 penetrations due to 5465 hits on the road, or 1.6 percent. Given the number of times that turbine missiles strike the roadway, the calculated number of penetrations is felt to be reasonable.

Other safety compromises involved strikes on the pipes inside the concrete bunker downstream from the road (MISIP target 517) and a few cases where as many as five of six service water pump motors were struck. For target 517, there were five strikes for 90° segments at rated speed, seven strikes for 90° segments at overspeed, one strike for 120° segments at rated speed, and one strike for 120° segments at overspeed. With regard to the service water pump motors, the safety compromises resulted from:

<u>90° segments, rated speed</u>:

Disc 16 - motors 31, 32, 33, 34, 35
Disc 17 - all motors
Disc 20 - motors 31, 32, 33, 35, 36
Disc 20 - all motors

<u>120° segments, rated speed</u>:

Disc 20 - motors 31, 32, 33, 35, 36

The previous model, which divided the service water pump motor enclosure into only two sections, resulted in a much larger number of calculated safety compromises. It is felt that the current model, in which each motor is in a separate cell, is more realistic and that the small number of safety compromises is reasonable.

Strikes on spent fuel storage were eliminated as possible safety compromises because only HTM strikes are possible. To produce an offsite

release from spent fuel storage a leak below the level of the stored elements would be required. It is concluded that an HTM strike cannot produce such a leak.

4.3 HAZARD DUE TO TURBINE MISSILES FROM UNIT 2

An analysis of the hazard to Indian Point 3 due to turbine missiles emanating from Unit 2 was performed. A MISIP model for both units was prepared and the code was executed to track missiles from the Unit 2 turbines. One thousand trials for failure of disc 16 and rated speed, and 1000 trials for disc 17 at 132 percent overspeed were examined. Both cases considered 90° segments because an earlier study [16] found 90° segments to result in the greater hazard in Unit 2. The execution of these two cases resulted in no strikes on IP3. This is considered adequate demonstration that turbine missiles from IP2 do not pose a significant threat to IP3.

5. CONCLUSIONS

This analysis is based on protection from an offsite release. In this regard, the current design coupled with emergency procedures is certainly adequate. The overall probability of compromising the plant's ability to achieve a safe shutdown due to turbine missiles is less than the NRC acceptance criteria of 10^{-7} per year.

The area of the plant that is most at risk is the service water system. Of those simulated missiles that entered areas of the plant containing safety-related equipment, the majority entered areas containing service water system components. However, this should not be considered a source of concern because in only a few of these cases were a sufficient number of components damaged as to disable the system. Most of these were due to strikes on the piping under the road, while a few cases resulted in strikes on 2 of 3 pump motors in each safety train. Additional shielding in these areas might reduce the number of safety compromises, but with the low frequency of safety compromises and the ability of the backup water system to perform the same function, such shielding is not considered necessary.

Besides the service water system, the other major areas of concern involve locations where electrical cables from both safety trains share a common room. This was found in the cable spreading room, at the start of the electrical tunnels, and in the electrical penetration area. Also, in the switchgear room, the four buses are relatively close together. Again, because of the low probability of safety compromise, no remedial action is necessary. In fact, the model is conservative in that it does not consider the shielding effect that the upper cable trays would have relative to the lower cable trays. Therefore, the probability of safety compromise may actually be lower than was calculated in this study.

In conclusion, it is felt that the results of this study show that Indian Point 3 plant is adequately protected from damage due to missiles generated by turbine failure. The probability that the plant will be unable to maintain a safe shutdown or that an offsite release will occur is well below the NRC acceptance criteria.

6. REFERENCES

1. Finn, S. P. and B. W. Johnson, Analysis of Hazards to Indian Point 3 Nuclear Generating Station Due to Missiles Generated by Turbine Failure, SAI01382-306LJ, Science Applications International Corp., January 1983.

2. Title 10, Code of Federal Regulations, Part 100 (10CFR100) "Reactor Site Criteria," Office of Federal Regulations, Washington, D.C.

3. "Turbine Missile Report - Results of Probability Analyses of Disc Rupture and Missile Generation," Westinghouse Electric Corporation, (Proprietary Data), May 1984.

4. The MIDAS Code Volume 1, Description, SAI/SR-12, Science Applications, Inc., June 1974.

5. Johnson, B. W. et al., Analysis of the Turbine Missile Hazard to the Nuclear Thermal Power Plant at Pebble Springs, Oregon, Portland General Electric Company, PGE-2012, January 1976.

6. "Turbine Missile Report (HP96-LP81-LP81-LP81)," CT-24081, Rev. 2, Westinghouse Electric Corporation, August 1982.

7. "Rotor Missile Report LP-3 Refurbished Rotor," CT-25210, Westinghouse Electric Corporation, September 1984.

8. "Missile Report for Turbines with 40-Inch Last Row Blades at Design, Intermediate and Destructive Overspeed," Report 296/380, Westinghouse Electric Co., June 1975.

9. Sliter, G. E., "Assessment of Empirical Concrete Impact Formulae," Journal of the Structural Division, ASCE, Vol. 106, No. ST, May 1980.

10. Sliter, G. E., "Status of EPRI Turbine Missile Research Program," Eighth Water Reactor Safety Research Information Meeting, October 1980.

11. Johnson, B. W., "Energy of Missiles Ricocheting from Concrete Walls," Draft Report, SAI-75-506-SV, Science Applications, Inc., October 1975.

12. Vasallo, F. A., "Missile Impact Testing of Reinforced Concrete Panels," Calspan Report No. HC-5609-D-1, January 1975, (Prepared for Bechtel Corporation, San Francisco, California).

13. Neville, A. M., Properties of Concrete, Sir Isaac Pitman & Sons, London, 1973, p. 303.

14. Hanst, J., Offshore Power Systems, Private Communication, October1975.

15. Hagg, A. C. and G. O. Sankey, "The Containment of Disc Burst Fragments by Cylindrical Shells," Research Report 73-1E7-STGRO-R1. See also Journal of Engineering for Power, TRANS. ASME, pp. 114-123, April 1974.

16. Johnson, B. W. and D. W. Buckley, Analysis of Hazards to the Indian Point 2 Nuclear Generating Station Due to Missiles Generated by Turbine Failure, SAI01381-138LJ/F, Science Applications, Inc., January 1982.

APPENDIX A - QUALITY ASSURANCE CHECKS

A.1 CHECK ON ADEQUACY OF PLANT SPECIFICATION

Two checks have been made on the plant specifications. One is the pre-process routine which is a small computer code which checks on a one-foot square grid that all points on the walls of the model of the plant are located adjacent to a valid neighboring room, or on a valid exterior wall. The routine also checks for duplicate designators of cells. This coded routine, MISREP, was utilized after the plant was first completely specified.

The second check was provided on a continuing basis in the main program MISIP, by an "error exit" option in the code. If, during a missile flight simulation, the missile enters an inappropriately specified region of the plant, a printout is provided of the valid location of the missile along with the missile characteristics. This printed information has been adequate to allow the plant specifications to be corrected.

A.2 VERIFICATION OF THE RANDOM PROCESS AND ANALYTICAL PROCEDURES

Random processes used in the code and calculated by Monte Carlo techniques were verified by selection of specific cases which could be calculated by hand to determine that the value obtained was within the appropriate ranges specified and occurred with the proper statistical frequency.

Analytical procedures and algorithms appearing in the code were verified by hand calculations as well as through the diagnostic printout used for the global checks.

A.3 GLOBAL CALCULATIONAL CHECK

A diagnostic option in the MISIP code traces the complete missile trajectory by successive impact points with emergent energies and directions for selected missile traces. Hand calculations of all the parameters listed have been made and the results verified for two of these complete traces.

APPENDIX B - MATHEMATICAL DERIVATIONS

B-1 Special Routine for Cylindrical Cells

B-2 Concrete Ricochet

B-3 Steel Wall Interactions

B-4 Statistical Confidence Limits

B-5 Effect of Turbine Base on Emergent Flight Paths

APPENDIX B-1 - SPECIAL ROUTINE FOR CYLINDRICAL CELLS

A special procedure is required for the cylindrical surface of the containment and the MSR's. Once the missile is located within a fictitious cell which encloses the containment or an MSR, the time required for the missile to reach the containment or MSR surface is calculated. The resulting equation for containment interaction is a quadratic whose discriminant, D, is

$$D = \left\{ \left(X-X_C\right)\dot{X} + \left(Y-Y_C\right)\dot{Y} \right\}^2 - \left(\dot{X}^2+\dot{Y}^2\right)\left\{\left(X-X_C\right)^2 + \left(Y-Y_C\right)^2 - R^2\right\} \qquad \text{B1-1}$$

where

X, Y	= horizontalcoordinatesofmissile
$\dot{X}, \dot{Y}$	= horizontal velocity components
X_C, Y_C	= coordinates of center of cylinder
R	= radius of cylinder

A negative discriminant indicates that the missile does not strike the containment. A positive discriminant permits solution for the time of interaction as the minimum positive value of

$$T = \frac{-(X-X_C)\dot{X} - (Y-Y_C)\dot{Y} \pm \sqrt{D}}{\dot{X}^2 + \dot{Y}^2} \qquad \text{B1-2}$$

Substitution of this T value in the component velocity equation locates the interaction point. The barrier interaction portion then either indicates penetration or returns the ricochet normal velocity and the angle of obliquity (angle of missile emergence with surface normal). The trace is stopped if the containment is penetrated.

From the normal ricochet velocity, V_{ne}, and the exit angle of obliquity, θ_e, the exit velocity components are specified as

$$\dot{X}_e = \frac{X-X_c}{R} Q - \dot{X}_i M$$

$$\dot{Y}_e = \frac{Y-Y_c}{c} Q - \dot{Y}_i M \qquad \text{B1-3}$$

$$\dot{Z}_e = M\dot{Z}_i$$

where

$$Q = V_{ne} \left\{ 1 + \frac{\tan\theta_e V_{ni}}{\sqrt{\dot{X}_i^2 + \dot{Y}_i^2 + \dot{Z}_i} \quad \sin\theta_i} \right\} \qquad \text{B1-4}$$

$$M = \frac{V_{ne} \tan\theta_e}{\sqrt{\dot{X}_i^2 + \dot{Y}_i^2 + \dot{Z}_i^2} \quad \sin\theta_i}$$

X, Y	= coordinates of strikepoint
X_c, Y_c	= coordinates of center of cylinder
V_{ni}	= incident normal velocity
θ_i	= incident angle of obliquity
$\dot{X}_i, \dot{Y}_i, \dot{Z}_i$	= incident velocity components

The moisture-separator reheaters are modeled in a similar manner but the X and Z coordinates are interchanged in all the above relations.

APPENDIX B-2 - CONCRETE RICOCHET ENERGY

For concrete ricochet energy considerations, we start from a static situation, ignoring the dynamic effects (i.e., stress waves engendered in both the steel and concrete) and we assume that the stress deformation (hence elastic strain energy) is statically determinable. These same assumptions are inherent in the Hagg-Sankey formulation for steel. There are three sources of elastic energy stored at the time the missile comes to rest.

These are:

(1) Elastic strain energy in the missile itself.

(2) Elastic strain energy associated with the local (missile-interface) deformation of the concrete. (May include local shear as well as compression.)

(3) Elastic strain energy associated with the gross deflection of the conrete wall.

It is difficult to ascribe elastic behavior to concrete, and thus difficult to quantify elastic strain energy. In fact almost any deformation of concrete involves a permanent set*. Therefore, rather than attempt to calculate exact elastic strain energy for the concrete, we estimate an upper limit on that portion of the concrete "elastic strain energy" which can be converted to kinetic energy in the ricocheting missile.

---

*See for example A.P. Mills, et al., Materials of Construction, John Wiley & Sons, New York, NY, 1955.

We assume an average modulus of elasticity for structural grade concrete of 3×10^6 psi. Therefore, consider the local strain energy in the concrete and that in the steel as the steel missile comes to rest after having crushed the concrete (i.e., stressed the interface to the σ_c value).

Figure B2-1 is an idealized case of a rectangular parallelepiped missile impinging on the concrete on one of its flat surfaces.

On the contacting surface the pressure is assumed to be σ_c; on the free surface, it has to be 0, of course. At any point in the materials local stress is proportional to local strain. To calculate the stored elastic strain energy at the time the missile has stopped, a stress distribution across the length L_c and L_s, as shown, must be assumed. In the absence of definitive data, it is assumed that stress is linear between 0 on the free surface and σ_c on the interface. Local energy stored is one-half the product of local stress: $\frac{X}{L}\sigma_c$, times local displacement; $\varepsilon dx = \frac{X}{L}\frac{\sigma_c}{E}dx$, where E is modulus of elasticity and X varies from 0 at the free face to D at interface. Therefore, concrete stored energy (neglecting the shear component) is

$$\xi = \frac{A\sigma_c^{\,2}}{2L^2E}\int_0^L X^2 dX \qquad \text{B2-1}$$

$$\xi = \frac{LA\sigma_c^{\,2}}{6\,E}$$

where A is the surface area in contact.

Since $E_c \approx 0.1E_s$, only one-tenth as much energy can be stored in a given thickness (L) of steel in the same thickness of concete, assuming both materials behave elastically. However, the stress distributions in both materials are purely hypothetical and it is not likely that stress will propagate as far from the disturbance in concrete as in steel, because of its more plastic response. Therefore, for concrete, an effective "length" of stress distribution which would be less than the actual depth, would seem more appropriate than the actual depth of the interacting member.

A similar analysis applies for shear, but it is even more difficult to ascribe an area of effective shear action in such a case. For purposes of this analysis, it has simply been assumed that the shear

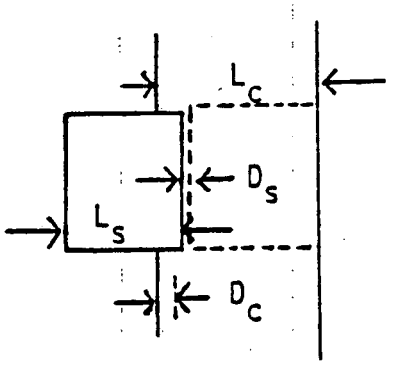

D_s = distortion in steel

D_c = distortion in concrete

Figure B2-1. Missile State at 0 Normal Velocity in the Concrete.

contributions to local elastic strain energy is equal to that of compression. Therefore, the total elastic strain energy is:

$$\xi = \frac{2LA\sigma_c^{\ 2}}{6E_c} + \frac{2L_sA\sigma_c^{\ 2}}{6E_s} \approx \frac{LA\sigma_c^{\ 2}}{3E_c} \qquad \text{B2-2}$$

where subscript s refers to the steel missiles.

A comparison with Calspan* measure ricochet velocities is contained in Table B2-1. The last column shows the values actually used in MISIP. It is obviously more conservative than the CALSPAN measured values. The values seem more conservative than needed. However, there are no tests at velocities at about 400 fps where many missile impacts occur. For this analysis, therefore, these conservative values are retained because of this fact and the fact that there is no mechanism in the ricochet analysis used to account for incident missile velocity. (Even though the Calspan tests show only a very weak correlation with impact velocity.)

*Vassallo, F.A., "Missile Impact Testing of Reinforced Concrete Panels," Calspan Report No. HC-5609-D-1, January 1975 (Prepared for Bechtel Corporation, San Francisco, California).

Table B2-1. Comparison of Measured and Calculated Ricochet Velocities.

Concrete Static Strength (psi)	Incident Velocity (ft/sec)	Concrete Thickness (in.)	Measured Rebound Velocity (ft/sec) [a]	Expected Rebound Velocity (ft/sec) [b]	Conservative Rebound Velocity (ft/sec) [c]
4950	337	18	10-15	12.7	16.4
4550	214	12	10	9.8	12.7
5770	122	12	4	12.1	15.7
4775	295	24	10	14	18.1
4500	377	24	15	13.2	17.1
4500	161	18	15	11.6	15

[a] These values are from Reference 8.

[b] Calculated with $\sigma_c\Big]_{dynamic}$ at an expected average for impact loading,*

$\sigma_c\Big]_{dynamic} = 1.55\sigma_c\Big]_{static}$.

[c] Calculated with $\sigma_c\Big]_{dynamic}$ used in the MIS code $= 2\sigma_c\Big]_{static}$.

This is a conservative approach and it also accounts for shear.

* Neville, A.M., Properties of Concrete, Sir Isaac Pitman & Sons, London, 1973, p. 303.

APPENDIX B-3 - MISSILE INTERACTIONS WITH STEEL BARRIERS

B3.1 PERFORATION

The Hagg-Sankey method[15] is utilized for interactions with steel walls. This method predicts steel wall perforation as a "two-phase" process. In the first phase wall resistance is affected only by local shear and compression. In the second phase the wall has had time to "stretch" in the plane of the wall, with tensile resistance also contributing. Perforation can occur in either phase. The equations involved are described below. The Hagg-Sankey formalism requires initially that M_2, the barrier mass which can be effectively accelerated along with the missile, be calculated. Its value is:

$$M_2 = \rho[A + 1.36\ \Phi\ (V_{ni})\ T\ \sqrt{A}]T \qquad \text{B3-1}$$

where

- ρ = density of steel (slugs/ft^3)
- A = effective impact area of missile (ft^2)
- T = barrier thickness (ft)
- V_{ni} = impact velocity component normal to barrier (fps)

$\Phi(V_{ni})$ is a function of impact velocity normal to the barrier which accounts for the distance in the wall from point of missile contact that is affected by the impact. From a private communication with Sankey, co-author of the method, we have derived the empirical relation

$$\Phi(V_{ni}) = \frac{2}{1-e^{.00138V_{ni}}} \qquad \text{B3-2}$$

which fits the measured results of Westinghouse on their turbine housing (which requires that Φ = 2 at 4000 fps, 3 at 800 fps, and 10 at 100 fps).

Also needed is the initial missile energy loss, ΔE_1, required to accommodate momentum conservation as M_2 is accelerated.

$$\Delta E_1 = \tfrac{1}{2} M_1 V_{ni}^2 \left(1 - \frac{M_1}{M - M_2}\right) \qquad \text{B3-3}$$

where M_1 is missile mass.

In order for Phase I failure to occur, ΔE_1 must exceed the effective strength of the barrier in local compression and shear ($E_c + E_s$).

$$E_c = AT\xi\sigma_d \qquad \text{B3-4}$$

$$E_s = K\tau_d PT^2 \qquad \text{B -5}$$

where

ξ = an effective compressive strain, (0.07)

σ_d = compressive yield strength (50,000 psi)

K = constant accounting for the amount of shear energy used

τ_d = the shear yield strength of the barrier

$$(K\tau_d = 0.27\sigma_d)$$

P = the periphery of the missile impact area.

Inserting appropriate constants and converting the ft-lb units, we have

E_c = 500 AT ft-lb

E_s = 4500 $A\sqrt{T}^2$ ft-lb

If ΔE_1 exceeds $E_c + E_s$, the barrier fails during the so-called Phase I and the missile has a residual normal velocity, V_{ne} given by[15]

$$V_{ne} = \frac{M_1 V_{ni}}{M_1 + M_2} + \sqrt{\left(\frac{M_1 V_{ni}}{M_1 + M_2}\right)^2 - \frac{2(E_c + E_s)\, m_3 - M_1 V_{ni}^2 (m_3 - M_1)}{(M_1 + M_2)(M_1 + m_2)}} \qquad \text{B3-6}$$

where

m_2 = the mass of the barrier having the same cross sectional area as the missile

$m_3 = M_2 - m_2$

If $E_c + E_s$ exceeds ΔE_1, then the tensile-strength phase or Phase II of the interaction ensues, and ΔE_2, the kinetic energy of the moving wall and missile which must be resisted by tensile strength in the barrier is determined.

The relations are

$$\Delta E_2 = \tfrac{1}{2} M_1 V_{ni}^2 \left(\frac{M_1}{M_1 + M_2}\right) \qquad \text{B3-7}$$

$$E_T = Q\xi_T\sigma_d \qquad \text{B3-8}$$

where

Q = the effective volume which can be stressed in tension (we assume it is approximately equal to the volume associated with M_2).

ξ_T = the effective tensile strain (0.05)

σ_d = the tensile ultimate strength (same as compression) in steel.

With appropriate constants,

$$E_T = \frac{208M_2}{\rho_{steel}}$$

If E_T exceeds ΔE_2 the breach of the barrier is prevented. If not, the missile exits with a velocity V_{ne} given by

$$V_{ne} = \sqrt{\left(\frac{M_1 V_{ni}}{M_1 + M_2}\right)^2 - \frac{2E_T}{M_1 + M_2}} \qquad \text{B3-9}$$

The missile is assumed to maintain its initial direction after perforation.

B3.2 RICOCHET OFF STEEL BARRIERS

The Hagg-Sankey formalism affords a means of calculating the ricochet conditions of a missile. We assume that the missile and wall mass, which initially move together at a velocity

$$V_2 = V_1 \left(\frac{M_1}{M_1 + M_2}\right),$$

are exactly reversed in direction as the wall reaches its maximum deflection and "unloads" in the approach direction. For perfectly elastic response this is true. Therefore, for non-perforation, or situations where no elastic limits have been exceeded, the exit normal velocity, V_{ne}, is given by

$$V_{ne} = -V_2$$

However, it is necessary to check that the elastic yield limit in compression, shear, and tension, as prescribed by Hagg and Sankey have not been exceeded. This means the kinetic energy of M_2 and M_1 moving together

$$E_K = \tfrac{1}{2} (M_1 + M_2) V_2^2 \qquad \text{B3-10}$$

does not exceed the elastic strain energy

$$E_E = \frac{A\, T\sigma_c^2}{2\, E_c} + \frac{PT^2\sigma_s^2}{2E_s} + \frac{M_2}{\rho steel} \quad \frac{\sigma_T^2}{2E_T}, \qquad \text{B3-11}$$

where

σ_c, σ_s, σ_T = elastic limit stress in compression, shear and tension, respectively

E_c, E_s, E_T = compression, shear, and tension moduli of elasticity, (previously defined).

If E_K exceeds E_E, V_{ne} is computed as

$$V_{ne} = \sqrt{\frac{2E_E}{M_1 + M_2}} \qquad \text{B3-12}$$

The direction after ricochet is determined by the same procedure that is used for concrete wall interactions (Section 2.4.1).

APPENDIX B-4 - STATISTICAL CONFIDENCE LIMITS

Adequacy of mathematical simulation of random events is established by calculating the confidence limits* given by**

$$p = \frac{x}{n} \pm z \left[x/n \left(1 - \frac{x}{n}\right) \Big/ n \right]^{\frac{1}{2}}$$

where

- n = number of trials
- x = number of times the event studied occurred in n trials
- p = the true probability of the event simulated
- z = value (+ and -) of the abscissa of the normal probability curve between which lies the area corresponding to the defined confidence.

For a 90 percent confidence, the normal probability distribution gives an abscissa of 1.65.

---

*Confidence limits specify the range of values such that the probability that the true value estimated lies within that range is equal to the confidence specified.

**Miller, I. and J.E. Freund, Probability and Statistics for Engineers, Prentice Hall, New York, NY, 1965.

APPENDIX B-5 - EFFECT OF TURBINE BASE ON EMERGENT FLIGHT PATHS

The effect of the turbine base on emergent flight paths apparently has never been analyzed before because of the complexity. In the missile hazard analysis described in this document, those missiles whose center of mass exits the turbine in the region of the base (0-to-42-inches above the turbine pedestal) are excluded. This exclusion is justified with aid of Figure B5-1.

In Figure B5-1 the missiles generated by the breakup of disc 2 are illustrated (2 of 4 sets for a 90° breakup). The disc sectors are located accurately in the radial dimension (prior to breakup). Location of blade ring fragments is assumed. The sizes of fragments are typical for all discs. It is obvious from the figure that only the smallest fragment could possibly exit the base region of the casing without interacting with one or both of the horizontal base plates on the top and bottom of this region. Such an exit is considered impossible for even the smallest fragment because it has a rotational component and could not maintain the precise orientation required to avoid these base plates during the perforation process. These base plates are heavy steel (three inches thick on top and six inches on bottom). Minimum width (on top) is eight inches. The bottom plates are much wider. These plates are separated by welded gusset plates and are also welded to the outer turbine casing. A missile exiting this region would have to tear these plates or separate them. The added energy required over that to perforate the casing is so great that the probability of emergence in this region is considered neglibible.

Researchers at Pacific Northwest Laboratory (PNL) of Battelle Memorial Institute report that they have also concluded that turbine missiles do not exit in the region of the base*.

---

*Spencer H. Bush, PNL, Private Communication, April 9, 1981

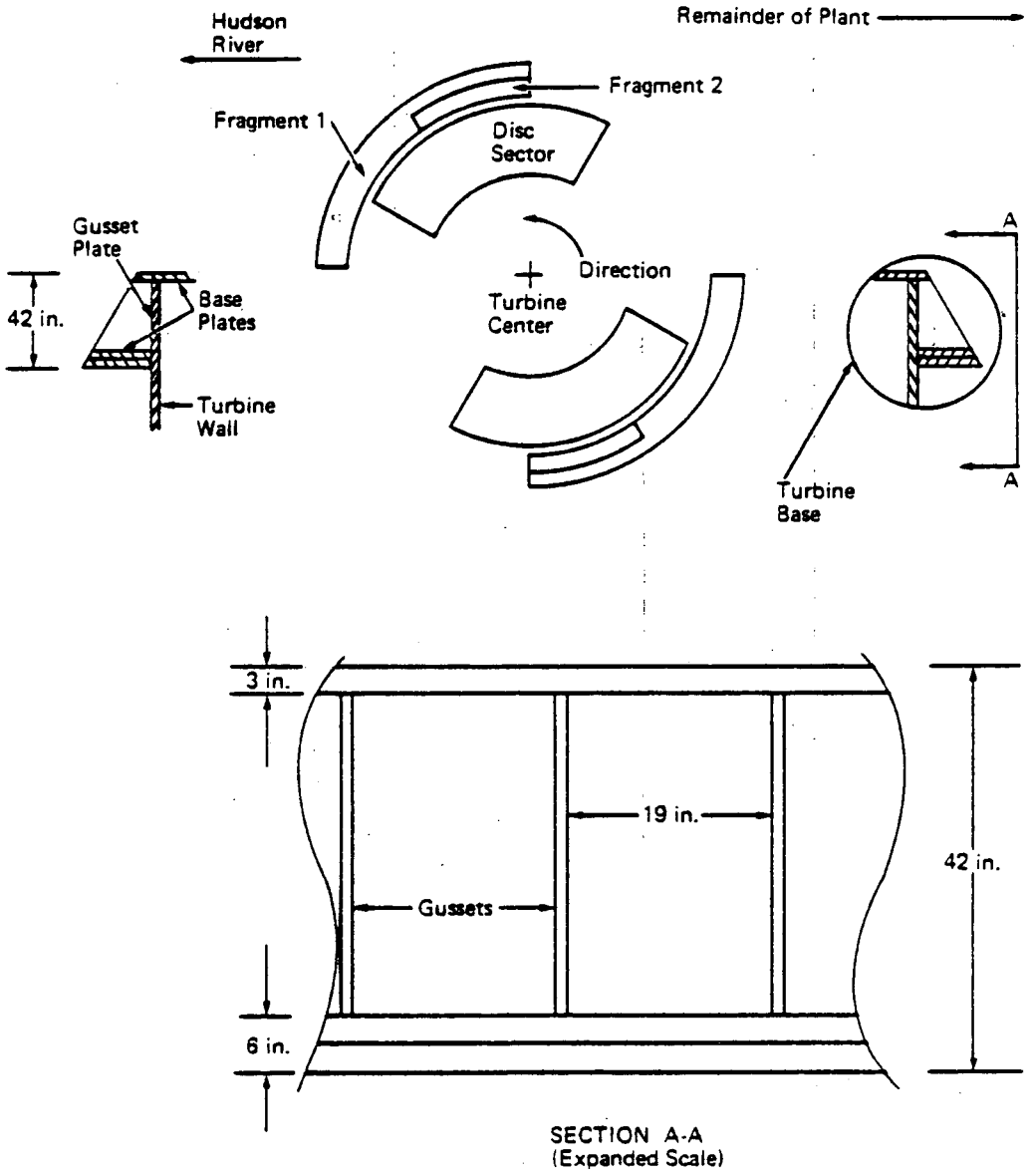

Figure B5-1. Disc and Blade Ring Fragments for Disc 2 Shown Relative to Turbine Base for Indian Point 3.

APPENDIX C - COMPUTER PRINTOUTS FOR MISIP

C-1 Computer Specifications of Indian Point 3

C-2 Sample Results

C-3 Indian Point 3 Plant Layout

APPENDIX C-1 - COMPUTER SPECIFICATIONS OF INDIAN POINT 3

Table C1-1 is a reproduction of the actual data used in the MISIP code for plant specification. Each line in the table represents one compartment (cell) of the plant. The first number listed is the room designator. For convenience, the rooms have been numbered consecutively from 1 to 529. Immediately following the room number either the letter "T" or "R" may appear for certain rooms. A "T" is used if the room is a safety target. An "R" is used if the room contains radioactive material, for example, waste holdup tanks. These latter rooms were not analyzed in this project because the aim was to determine the plant's ability to maintain a safety shutdown condition. They are included for possible future reference. The remaining numbers and designators are grouped in six sets, one set for each of the six walls of each compartment. The first number is the wall location (in feet) and the second is the wall thickness (in inches). The two letters which follow designate the wall material and plant exit characteristics.

The material designations are:

A - air
C - 4,000 psi concrete
D - dirt

The plant exit designations are:

R - roof exit
G - exit through floor slab
E - exit through an exterior wall below grade level
S - exit through x_{max} side of plant
N - exit through x_{min} side of plant
W - exit through y_{min} side of plant
T - exit through y_{max} side of plant

The containment wall is modeled to be 54 inches thick (concrete).

Table C1-1. Computer Specification of the Indian Point 3 Plant.

1	125.0	0.AL	476.0	0.AW	0.0	0.AS	34.0	0.A	14.0	36.DG	262.0	0.AR
2	125.0	0.AL	302.0	0.A	34.0	0.A	58.0	0.A	14.0	36.DG	262.0	0.AR
3	305.5	10.CE	326.5	10.CE	34.0	36.CE	49.0	10.CE	2.0	10.CG	14.0	24.C
4	330.0	0.A	476.0	0.AW	34.0	0.A	58.0	0.A	14.0	36.DG	262.0	0.AR
5	125.0	0.A	177.0	0.A	58.0	0.A	158.0	0.A	14.0	36.DG	262.0	0.AR
6	177.0	0.A	302.0	12.C	58.0	0.A	76.0	0.A	14.0	36.D	17.0	0.A
7	302.0	0.A	305.5	0.A	34.0	0.A	58.0	12.C	14.0	36.D	17.0	0.A
8	326.5	0.A	330.0	0.A	34.0	0.A	58.0	12.C	14.0	36.DG	17.0	0.A
9	302.0	12.C	330.0	12.C	58.0	12.C	76.0	12.C	14.0	1.S	17.0	0.A
10	302.0	0.A	330.0	0.A	58.0	0.A	76.0	0.A	17.0	0.A	262.0	0.AR
11	330.0	12.C	456.0	0.A	58.0	0.A	76.0	0.A	14.0	36.D	17.0	0.A
12	456.0	0.A	476.0	0.AW	58.0	0.A	339.0	0.A	14.0	36.DG	262.0	0.AR
13	330.0	0.A	456.0	0.A	76.0	0.A	185.0	0.A	14.0	36.D	262.0	0.AR
14	302.0	0.A	330.0	0.A	76.0	12.C	114.0	0.A	11.0	96.D	17.0	0.A
15	302.0	0.A	330.0	0.A	76.0	0.A	114.0	0.A	17.0	0.A	262.0	0.AR
16	177.0	0.A	302.0	0.A	76.0	0.A	185.0	0.A	14.0	36.D	262.0	0.AR
17	177.0	0.A	197.0	0.A	185.0	0.A	232.0	0.A	24.0	0.A	262.0	0.AR
18	197.0	12.C	456.0	12.C	185.0	12.C	232.0	18.C	14.0	36.D	15.0	12.C
19	197.0	0.AE	456.0	0.AE	185.0	0.AE	232.0	12.C	12.0	0.AG	14.0	999.D
20	197.0	0.A	456.0	0.A	185.0	0.A	232.0	0.A	15.0	12.C	67.0	0.A
21	197.0	0.A	456.0	0.A	185.0	0.A	232.0	0.A	67.0	0.A	262.0	0.AR
22	177.0	10.CE	456.0	10.CE	232.0	12.C	339.0	10.CE	12.0	8.CG	15.0	0.A
23	177.0	0.A	456.0	0.A	232.0	0.A	339.0	10.CE	15.0	0.A	18.0	0.A
24	261.0	48.C	377.4	48.C	267.5	109.C	303.5	109.C	43.0	0.A	53.0	6.C
25	177.0	0.A	261.0	0.A	232.0	0.A	250.8	0.A	53.0	6.C	64.0	0.A
26	177.0	0.A	261.0	0.	250.8	0.A	259.8	0.A	53.0	6.C	64.0	0.A
27	177.0	0.A	261.0	0.A	259.8	0.A	311.0	0.A	53.0	6.C	64.0	0.A
28	177.0	0.A	261.0	0.	311.0	0.A	320.0	0.A	53.0	6.C	64.0	0.A
29	177.0	0.A	261.0	0.A	320.0	0.A	339.0	0.A	53.0	6.C	64.0	0.A
30	261.0	0.A	298.0	0.A	232.0	0.A	243.7	0.A	53.0	6.C	64.0	0.A
31	261.0	0.A	298.0	0.	243.7	0.A	250.8	0.	53.0	6.C	64.0	0.A
32	261.0	0.	298.0	0.	250.8	0.	259.8	0.	53.0	6.C	64.0	0.A
33	261.0	0.A	298.0	0.A	259.8	0.	270.0	0.A	53.0	0.A	64.0	0.A
34	261.0	0.A	298.0	0.A	301.0	0.A	311.0	0.	53.0	0.A	64.0	0.A
35	261.0	0.	298.0	0.	311.0	0.	320.0	0.	53.0	6.C	64.0	0.A
36	261.0	0.A	298.0	0.	320.0	0.	327.0	0.A	53.0	6.C	64.0	0.A
37	261.0	0.A	298.0	0.A	327.0	0.A	339.0	0.A	53.0	6.C	64.0	0.A
38	298.0	0.A	337.4	0.A	232.0	0.A	243.7	0.	53.0	6.C	64.0	0.A
39	298.0	0.	337.4	0.	243.7	0.	252.7	0.	53.0	6.C	64.0	0.A
40	298.0	0.	337.4	0.	252.7	0.	259.8	0.A	53.0	6.C	64.0	0.A
41	298.0	0.A	337.4	0.A	259.8	0.A	270.0	0.A	53.0	6.C	64.0	0.A
42	298.0	0.A	337.4	0.A	301.0	0.A	311.0	0.A	53.0	6.C	64.0	0.A
43	298.0	0.	337.4	0.	311.0	0.A	318.0	0.	53.0	6.C	64.0	0.A
44	298.0	0.	337.4	0.	318.0	0.	327.0	0.	53.0	6.C	64.0	0.A
45	298.0	0.A	337.4	0.A	327.0	0.	339.0	0.A	53.0	6.C	64.0	0.A
46	337.4	0.A	377.4	0.A	232.0	0.A	243.7	0.A	53.0	6.C	64.0	0.A
47	337.4	0.	377.4	0.A	243.7	0.A	250.8	0.	53.0	6.C	64.0	0.A
48	337.4	0.	377.4	0.	250.8	0.	259.8	0.	53.0	6.C	64.0	0.A
49	337.4	0.A	377.4	0.A	259.8	0.	270.0	0.A	53.0	0.A	64.0	0.A
50	337.4	0.A	377.4	0.A	301.0	0.A	311.0	0.	53.0	0.A	64.0	0.A
51	337.4	0.	377.4	0.	311.0	0.	320.0	0.	53.0	6.C	64.0	0.A
52	337.4	0.	377.4	0.A	320.0	0.	327.0	0.A	53.0	6.C	64.0	0.A
53	337.4	0.A	377.4	0.A	327.0	0.A	339.0	0.A	53.0	6.C	64.0	0.A
54	377.4	0.A	456.0	0.A	232.0	0.A	250.8	0.A	53.0	6.C	64.0	0.A
55	377.4	0.	456.0	0.A	250.8	0.A	259.8	0.A	53.0	6.C	64.0	0.A
56	377.4	0.A	456.0	0.A	259.8	0.A	311.0	0.A	53.0	6.C	64.0	0.A
57	377.4	0.	456.0	0.A	311.0	0.A	320.0	0.A	53.0	6.C	64.0	0.A
58	377.4	0.A	456.0	0.A	320.0	0.A	339.0	0.A	53.0	6.C	64.0	0.A
59	177.0	0.A	456.0	0.A	232.0	0.A	339.0	0.A	64.0	0.A	134.0	0.A

Table C1-1. Computer Specification of the Indian Point 3 Plant (Continued).

60	177.0	0.A	456.0	0.A	232.0	0.A	339.0	0.A	134.0	0.A	262.0	0.AR
61	310.0	0.A	442.0	0.A	339.0	0.A	385.0	0.A	18.0	36.D	262.0	0.AR
62	397.0	0.A	442.0	0.A	385.0	0.A	464.0	0.A	18.0	36.D	262.0	0.AR
63	397.0	0.A	406.0	0.A	480.0	0.A	500.0	144.CE	18.0	36.D	33.0	0.A
64T	397.0	0.A	442.0	0.A	480.0	0.A	500.0	144.CE	33.0	0.A	43.0	12.C
65	397.0	0.A	442.0	0.A	464.0	0.A	500.0	144.CE	54.0	20.C	72.0	0.A
66	397.0	0.A	442.0	0.A	464.0	0.A	500.0	0.A	72.0	0.A	262.0	0.AR
67T	442.0	18.C	453.0	15.C	482.0	0.A	500.0	0.AE	33.0	20.CG	43.0	12.C
68	442.0	0.A	453.0	0.A	464.0	0.A	500.0	0.A	54.0	20.C	262.0	0.AR
69	453.0	15.C	476.0	999.DE	464.0	0.A	500.0	999.DE	33.0	36.DG	43.0	999.DG
70	453.0	0.A	476.0	0.AW	464.0	0.A	500.0	0.A	43.0	36.D	262.0	0.AR
71	453.0	0.AE	476.0	0.AW	500.0	0.A	540.0	0.AE	43.0	36.DG	50.0	0.A
72	453.0	15.C	476.0	0.AW	500.0	0.A	540.0	0.AE	50.0	0.A	62.0	0.A
73	453.0	0.A	476.0	0.AW	500.0	0.A	540.0	0.AE	62.0	0.A	68.0	0.A
74	453.0	0.A	476.0	0.AW	500.0	0.A	538.0	0.A	68.0	0.A	262.0	0.AR
75	453.0	15.C	476.0	0.AW	540.0	0.A	552.0	0.AE	68.0	0.AG	80.0	0.A
76	453.0	0.A	476.0	0.AW	540.0	0.A	552.0	0.A	80.0	0.A	262.0	0.AR
77	442.0	0.A	453.0	15.C	540.0	36.D	552.0	18.C	68.0	20.C	80.0	20.C
78	442.0	0.A	453.0	0.A	540.0	0.A	552.0	0.A	80.0	20.C	262.0	0.AR
79	397.0	80.A	442.0	80.A	540.0	18.C	552.0	18.C	68.0	20.C	80.0	20.C
80	397.0	24.C	442.0	0.A	540.0	0.A	552.0	0.A	80.0	20.C	116.0	0.A
81	397.0	0.A	442.0	0.A	540.0	0.A	552.0	0.A	116.0	0.A	262.0	0.AR
82	397.0	48.C	442.0	0.A	500.0	0.A	540.0	18.C	72.0	36.DG	80.0	0.A
83	397.0	10.C	442.0	0.A	500.0	0.A	540.0	0.A	80.0	0.A	116.0	0.A
84	397.0	0.A	442.0	0.A	500.0	0.A	540.0	0.A	116.0	0.A	262.0	0.A
85T	442.0	18.CE	453.0	0.A	500.0	0.A	540.0	0.AE	50.0	20.C	62.0	20.C
86	442.0	18.CE	453.0	0.A	500.0	0.A	540.0	0.AE	62.0	20.C	68.0	0.A
87	442.0	18.CE	453.0	0.A	500.0	0.A	538.0	0.A	68.0	0.A	72.0	0.A
88	442.0	0.A	453.0	0.A	500.0	0.A	540.0	0.A	72.0	0.A	262.0	0.AR
89	287.0	54.C	310.0	36.C	406.0	0.A	478.0	36.CE	46.0	36.CG	51.0	0.A
90T	287.0	54.C	310.0	36.C	406.0	0.A	500.0	36.C	34.0	12.CG	51.0	12.C
91	287.0	0.A	310.0	0.A	406.0	0.A	478.0	0.A	73.0	30.C	262.0	0.A
92	287.0	0.A	310.0	36.C	385.0	0.A	406.0	0.A	46.0	36.CG	63.0	12.C
93	287.0	0.A	310.0	0.A	385.0	0.A	406.0	0.A	63.0	10.C	262.0	0.AR
94	258.0	48.C	287.0	0.A	385.0	48.C	406.0	54.C	46.0	36.C	63.0	18.C
95	258.0	0.A	287.0	0.A	385.0	0.A	406.0	0.A	63.0	10.C	262.0	0.AR
96	240.0	0.A	258.0	48.C	385.0	12.C	406.0	54.C	18.0	9.CG	33.0	24.C
97	240.0	0.A	258.0	48.C	385.0	12.C	406.0	66.C	33.0	24.C	43.0	24.C
98	240.0	0.A	258.0	48.C	385.0	0.A	406.0	0.A	43.0	24.C	46.0	0.A
99T	240.0	0.A	258.0	0.A	385.0	0.A	406.0	0.A	46.0	0.A	80.0	0.A
100T	189.0	0.A	240.0	0.A	385.0	48.C	406.0	0.A	18.0	9.CG	33.0	24.C
101T	189.0	12.C	240.0	0.A	385.0	48.C	406.0	66.C	33.0	24.C	43.0	24.C
102T	189.0	0.A	214.5	0.A	385.0	48.C	406.0	0.A	43.0	24.C	80.0	0.A
103	189.0	0.A	240.0	0.A	385.0	0.A	406.0	0.A	80.0	0.A	262.0	0.AR
104	152.0	0.A	189.0	0.A	373.0	0.A	406.0	0.A	18.0	9.CG	33.0	0.A
105	152.0	0.A	189.0	0.A	373.0	0.A	406.0	0.A	33.0	0.A	43.0	0.A
106	152.0	0.A	189.0	0.A	373.0	0.A	406.0	0.A	80.0	0.A	262.0	0.AR
107	310.0	0.A	320.0	0.A	385.0	0.A	500.0	0.A	73.0	0.A	262.0	0.AR
108	143.0	0.A	152.0	0.A	373.0	0.A	406.0	0.A	18.0	36.DG	262.0	0.AR
109	125.0	0.A	143.0	0.A	373.0	0.A	406.0	0.A	18.0	36.DG	262.0	0.AR
110	199.0	0.A	310.0	0.A	339.0	0.A	371.0	0.A	18.0	36.D	262.0	0.AR
111	189.0	0.A	240.0	0.A	373.0	0.A	385.0	48.C	18.0	36.D	80.0	0.A
112	189.0	0.A	240.0	0.A	373.0	0.A	385.0	0.A	80.0	0.A	262.0	0.AR
113	240.0	0.A	256.0	0.A	373.0	0.A	385.0	12.C	18.0	0.A	43.0	0.A
114	240.0	0.A	258.0	0.A	373.0	0.A	385.0	0.A	43.0	0.A	262.0	0.AR
115	258.0	0.A	310.0	0.A	373.0	0.A	385.0	144.CE	18.0	36.D	46.0	0.A
116	258.0	0.A	310.0	0.A	373.0	0.A	385.0	36.C	46.0	0.A	63.0	0.A
117	258.0	0.A	310.0	0.A	373.0	0.A	385.0	0.A	63.0	0.A	262.0	0.AR
118	125.0	0.A	143.0	0.A	406.0	0.A	550.0	0.AE	18.0	0.A	79.0	0.A
119	125.0	0.AL	143.0	0.A	406.0	0.A	550.0	0.A	79.0	36.DG	262.0	0.AR

Table C1-1. Computer Specification of the Indian Point 3 Plant (Continued).

120	143.0	0.AE	258.0	0.A	406.0	0.A	550.0	0.AE	43.0	108.CG	79.0	0.A
121	143.0	0.A	258.0	0.A	406.0	0.A	550.0	0.A	79.0	0.A	262.0	0.AR
122	258.0	0.A	287.0	0.AE	406.0	0.A	500.0	0.A	43.0	108.CG	46.0	0.A
123	258.0	0.A	287.0	54.C	406.0	0.A	500.0	0.A	46.0	0.A	262.0	0.AR
124	258.0	0.A	287.0	0.AE	500.0	0.A	550.0	0.AE	43.0	108.CG	51.0	0.A
125	258.0	0.A	287.0	0.A	500.0	0.A	550.0	0.AE	51.0	0.A	79.0	0.A
126	258.0	0.A	287.0	0.A	500.0	0.A	550.0	0.A	79.0	0.A	262.0	0.AR
127T	287.0	0.A	310.0	0.A	540.0	0.A	550.0	36.CE	51.0	12.CG	73.0	42.C
128	287.0	0.A	310.0	0.A	540.0	0.A	550.0	0.A	73.0	42.C	262.0	0.AR
129T	287.0	54.C	310.0	36.C	406.0	0.A	452.0	0.A	51.0	0.A	73.0	12.C
130T	287.0	0.A	310.0	36.C	500.0	36.C	540.0	0.A	51.0	12.CG	73.0	42.C
131	287.0	0.A	310.0	0.A	500.0	0.A	540.0	0.A	73.0	42.C	262.0	0.AR
132	310.0	36.C	320.0	24.C	500.0	0.A	540.0	0.A	51.0	36.DG	80.0	0.A
133	310.0	36.C	320.0	10.C	500.0	0.A	540.0	0.A	80.0	0.A	98.0	0.A
134	310.0	0.A	320.0	0.A	500.0	0.A	540.0	0.A	98.0	0.A	262.0	0.AR
135T	310.0	36.C	320.0	36.C	540.0	36.C	550.0	0.A	51.0	12.CG	73.0	12.C
136	310.0	0.A	320.0	24.C	540.0	0.A	550.0	0.A	73.0	12.C	116.0	0.A
137	310.0	0.A	320.0	0.A	540.0	0.A	550.0	0.A	116.0	0.A	262.0	0.AR
138	310.0	36.C	320.0	36.CE	550.0	0.A	561.0	36.CE	51.0	12.CG	73.0	42.C
139	310.0	0.A	320.0	24.C	550.0	0.A	561.0	36.DE	73.0	42.C	79.0	0.A
140	310.0	0.A	320.0	24.C	550.0	0.A	561.0	0.A	79.0	0.A	116.0	0.A
141	310.0	0.A	320.0	0.A	550.0	0.A	561.0	0.A	116.0	0.A	262.0	0.AR
142	310.0	0.A	320.0	30.C	561.0	0.A	604.0	0.A	79.0	36.DG	98.0	0.A
143	310.0	0.A	320.0	24.C	561.0	0.A	604.0	0.A	98.0	0.A	116.0	0.A
144	310.0	0.A	320.0	0.A	561.0	0.A	604.0	0.A	116.0	0.A	262.0	0.AR
145	125.0	0.AL	320.0	10.C	604.0	0.A	664.0	0.A	79.0	36.DG	98.0	0.A
146	125.0	0.AL	320.0	0.A	604.0	0.A	664.0	0.A	98.0	0.A	262.0	0.AR
147	213.0	0.A	255.0	0.A	550.0	0.A	604.0	0.A	81.0	0.A	136.0	0.A
148	213.0	0.A	255.0	0.A	550.0	0.A	604.0	0.A	136.0	0.A	262.0	0.AR
149	287.0	0.A	310.0	0.A	550.0	0.A	604.0	0.A	79.0	10.CG	136.0	0.A
150	287.0	0.A	310.0	0.A	550.0	0.A	604.0	0.A	136.0	0.A	262.0	0.AR
151	143.0	0.A	213.0	0.A	550.0	0.A	604.0	0.A	79.0	36.DG	262.0	0.AR
152	125.0	0.AL	143.0	0.A	550.0	0.A	604.0	0.A	79.0	36.DG	262.0	0.AR
153	397.0	0.A	476.0	0.AW	664.0	0.A	681.0	0.A	79.0	36.DG	262.0	0.AR
154	436.0	0.A	476.0	0.AW	681.0	0.A	724.0	0.A	79.0	36.DG	262.0	0.AR
155	425.0	0.A	476.0	0.AW	724.0	0.A	756.0	0.A	79.0	36.DG	262.0	0.AR
156T	397.0	0.A	436.0	0.A	681.0	0.A	724.0	0.A	79.0	24.CG	129.0	0.A
157	397.0	0.A	436.0	0.A	681.0	0.A	724.0	0.A	129.0	0.A	262.0	0.AR
158	397.0	0.A	425.0	0.A	724.0	0.A	756.0	0.A	79.0	24.CG	122.0	0.A
159	397.0	0.A	425.0	0.A	724.0	0.A	756.0	0.A	122.0	0.A	262.0	0.AR
160	397.0	0.A	453.0	0.A	600.0	0.A	664.0	0.A	72.0	36.D	262.0	0.AR
161	177.0	36.DE	456.0	36.DE	76.0	36.DE	185.0	36.DE	8.0	36.DG	14.0	36.D
162	177.0	36.DE	301.0	36.DE	49.0	36.DE	76.0	36.D	8.0	36.DG	14.0	36.D
163	301.0	36.DE	331.0	36.DE	49.0	36.DE	58.0	36.DE	8.0	36.DG	14.0	36.D
164	331.0	36.DE	456.0	36.DE	49.0	36.DE	76.0	36.D	8.0	36.DG	14.0	36.D
165	173.0	0.A	189.0	0.A	373.0	0.A	385.0	0.A	53.0	0.A	80.0	0.A
166	125.0	36.DE	310.0	36.DE	339.0	36.DE	373.0	36.D	12.0	36.DG	18.0	36.D
167	189.0	36.D	310.0	36.D	373.0	36.D	385.0	36.DE	12.0	36.DG	18.0	36.D
168	397.0	36.DE	476.0	36.DE	552.0	36.DE	681.0	36.DE	66.0	36.DG	72.0	36.D
169	125.0	36.DE	397.0	36.DE	664.0	36.DE	756.0	36.DE	73.0	36.DG	79.0	36.D
170	261.0	0.A	377.4	0.A	270.0	0.A	301.0	0.A	53.0	0.A	64.0	0.A
171	261.0	0.A	377.4	0.A	232.0	0.A	267.5	109.C	43.0	0.A	53.0	6.C
172	261.0	0.A	377.4	0.A	303.5	109.C	339.0	0.A	43.0	0.A	53.0	6.C
173	177.0	0.A	456.0	0.A	232.0	0.A	339.	0.A	18.0	0.A	43.0	6.C
174	177.0	0.A	261.0	0.A	232.0	0.A	267.5	0.A	43.0	0.A	53.0	0.A
175	377.4	48.C	456.0	0.A	232.0	0.A	339.0	0.A	43.0	0.A	53.0	6.C
176T	213.0	0.A	255.0	0.A	550.0	0.A	604.0	0.A	79.0	10.CG	81.0	0.A
177	255.0	0.A	287.0	0.A	550.0	0.A	604.0	0.A	79.0	10.CG	136.0	0.A
178	255.0	0.A	287.0	0.A	550.0	0.A	604.0	0.A	136.0	0.A	262.0	0.AR
179	397.0	0.A	453.0	0.A	552.0	0.A	600.0	0.A	72.0	36.D	95.0	0.A

Table C1-1. Computer Specification of the Indian Point 3 Plant (Continued).

180	397.0	0.A	453.0	0.A	552.0	0.A	600.0	0.A	95.0	0.A	262.0	0.AR
181	406.0	0.A	426.0	0.A	480.0	0.A	500.0	144.CE	18.0	36.D	33.0	0.A
182	426.0	0.A	442.0	18.CE	480.0	0.A	500.0	144.CE	18.0	36.D	33.0	0.A
183	397.0	0.A	442.0	18.CE	464.0	0.A	480.0	0.A	18.0	36.D	33.0	0.A
184T	397.0	0.A	442.0	0.A	480.0	0.A	500.0	144.CE	43.0	12.C	54.0	20.C
185T	442.0	18.C	453.0	15.C	482.0	0.A	500.0	0.AE	43.0	12.C	54.0	20.C
186	397.0	0.A	442.0	18.C	464.0	0.A	480.0	0.A	33.0	0.A	54.0	0.A
187	152.0	0.A	189.0	0.A	373.0	0.A	406.0	0.A	43.0	0.A	53.0	0.A
188	125.0	0.A	197.0	0.A	339.0	0.A	373.0	0.A	18.0	36.D	43.0	0.A
189	125.0	0.A	177.0	0.A	339.0	0.A	373.0	0.A	43.0	0.A	53.0	0.A
190	125.0	0.A	197.0	0.A	339.0	0.A	373.0	0.A	53.0	0.A	262.0	0.AR
191	177.0	0.A	197.0	0.A	339.0	0.A	373.0	0.A	43.0	0.A	53.0	0.A
192	177.0	0.A	261.0	48.C	267.5	0.A	303.5	0.A	43.0	0.A	53.0	6.C
193	177.0	0.A	197.0	0.A	303.5	0.A	339.0	0.A	43.0	0.A	53.0	6.C
194	197.0	0.A	261.0	0.A	303.5	0.A	339.0	0.A	43.0	0.A	53.0	0.A
195	305.5	0.A	326.5	0.A	34.0	0.A	53.0	0.A	22.0	0.A	262.0	0.AR
196	125.0	0.A	177.0	0.A	232.0	0.A	339.0	0.A	14.0	36.DG	262.0	0.AR
197T	125.0	0.A	177.0	0.A	158.0	0.A	232.0	0.A	14.0	36.DG	24.0	0.A
198T	177.0	0.A	197.0	0.A	185.0	0.A	232.0	0.A	14.0	36.DG	24.0	0.A
199	453.0	0.A	476.0	0.AW	552.0	0.A	664.0	0.A	72.0	36.D	262.0	0.AR
200T	258.0	36.DE	310.0	0.A	385.0	36.DE	388.0	36.DE	12.5	36.DG	15.0	36.D
201T	310.0	0.A	332.0	36.DE	385.0	36.DE	388.0	36.DE	12.5	36.DG	15.0	36.D
202T	329.0	36.DE	332.0	36.DE	388.0	36.DE	403.0	36.DE	12.5	36.DG	15.0	36.D
203T	332.0	0.A	424.0	0.A	400.0	36.DE	403.0	36.DE	12.5	36.DG	15.0	36.D
204T	424.0	36.DE	427.0	36.DE	378.0	36.DE	403.0	36.DE	12.5	36.DG	15.0	36.D
205T	427.0	0.A	442.0	36.DE	378.0	36.DE	381.0	36.DE	12.5	36.DG	15.0	36.D
206	258.0	36.DE	310.0	0.A	385.0	36.DE	388.0	36.DE	15.0	36.D	18.0	36.D
207	310.0	0.A	332.0	36.DE	385.0	36.DE	388.0	36.DE	15.0	36.D	18.0	36.D
208	329.0	36.DE	332.0	36.DE	388.0	36.DE	403.0	36.DE	15.0	36.D	18.0	36.D
209	332.0	0.A	424.0	0.A	400.0	36.DE	403.0	36.DE	15.0	36.D	18.0	36.D
210	424.0	36.DE	427.0	36.DE	378.0	36.DE	403.0	36.DE	15.0	36.D	18.0	36.D
211	427.0	0.A	442.0	36.DE	378.0	36.DE	381.0	36.DE	15.0	36.D	18.0	36.D
212	197.0	0.A	199.0	0.A	339.0	0.A	373.0	0.A	18.0	36.D	43.0	0.A
213T	197.0	0.A	199.0	0.A	339.0	0.A	373.0	0.A	43.0	0.A	45.0	0.A
214	197.0	0.A	199.0	0.A	339.0	0.A	373.0	0.A	45.0	0.A	262.0	0.AR
215	199.0	0.A	256.0	0.A	371.0	0.A	373.0	0.A	18.0	36.D	43.0	0.A
216T	199.0	0.A	258.0	0.A	371.0	0.A	373.0	0.A	43.0	0.A	45.0	0.A
217	199.0	0.A	258.0	0.A	371.0	0.A	373.0	0.A	45.0	0.A	262.0	0.AR
218T	256.0	0.A	258.0	0.A	371.0	0.A	373.0	0.A	18.0	36.D	43.0	0.A
219	258.0	0.A	310.0	0.A	371.0	0.A	373.0	0.A	18.0	36.D	262.0	0.AR
220T	256.0	0.A	258.0	0.A	373.0	0.A	385.0	12.C	18.0	36.D	20.0	0.A
221	256.0	0.A	258.0	0.A	373.0	0.A	385.0	12.C	20.0	0.A	43.0	0.A
222	442.0	0.A	476.0	0.AW	538.0	0.A	540.0	36.D	68.0	0.A	72.0	0.A
223	397.0	0.A	442.0	0.A	538.0	36.DG	540.0	18.C	68.0	36.DG	72.0	0.A
224	453.0	0.A	476.0	0.AW	538.0	0.A	540.0	0.A	72.0	0.A	262.0	0.AR
225	287.0	54.C	310.0	36.C	478.0	36.C	489.0	12.C	73.0	42.C	91.0	12.C
226T	287.0	54.C	298.5	0.A	452.0	0.A	500.0	36.C	51.0	12.C	73.0	12.C
227T	298.5	0.A	310.0	36.C	452.0	0.A	500.0	36.C	51.0	12.C	73.0	12.C
228	287.0	0.A	310.0	0.A	478.0	0.A	489.0	0.A	91.0	12.C	262.0	0.AR
229	287.0	0.A	310.0	0.A	489.0	12.C	500.0	0.A	73.0	12.C	91.0	0.A
230	287.0	0.A	310.0	0.A	489.0	0.A	500.0	0.A	91.0	0.A	262.0	0.AR
231	240.0	0.A	258.0	0.A	385.0	0.A	406.0	0.A	80.0	0.A	262.0	0.AR
232T	214.5	0.A	240.0	0.A	385.0	48.C	406.0	54.C	43.0	24.C	80.0	0.A
233T	173.0	0.A	189.0	0.A	385.0	0.A	406.0	0.A	53.0	0.A	80.0	0.A
234	152.0	0.A	173.0	0.A	385.0	0.A	406.0	0.A	53.0	0.A	80.0	0.A
235T	320.0	24.CE	339.0	24.C	490.0	24.C	539.0	24.C	15.0	36.DG	31.0	24.C
236T	339.0	24.C	354.0	24.C	490.0	24.C	539.0	24.C	15.0	36.DG	31.0	24.C
237	354.0	24.C	369.0	0.A	490.0	0.A	500.0	0.A	18.0	36.DG	31.0	0.A
238	354.0	24.C	369.0	48.C	500.0	0.A	516.0	0.A	15.0	36.DG	31.0	24.C
239	354.0	24.C	369.0	0.A	516.0	0.A	529.0	0.A	15.0	36.DG	31.0	24.C

Table C1-1. Computer Specification of the Indian Point 3 Plant (Continued).

240	354.0	24.C	369.0	0.A	529.0	0.A	539.0	0.A	15.0	36.DG	31.0	24.C
241	369.0	0.A	397.0	0.AE	490.0	0.A	500.0	48.C	18.0	36.DG	31.0	0.A
242R	369.0	48.C	397.0	48.CE	500.0	48.C	516.0	48.C	15.0	36.DG	31.0	48.C
243	369.0	0.A	378.0	24.C	516.0	48.C	529.0	0.A	15.0	36.DG	31.0	48.C
244	369.0	0.A	378.0	0.A	529.0	0.A	550.0	0.A	15.0	36.DG	31.0	48.C
245R	378.0	24.C	397.0	24.CE	516.0	48.C	529.0	24.C	15.0	36.DG	31.0	48.C
246	378.0	0.A	388.0	18.C	529.0	24.C	550.0	48.C	15.0	36.DG	31.0	48.C
247	388.0	18.C	397.0	24.CE	529.0	24.C	550.0	48.C	15.0	36.DG	31.0	48.C
248	320.0	24.CE	342.0	0.A	539.0	24.C	550.0	24.C	15.0	36.DG	31.0	24.C
249T	320.0	24.CE	342.0	24.C	550.0	24.C	560.0	24.C	15.0	36.DG	31.0	24.C
250T	320.0	24.CE	342.0	24.C	560.0	24.C	570.0	24.C	15.0	36.DG	31.0	24.C
251T	320.0	24.CE	342.0	24.C	570.0	24.C	578.0	24.C	15.0	36.DG	31.0	24.C
252T	320.0	24.CE	342.0	24.C	578.0	24.C	588.0	24.CE	15.0	36.DG	31.0	24.C
253	342.0	0.A	354.0	0.A	539.0	24.C	550.0	0.A	15.0	36.DG	31.0	24.C
254	342.0	24.C	354.0	24.C	550.0	0.A	569.0	0.A	15.0	36.DG	31.0	24.C
255	354.0	0.A	369.0	0.A	539.0	0.A	550.0	24.C	15.0	36.DG	31.0	24.C
256R	354.0	24.C	369.0	24.C	550.0	24.C	569.0	24.C	15.0	36.DG	31.0	24.C
257R	354.0	42.C	369.0	0.A	569.0	24.C	577.0	33.C	15.0	36.DG	31.0	24.C
258R	354.0	42.C	382.0	33.C	577.0	33.C	588.0	42.CE	15.0	36.DG	31.0	42.C
259T	369.0	24.C	382.0	33.C	550.0	48.C	569.0	0.A	15.0	36.DG	31.0	24.C
260T	369.0	0.A	382.0	33.C	569.0	0.A	577.0	33.C	15.0	36.DG	31.0	24.C
261	342.0	24.C	354.0	42.C	569.0	0.A	588.0	24.CE	15.0	36.DG	31.0	24.C
262T	320.0	0.A	354.0	24.C	490.0	24.C	500.0	24.C	31.0	24.C	43.0	12.C
263T	320.0	0.A	332.0	24.C	500.0	24.C	522.0	0.A	31.0	24.C	54.0	24.C
264T	320.0	24.CE	332.0	24.C	522.0	0.A	528.0	0.A	31.0	24.C	54.0	24.C
265T	320.0	24.CE	332.0	24.C	528.0	0.A	569.0	0.A	31.0	24.C	40.0	12.C
266T	332.0	24.C	354.0	24.C	500.0	24.C	529.0	0.A	31.0	24.C	54.0	24.C
267T	354.0	24.C	397.0	0.A	490.0	0.A	500.0	24.C	31.0	24.C	43.0	12.C
268	354.0	24.C	369.0	0.A	500.0	24.C	511.0	24.C	31.0	24.C	40.0	24.C
269	354.0	24.C	369.0	48.C	511.0	24.C	525.0	0.A	31.0	24.C	54.0	24.C
270	369.0	0.A	397.0	0.A	500.0	24.C	511.0	48.C	31.0	48.C	40.0	24.C
271R	369.0	48.C	385.0	0.A	511.0	48.C	525.0	36.C	31.0	48.C	54.0	24.C
272T	369.0	0.A	385.0	36.C	525.0	36.C	538.0	36.C	31.0	48.C	54.0	24.C
273R	369.0	48.C	382.0	0.A	538.0	36.C	550.0	0.A	31.0	48.C	54.0	24.C
274R	382.0	0.A	385.0	0.A	538.0	36.C	550.0	48.C	31.0	48.C	54.0	24.C
275T	369.0	24.C	382.0	33.C	550.0	0.A	569.0	0.A	31.0	24.C	40.0	0.A
276R	385.0	0.A	397.0	48.CE	511.0	48.C	525.0	0.A	31.0	48.C	54.0	48.C
277R	385.0	36.C	397.0	48.CE	525.0	0.A	538.0	0.A	31.0	48.C	54.0	48.C
278R	385.0	0.A	397.0	48.CE	538.0	0.A	550.0	48.C	31.0	48.C	54.0	48.C
279T	320.0	0.A	332.0	0.A	569.0	0.A	588.0	24.CE	31.0	24.C	40.0	24.C
280T	332.0	0.A	369.0	0.A	569.0	24.C	588.0	24.CE	31.0	24.C	40.0	24.C
281T	369.0	0.A	382.0	33.C	569.0	0.A	588.0	24.CE	31.0	24.C	40.0	0.A
282R	382.0	33.C	397.0	42.CE	550.0	48.C	588.0	42.CE	15.0	36.DG	40.0	48.C
283T	320.0	24.CE	332.0	24.C	528.0	0.A	539.0	0.A	40.0	0.A	54.0	0.A
284T	320.0	24.CE	332.0	24.C	539.0	0.A	569.0	0.A	40.0	12.C	54.0	24.C
285T	320.0	0.A	332.0	0.A	569.0	0.A	588.0	24.C	40.0	12.C	54.0	48.C
286T	332.0	0.A	347.0	0.A	569.0	24.C	588.0	24.C	40.0	24.C	54.0	48.C
287T	347.0	0.A	356.0	0.A	569.0	24.C	588.0	0.A	40.0	24.C	54.0	48.C
288T	356.0	0.A	364.0	0.A	569.0	24.C	588.0	24.C	40.0	24.C	54.0	24.C
289T	364.0	0.A	369.0	24.C	569.0	24.C	588.0	0.A	40.0	24.C	54.0	24.C
290	369.0	24.C	382.0	24.C	550.0	48.C	569.0	0.A	40.0	0.A	54.0	24.C
291	369.0	24.C	373.0	0.A	576.0	0.A	583.0	0.A	40.0	0.A	54.0	24.C
292	382.0	24.C	397.0	24.CE	550.0	48.C	588.0	0.A	40.0	42.C	54.0	24.C
293T	320.0	24.CE	333.0	0.A	588.0	24.C	611.0	0.A	40.0	24.CG	54.0	30.C
294T	347.0	0.A	356.0	24.C	588.0	0.A	611.0	0.A	40.0	24.CG	54.0	30.C
295T	356.0	24.C	364.0	24.C	588.0	24.C	664.0	0.AE	40.0	24.CG	49.0	24.C
296T	356.0	24.C	364.0	0.A	588.0	24.C	664.0	0.AE	49.0	24.C	54.0	12.C
297	364.0	24.C	369.0	0.A	588.0	0.A	664.0	24.CE	40.0	24.CG	49.0	0.A
298T	369.0	0.A	382.0	0.A	588.0	24.C	607.0	0.A	40.0	24.CG	54.0	30.C
299T	382.0	0.A	397.0	24.CE	588.0	0.A	607.0	0.A	40.0	24.CG	54.0	30.C

Table C1-1. Computer Specification of the Indian Point 3 Plant (Continued).

300R	320.0	24.CE	327.0	0.A	611.0	0.A	654.0	0.A	40.0	24.CG	54.0	12.C
301	327.0	0.A	333.0	0.A	611.0	0.A	626.0	0.A	40.0	24.CG	54.0	12.C
302	327.0	0.A	333.0	0.A	626.0	0.A	632.0	0.A	40.0	24.CG	54.0	0.A
303	327.0	0.A	333.0	0.A	632.0	0.A	654.0	0.A	40.0	24.CG	54.0	12.C
304	320.0	24.CE	339.0	24.C	654.0	0.A	664.0	24.CE	40.0	24.CG	54.0	0.A
305	333.0	0.A	347.0	0.A	611.0	0.A	654.0	0.A	40.0	24.CG	54.0	12.C
306R	339.0	24.C	356.0	24.C	654.0	0.A	664.0	24.CE	40.0	24.CG	54.0	12.C
307	347.0	0.A	356.0	24.C	611.0	0.A	635.0	0.A	40.0	24.CG	54.0	0.A
308R	347.0	0.A	356.0	24.C	635.0	0.A	654.0	0.A	40.0	24.CG	54.0	12.C
309R	369.0	0.A	397.0	24.CE	607.0	0.A	625.0	0.A	40.0	24.CG	54.0	30.C
310	369.0	0.A	372.0	0.A	625.0	0.A	636.0	0.A	40.0	24.CG	54.0	30.C
311	372.0	0.A	397.0	24.CE	625.0	0.A	636.0	0.A	40.0	24.CG	54.0	0.A
312T	369.0	0.A	397.0	24.CE	636.0	0.A	648.0	0.A	40.0	24.CG	54.0	12.C
313	320.0	0.AE	354.0	0.A	490.0	0.A	500.0	24.C	54.0	24.C	72.0	0.A
314T	320.0	24.CE	354.0	0.A	500.0	24.C	528.0	24.C	54.0	24.C	72.0	24.CR
315	354.0	0.A	373.0	24.C	500.0	24.C	511.0	0.A	54.0	24.C	72.0	24.CR
316	354.0	0.A	373.0	0.A	511.0	0.A	528.0	0.A	54.0	24.C	72.0	24.CR
317R	373.0	24.C	397.0	24.CE	500.0	24.C	511.0	24.C	54.0	24.C	72.0	24.CR
318	373.0	0.A	385.0	0.A	528.0	0.A	550.0	24.C	54.0	24.C	72.0	24.C
319T	320.0	24.CE	332.0	24.C	528.0	24.C	539.0	24.C	54.0	0.A	72.0	0.A
320R	332.0	24.C	354.0	24.C	528.0	24.C	539.0	24.C	54.0	24.C	72.0	42.C
321	354.0	24.C	373.0	0.A	528.0	0.A	550.0	0.A	54.0	24.C	72.0	24.C
322	320.0	24.CE	350.0	18.C	539.0	24.C	544.0	0.A	54.0	24.C	63.0	0.A
323	320.0	24.CE	331.0	18.C	544.0	0.A	554.0	0.A	54.0	24.C	63.0	0.A
324	320.0	24.CE	331.0	0.A	554.0	0.A	568.0	30.C	54.0	48.C	63.0	0.A
325R	331.0	18.C	350.0	18.C	544.0	0.A	554.0	18.C	54.0	24.C	63.0	0.A
326	331.0	0.A	350.0	0.A	554.0	18.C	568.0	30.C	54.0	48.C	63.0	0.A
327R	350.0	18.C	354.0	24.C	539.0	24.C	554.0	0.A	54.0	24.C	63.0	0.A
328	350.0	0.A	354.0	24.C	554.0	0.A	568.0	30.C	54.0	48.C	63.0	0.A
329	320.0	24.CE	354.0	24.C	539.0	24.C	568.0	30.C	63.0	0.A	72.0	42.C
330	354.0	24.C	373.0	24.C	550.0	0.A	568.0	0.A	54.0	24.C	72.0	24.C
331R	373.0	24.C	391.0	0.A	550.0	24.C	576.0	24.C	54.0	24.C	72.0	24.C
332	391.0	0.A	397.0	24.CE	550.0	24.C	588.0	30.C	54.0	24.C	72.0	24.C
333T	320.0	30.CE	348.0	30.C	568.0	30.C	582.0	30.C	54.0	30.C	72.0	24.C
334T	320.0	30.CE	348.0	30.C	582.0	30.C	597.0	30.C	54.0	30.C	72.0	24.C
335T	320.0	30.CE	348.0	30.C	597.0	30.C	611.0	30.C	54.0	30.C	72.0	24.C
336	348.0	30.C	354.0	0.A	568.0	30.C	611.0	30.C	54.0	30.C	72.0	24.C
337	354.0	0.A	373.0	24.C	568.0	0.A	583.0	0.A	54.0	24.C	72.0	24.C
338T	373.0	24.C	382.0	24.C	576.0	24.C	583.0	24.C	54.0	0.A	72.0	0.A
339	373.0	30.C	380.0	0.A	583.0	24.C	588.0	0.A	54.0	24.C	72.0	24.C
340	373.0	30.C	380.0	30.C	588.0	0.A	596.0	0.A	54.0	30.C	72.0	30.C
341R	373.0	30.C	397.0	30.CE	596.0	0.A	606.0	30.C	54.0	30.C	72.0	30.C
342	380.0	0.A	382.0	0.A	583.0	24.C	588.0	30.C	54.0	24.C	72.0	24.C
343	382.0	24.C	391.0	0.A	576.0	24.C	583.0	0.A	54.0	24.C	72.0	24.C
344	382.0	0.A	391.0	0.A	583.0	0.A	588.0	30.C	54.0	24.C	72.0	24.C
345R	380.0	30.C	397.0	30.CE	588.0	30.C	596.0	0.A	54.0	30.C	72.0	30.C
346T	320.0	24.CE	339.0	0.A	611.0	30.C	626.0	0.A	54.0	12.C	72.0	12.C
347	320.0	24.CE	327.0	0.A	626.0	0.A	632.0	0.A	54.0	12.C	72.0	12.C
348	327.0	0.A	333.0	0.A	626.0	0.A	632.0	0.A	54.0	0.A	72.0	12.C
349	333.0	0.A	339.0	0.A	626.0	0.A	632.0	0.A	54.0	12.C	72.0	12.C
350T	320.0	24.CE	339.0	0.A	632.0	0.A	654.0	24.C	54.0	12.C	72.0	12.C
351	320.0	24.CE	339.0	24.C	654.0	24.C	664.0	0.AE	54.0	0.A	72.0	12.C
352T	339.0	0.A	348.0	0.A	611.0	30.C	654.0	0.A	54.0	12.C	72.0	12.C
353	339.0	24.C	348.0	0.A	654.0	0.A	664.0	24.CE	54.0	12.C	72.0	12.C
354	348.0	0.A	354.0	0.A	611.0	30.C	635.0	0.A	54.0	0.A	72.0	12.C
355	348.0	0.A	354.0	0.A	635.0	0.A	664.0	24.CE	54.0	12.C	72.0	12.C
356	354.0	0.A	373.0	0.A	606.0	0.A	664.0	24.CE	54.0	24.C	72.0	24.C
357T	373.0	0.A	397.0	24.CE	606.0	30.C	625.0	0.A	54.0	12.C	72.0	24.C
358	373.0	0.A	397.0	24.CE	625.0	0.A	636.0	24.C	54.0	0.A	72.0	24.C
359T	373.0	0.A	397.0	24.CE	636.0	24.C	664.0	24.CE	54.0	12.C	72.0	24.C

Table C1-1. Computer Specification of the Indian Point 3 Plant (Continued).

360	320.0	0.A	397.0	0.A	490.0	0.A	500.0	0.A	72.0	0.A	92.0	0.A
361	320.0	0.A	397.0	0.A	500.0	0.A	528.0	24.C	72.0	24.CR	92.0	0.A
362	320.0	24.C	332.0	42.C	528.0	24.C	539.0	42.C	72.0	0.A	92.0	24.CR
363T	320.0	42.C	337.0	42.C	539.0	42.C	554.0	42.C	72.0	42.C	92.0	24.CR
364	320.0	42.C	337.0	0.A	554.0	42.C	568.0	24.C	72.0	42.C	92.0	24.CR
365T	337.0	42.C	343.0	12.C	539.0	42.C	554.0	0.A	72.0	42.C	92.0	24.CR
366T	337.0	0.A	343.0	12.C	554.0	0.A	568.0	24.C	72.0	42.C	92.0	24.CR
367	343.0	12.C	350.0	0.A	539.0	42.C	568.0	24.C	72.0	42.C	92.0	24.CR
368	350.0	0.A	354.0	0.A	539.0	42.C	568.0	0.A	72.0	42.C	92.0	24.CR
369	354.0	42.C	356.0	0.A	528.0	24.C	539.0	0.A	72.0	24.C	92.0	24.CR
370	354.0	0.A	356.0	0.A	539.0	0.A	568.0	0.A	72.0	24.C	92.0	24.CR
371	356.0	0.A	368.0	24.C	528.0	24.C	538.0	0.A	72.0	24.C	92.0	24.CR
372	356.0	0.A	368.0	0.A	538.0	0.A	568.0	0.A	72.0	24.C	92.0	24.CR
373T	368.0	24.C	397.0	24.C	528.0	24.C	538.0	24.C	72.0	24.C	92.0	24.CR
374	368.0	0.A	373.0	24.C	538.0	24.C	568.0	0.A	72.0	24.C	92.0	24.CR
375R	373.0	24.C	397.0	24.C	538.0	24.C	571.0	24.C	72.0	24.C	92.0	24.CR
376R	320.0	24.C	350.0	24.C	568.0	24.C	582.0	24.C	72.0	24.C	92.0	24.CR
377T	320.0	24.C	350.0	24.C	582.0	24.C	597.0	24.C	72.0	24.C	92.0	24.CR
378T	320.0	24.C	350.0	0.A	597.0	24.C	605.0	0.A	72.0	24.C	92.0	24.CR
379	350.0	24.C	373.0	24.C	568.0	0.A	597.0	0.A	72.0	24.C	92.0	24.CR
380	350.0	0.A	373.0	24.C	597.0	0.A	611.0	0.A	72.0	24.C	92.0	24.CR
381	373.0	24.C	382.0	0.A	571.0	24.C	576.0	24.C	72.0	24.C	92.0	24.CR
382T	373.0	24.C	382.0	24.C	576.0	24.C	583.0	24.C	72.0	0.A	92.0	24.CR
383	382.0	0.A	397.0	24.C	571.0	24.C	576.0	0.A	72.0	24.C	92.0	24.CR
384	382.0	24.C	397.0	24.C	576.0	0.A	583.0	24.C	72.0	24.C	92.0	24.CR
385R	373.0	24.C	397.0	24.C	588.0	0.A	606.0	0.A	72.0	30.C	92.0	24.CR
386T	339.0	24.C	354.0	0.A	627.0	0.A	664.0	24.C	72.0	12.C	92.0	24.CR
387	354.0	0.A	373.0	24.C	611.0	0.A	618.0	0.A	72.0	24.C	92.0	24.CR
388	354.0	0.A	373.0	0.A	618.0	0.A	664.0	24.C	72.0	24.C	92.0	24.CR
389	373.0	0.A	397.0	24.C	618.0	24.C	664.0	24.C	72.0	24.C	92.0	24.CR
390	354.0	0.A	373.0	30.C	583.0	0.A	606.0	0.A	54.0	24.C	72.0	24.C
391T	320.0	0.A	354.0	24.C	490.0	24.C	500.0	24.C	43.0	12.C	54.0	24.CR
392	354.0	24.C	369.0	0.A	500.0	24.C	511.0	24.C	40.0	24.C	54.0	24.C
393	354.0	24.C	369.0	0.A	525.0	0.A	538.0	0.A	31.0	24.C	54.0	24.C
394	354.0	24.C	369.0	48.C	538.0	0.A	550.0	0.A	31.0	24.C	54.0	24.C
395	354.0	24.C	369.0	24.C	550.0	0.A	569.0	24.C	31.0	24.C	54.0	24.C
396	369.0	24.C	382.0	24.C	569.0	0.A	576.0	0.A	40.0	0.A	54.0	24.C
397	373.0	0.A	382.0	24.C	576.0	0.A	583.0	0.A	40.0	0.A	54.0	0.A
398	369.0	24.C	382.0	24.C	583.0	0.A	588.0	24.C	40.0	0.A	54.0	24.C
399	369.0	0.A	397.0	0.A	500.0	24.C	511.0	48.C	40.0	24.C	54.0	24.C
400	364.0	0.A	369.0	0.A	588.0	0.A	664.0	24.CE	49.0	0.A	54.0	24.C
401	354.0	0.A	397.0	0.A	490.0	0.A	500.0	24.C	54.0	0.A	72.0	0.A
402	385.0	0.A	397.0	24.C	528.0	0.A	550.0	24.C	54.0	48.C	72.0	24.C
403	332.0	42.C	354.0	42.C	528.0	42.C	539.0	42.C	72.0	42.C	92.0	42.CR
404R	373.0	24.C	397.0	24.C	583.0	24.C	588.0	0.A	72.0	24.C	92.0	24.CR
405R	373.0	24.C	397.0	24.C	606.0	0.A	618.0	24.C	72.0	24.C	92.0	24.CR
406	373.0	0.A	385.0	0.A	511.0	24.C	528.0	0.A	54.0	48.C	72.0	24.CR
407	385.0	0.A	397.0	24.C	511.0	24.C	528.0	0.A	54.0	48.C	72.0	24.CR
408	320.0	0.A	397.0	0.A	490.0	0.A	528.0	0.A	92.0	0.A	262.0	0.AR
409	320.0	0.A	397.0	0.A	528.0	0.A	664.0	0.A	92.0	24.C	262.0	0.AR
410	320.0	0.A	354.0	0.A	385.0	0.A	490.0	24.CE	18.0	36.DG	54.0	0.A
411	354.0	0.A	397.0	0.A	385.0	0.A	490.0	0.A	18.0	36.DG	54.0	0.A
412	320.0	0.A	397.0	0.A	385.0	0.A	490.0	0.A	54.0	0.A	262.0	0.AR
413	310.0	144.CE	320.0	0.A	385.0	0.A	490.0	144.CE	18.0	36.D	46.0	0.A
414	310.0	36.C	320.0	0.A	385.0	0.A	490.0	144.CE	46.0	0.A	63.0	0.A
415	310.0	0.A	320.0	0.A	385.0	0.A	490.0	144.CE	63.0	0.A	73.0	0.A
416	310.0	144.CE	320.0	24.CE	490.0	24.C	500.0	24.C	15.0	36.DG	31.0	24.C
417T	310.0	0.AE	320.0	0.AE	490.0	24.C	500.0	24.CE	31.0	24.C	43.0	12.C
418T	310.0	0.AE	320.0	0.AE	490.0	24.C	500.0	24.CE	43.0	12.C	54.0	24.C
419	310.0	0.A	320.0	0.A	490.0	0.A	500.0	0.A	54.0	24.C	73.0	0.A

Table C1-1. Computer Specification of the Indian Point 3 Plant (Continued).

420T	442.0	24.C	454.0	0.A	390.0	0.A	412.0	0.A	15.0	36.DG	33.0	24.C
421T	442.0	24.C	454.0	0.A	412.0	0.A	420.0	0.A	15.0	36.DG	33.0	24.C
422T	442.0	24.C	454.0	0.A	420.0	0.A	444.0	6.C	15.0	36.DG	33.0	24.C
423T	454.0	0.A	459.0	0.A	390.0	0.A	412.0	0.A	15.0	36.DG	33.0	24.C
424T	454.0	0.A	459.0	0.A	412.0	0.A	420.0	0.A	15.0	36.DG	33.0	24.C
425T	454.0	0.A	459.0	0.A	420.0	0.A	444.0	6.C	15.0	36.DG	33.0	24.C
426T	459.0	0.A	471.0	24.C	390.0	0.A	412.0	0.A	15.0	36.DG	33.0	24.C
427T	459.0	0.A	471.0	24.C	412.0	0.A	420.0	0.A	15.0	36.DG	33.0	24.C
428T	459.0	0.A	471.0	24.C	420.0	0.A	444.0	6.C	15.0	36.DG	33.0	24.C
429T	442.0	24.C	452.0	0.A	339.0	24.C	445.0	0.A	33.0	24.C	53.0	24.C
430T	452.0	0.A	455.0	0.A	339.0	24.C	385.0	0.A	33.0	24.C	53.0	24.C
431T	452.0	0.A	455.0	0.A	385.0	0.A	394.0	0.A	33.0	24.C	53.0	24.C
432T	452.0	0.A	455.0	0.A	394.0	0.A	412.0	0.A	33.0	24.C	53.0	24.C
433T	452.0	0.A	455.0	0.A	412.0	0.A	421.0	0.A	33.0	24.C	53.0	24.C
434T	452.0	0.A	455.0	0.A	421.0	0.A	464.0	24.C	33.0	24.C	53.0	24.C
435T	455.0	0.A	461.0	0.A	339.0	24.C	357.0	0.A	33.0	24.C	53.0	24.C
436T	461.0	0.A	476.0	24.C	339.0	24.C	357.0	8.C	33.0	24.C	53.0	24.C
437T	461.0	8.C	476.0	24.C	357.0	8.C	378.0	8.C	33.0	24.C	53.0	24.C
438T	461.0	8.C	476.0	24.C	378.0	8.C	397.0	8.C	33.0	24.C	53.0	24.C
439T	461.0	0.A	476.0	24.C	397.0	8.C	402.0	0.A	33.0	24.C	53.0	24.C
440T	461.0	0.A	465.0	0.A	402.0	0.A	405.0	0.A	33.0	24.C	53.0	24.C
441T	461.0	0.A	465.0	0.A	405.0	0.A	408.0	0.A	33.0	24.C	53.0	24.C
442T	461.0	0.A	465.0	0.A	408.0	0.A	464.0	24.C	33.0	24.C	53.0	24.C
443T	465.0	0.A	476.0	24.C	402.0	0.A	464.0	24.C	33.0	24.C	53.0	24.C
444T	455.0	0.A	461.0	8.C	357.0	0.A	397.0	0.A	33.0	24.C	53.0	24.C
445T	455.0	0.A	461.0	0.A	397.0	0.A	464.0	24.C	33.0	24.C	53.0	24.C
446T	442.0	24.C	476.0	24.C	339.0	24.C	464.0	24.C	53.0	24.C	72.0	31.C
447	476.0	0.A	528.0	36.DS	0.0	0.AW	339.0	0.A	15.0	36.DG	72.0	0.A
448T	476.0	24.C	528.0	24.C	394.0	24.C	410.0	24.C	15.0	36.DG	53.0	24.C
449T	476.0	24.C	528.0	24.C	410.0	24.C	426.0	24.C	15.0	36.DG	53.0	24.C
450T	476.0	24.C	528.0	24.C	426.0	24.C	443.0	24.C	15.0	36.DG	53.0	24.C
451T	528.0	24.C	539.0	36.DS	394.0	24.C	410.0	12.C	28.0	36.C	38.0	18.C
452T	528.0	24.C	539.0	36.DS	410.0	12.C	426.0	12.C	28.0	36.C	38.0	18.C
453T	528.0	24.C	539.0	36.DS	426.0	12.C	443.0	36.C	28.0	36.C	38.0	18.C
454	476.0	24.C	528.0	0.AS	339.0	0.A	394.0	24.C	15.0	36.DG	53.0	0.A
455	476.0	24.C	528.0	0.AS	339.0	0.A	394.0	0.A	53.0	0.A	72.0	0.A
456	476.0	24.C	528.0	0.A	394.0	0.A	443.0	0.A	53.0	24.C	72.0	0.A
457	528.0	24.C	539.0	0.AS	394.0	0.A	443.0	0.A	38.0	18.C	53.0	0.A
458	528.0	0.A	539.0	0.AS	394.0	0.A	443.0	0.A	53.0	0.A	72.0	0.A
459	528.0	24.C	539.0	36.DS	394.0	36.C	443.0	36.C	15.0	36.DG	28.0	36.C
460	528.0	0.A	539.0	0.AS	0.0	0.AW	394.0	36.C	15.0	36.DG	28.0	0.A
461	528.0	0.A	539.0	0.AS	0.0	0.AW	394.0	24.C	28.0	0.A	38.0	0.A
462	528.0	0.A	539.0	0.AS	0.0	0.AW	394.0	0.A	38.0	0.A	72.0	0.A
463	528.0	0.A	539.0	0.AS	443.0	36.C	464.0	0.A	15.0	36.DG	38.0	0.A
464	528.0	0.A	539.0	0.AS	443.0	0.A	464.0	0.A	38.0	0.A	72.0	0.A
465	476.0	24.C	528.0	0.A	443.0	24.C	464.0	0.A	15.0	36.DG	53.0	0.A
466	476.0	24.C	528.0	0.A	443.0	0.A	464.0	0.A	53.0	0.A	72.0	0.A
467	476.0	0.A	539.0	0.AS	464.0	0.A	756.0	0.AT	15.0	36.DG	72.0	0.A
468	476.0	0.A	539.0	0.AS	0.0	0.AW	756.0	0.AT	72.0	0.A	2620	0.AR
469	125.0	0.AN	397.0	0.A	664.0	0.A	695.0	0.A	79.0	36.DG	122.0	0.A
470	125.0	0.AN	189.0	0.A	695.0	0.A	738.0	0.A	79.0	36.DG	122.0	0.A
471T	189.0	0.A	232.0	0.A	695.0	0.A	738.0	0.A	79.0	36.DG	122.0	0.A
472	232.0	0.A	397.0	0.A	695.0	0.A	738.0	0.A	79.0	36.DG	122.0	0.A
473	125.0	0.AN	397.0	0.A	738.0	0.A	756.0	0.AT	79.0	36.DG	122.0	0.A
474	320.0	36.D	329.0	36.D	388.0	36.D	490.0	24.C	15.0	36.DG	18.0	36.D
475	329.0	36.D	354.0	36.D	403.0	36.D	490.0	24.C	15.0	36.DG	18.0	36.D
476	354.0	36.D	397.0	36.D	403.0	36.D	490.0	36.D	15.0	36.DG	18.0	36.D
477	354.0	36.D	397.0	36.D	490.0	36.D	500.0	48.C	15.0	36.DG	18.0	36.DR
478T	320.0	24.C	350.0	0.A	605.0	0.A	611.0	0.A	72.0	24.C	92.0	24.CR
479T	320.0	24.C	339.0	0.A	611.0	0.A	627.0	0.A	72.0	12.C	92.0	24.CR

Table C1-1. Computer Specification of the Indian Point 3 Plant (Continued).

480T	339.0	0.A	354.0	0.A	611.0	0.A	627.0	0.A	72.0	12.C	92.0	24.CR
481T	320.0	24.C	339.0	0.A	627.0	0.A	664.0	24.C	72.0	12.C	92.0	24.CR
482T	369.0	0.A	397.0	24.CE	648.0	0.A	664.0	24.C	40.0	24.CG	54.0	12.C
483T	332.0	24.C	354.0	24.C	529.0	0.A	549.0	0.A	31.0	24.C	54.0	24.C
484T	332.0	24.C	354.0	24.C	549.0	0.A	569.0	24.C	31.0	24.C	54.0	24.C
485T	333.0	0.A	347.0	0.A	588.0	24.C	611.0	0.A	40.0	24.CG	54.0	30.C
486	152.0	0.A	173.0	0.A	373.0	0.A	385.0	0.A	53.0	0.A	80.0	0.A
487	442.0	24.C	476.0	24.C	339.0	24.C	390.0	0.A	15.0	36.DG	33.0	24.C
488T	354.0	24.C	397.0	0.A	490.0	0.A	500.0	24.C	43.0	12.C	54.0	0.A
489T	442.0	18.C	453.0	15.C	464.0	12.C	482.0	0.A	33.0	20.CG	43.0	0.A
490T	442.0	18.C	453.0	15.C	464.0	12.C	482.0	0.A	43.0	0.A	54.0	20.C
491T	0.0	0.AL	57.0	0.A	504.0	0.AE	561.0	0.AE	71.0	36.DG	108.0	0.AR
492	57.0	0.AL	125.0	0.A	50.0	0.A	561.0	0.AE	18.0	36.DG	108.0	0.AR
493	442.0	24.C	471.0	24.C	444.0	6.C	464.0	24.C	15.0	36.DG	33.0	24.C
494	471.0	24.C	476.0	0.A	390.0	24.C	464.0	24.C	15.0	36.DG	33.0	24.C
495	305.5	0.A	326.5	0.A	53.0	0.A	58.0	12.C	14.0	36.DG	17.0	0.A
496	322.0	0.A	326.5	0.A	47.0	0.A	53.0	0.A	14.0	24.C	22.0	0.A
497T	316.0	0.A	322.0	0.A	47.0	0.A	53.0	0.A	14.0	24.C	22.0	0.A
498T	310.0	0.A	316.0	0.A	47.0	0.A	53.0	0.A	14.0	24.C	22.0	0.A
499	305.5	0.A	310.0	0.A	47.0	0.A	53.0	0.A	14.0	24.C	22.0	0.A
500T	316.5	0.A	326.5	0.A	41.0	0.A	47.0	0.A	14.0	24.C	22.0	0.A
501T	305.5	0.A	316.5	0.A	41.0	0.A	47.0	0.A	14.0	24.C	22.0	0.A
502T	318.5	0.A	326.5	0.A	34.0	0.A	41.0	0.A	14.0	24.C	22.0	0.A
503	313.5	0.A	318.5	0.A	34.0	0.A	41.0	0.A	14.0	24.C	22.0	0.A
504T	305.5	0.A	313.5	0.A	34.0	0.A	41.0	0.A	14.0	24.C	22.0	0.A
505T	324.3	0.A	330.0	12.CE	58.0	12.CE	76.0	12.CE	2.0	6.CG	14.0	1.S
506T	320.0	0.A	324.3	0.A	58.0	12.CE	76.0	12.CE	2.0	6.CG	14.0	1.S
507T	315.9	0.A	320.0	0.A	58.0	12.CE	76.0	12.CE	2.0	6.CG	14.0	1.S
508T	311.8	0.A	315.9	0.A	58.0	12.CE	76.0	12.CE	2.0	6.CG	14.0	1.S
509T	307.7	0.A	311.8	0.A	58.0	12.CE	76.0	12.CE	2.0	6.CG	14.0	1.S
510T	302.0	12.CE	307.7	0.A	58.0	12.CE	76.0	12.CE	2.0	6.CG	14.0	1.S
511	177.0	0.A	302.0	0.A	58.0	0.A	76.0	0.A	17.0	0.A	262.0	0.AR
512	330.0	0.A	456.0	0.A	58.0	0.A	76.0	0.A	17.0	0.A	262.0	0.AR
513	302.0	0.A	305.5	0.A	34.0	0.A	58.0	0.A	17.0	0.A	262.0	0.AR
514	326.5	0.A	330.0	0.A	34.0	0.A	58.0	0.A	17.0	0.A	262.0	0.AR
515	305.5	0.A	326.5	0.A	53.0	0.A	58.0	0.A	17.0	0.A	262.0	0.AR
516T	302.0	36.DE	330.0	36.DE	76.0	36.DE	114.0	36.DE	2.0	24.DG	11.0	96.D
517T	302.0	24.CE	330.0	24.CE	114.0	24.CE	158.0	24.CE	2.0	24.DG	14.0	24.C
518	302.0	0.A	330.0	0.A	114.0	0.A	158.0	0.A	14.0	24.C	262.0	0.AR
519	302.0	0.A	330.0	0.A	158.0	0.A	185.0	0.A	14.0	36.DG	262.0	0.AR
520	301.0	0.A	302.0	0.A	174.5	0.A	185.0	0.A	14.0	36.DG	262.0	0.AR
521	289.5	0.A	301.0	0.A	184.0	0.A	185.0	0.A	14.0	36.DG	262.0	0.AR
522	289.5	0.A	301.0	0.A	174.5	0.A	184.0	0.A	14.0	1.S	262.0	0.AR
523	289.5	0.A	302.0	0.A	76.0	0.A	174.5	0.A	14.0	36.DG	262.0	0.AR
524T	289.5	9.CE	295.0	0.A	174.5	9.CE	184.0	9.CE	2.0	24.DG	14.0	1.S
525T	295.0	0.A	297.0	0.A	174.5	9.CE	182.0	0.A	2.0	24.DG	14.0	1.S
526T	295.0	0.A	297.0	0.A	182.0	0.A	184.0	9.CE	2.0	24.DG	14.0	1.S
527T	297.0	0.A	301.0	9.CE	174.5	9.CE	184.0	9.CE	2.0	24.DG	14.0	1.S
528	125.0	0.A	177.0	0.A	158.0	0.A	232.0	0.A	24.0	0.A	262.0	0.AR
529T	442.0	24.C	452.0	0.A	445.0	0.A	464.0	24.C	33.0	24.C	53.0	24.C
999												

APPENDIX C-2 - SAMPLE RESULTS

Table C2-1 illustrates the results of a run for 2000 trials for disc 16. The specific case is 90° breakup at 132 percent overspeed. The line starting with "INPUT DATA" lists the input parameters to set up this case. The output shows the number of each trial in which a safety target was hit, the number of target rooms penetrated, and the MISIP identification numbers for these rooms. For example, the first trial which resulted in penetration of a target was trial number 1. In this trial 1 target room was hit: room 232. In trial number 7, three targets were hit: rooms 498, 501, and 504.

There were 17 trials which resulted in safety compromises after redundancy modeling was considered:

Trial Number	Room Struck	Description of Rooms
69	226	Common Electrical Penetration Area
235	517	Service Water Piping Bunker
343	516	Service Water Piping Under Roadway
362	516	Service Water Piping Under Roadway
454	516	Service Water Piping Under Roadway
597	516	Service Water Piping Under Roadway
636	516	Service Water Piping Under Roadway
740	516	Service Water Piping Under Roadway
793	516	Service Water Piping Under Roadway
1074	516	Service Water Piping Under Roadway
1160	516	Service Water Piping Under Roadway
1400	135	Piping Penetration Area
1472	516	Service Water Piping Under Roadway
1546	516	Service Water Piping Under Roadway
1657	516	Service Water Piping Under Roadway
1729	516	Service Water Piping Under Roadway
1973	517	Service Water Piping Bunker

Table C2-2 is an output summary showing the number of times each safety target room was hit, and the number of penetrations. In this table disregard the listed probablity of safety compromise as this does not as yet include redundancy considerations.

Table C2-1. Example Computer Printout - Targets Struck During Each Trial.

INPUT DATA	16	2	1	2000				
SAFETY	TARGETS	HIT	1	1	232			
SAFETY	TARGETS	HIT	6	1	501			
SAFETY	TARGETS	HIT	7	3	498	501	504	
SAFETY	TARGETS	HIT	23	3	497	500	502	
SAFETY	TARGETS	HIT	29	3	498	501	504	
SAFETY	TARGETS	HIT	46	2	500	502		
SAFETY	TARGETS	HIT	69	3	129	129	226	
SAFETY	TARGETS	HIT	113	1	504			
SAFETY	TARGETS	HIT	143	2	129	129		
SAFETY	TARGETS	HIT	175	2	501	504		
SAFETY	TARGETS	HIT	191	1	129			
SAFETY	TARGETS	HIT	200	1	500			
SAFETY	TARGETS	HIT	215	2	501	504		
SAFETY	TARGETS	HIT	219	2	510	197		
SAFETY	TARGETS	HIT	230	1	156			
SAFETY	TARGETS	HIT	235	1	517			
SAFETY	TARGETS	HIT	248	1	156			
SAFETY	TARGETS	HIT	252	1	505			
SAFETY	TARGETS	HIT	283	1	422			
SAFETY	TARGETS	HIT	300	1	500			
SAFETY	TARGETS	HIT	319	1	501			
SAFETY	TARGETS	HIT	329	3	497	500	502	
SAFETY	TARGETS	HIT	334	1	232			
SAFETY	TARGETS	HIT	339	1	502			
SAFETY	TARGETS	HIT	343	1	516			
SAFETY	TARGETS	HIT	350	2	99	232		
SAFETY	TARGETS	HIT	352	1	232			
SAFETY	TARGETS	HIT	362	1	516			
SAFETY	TARGETS	HIT	376	1	504			
SAFETY	TARGETS	HIT	387	2	500	502		
SAFETY	TARGETS	HIT	390	1	129			
SAFETY	TARGETS	HIT	410	3	498	501	504	
SAFETY	TARGETS	HIT	438	2	500	502		
SAFETY	TARGETS	HIT	442	1	505			
SAFETY	TARGETS	HIT	454	1	516			
SAFETY	TARGETS	HIT	486	2	500	502		
SAFETY	TARGETS	HIT	502	1	429			
SAFETY	TARGETS	HIT	507	2	498	501		
SAFETY	TARGETS	HIT	511	2	500	502		
SAFETY	TARGETS	HIT	516	2	497	501		
SAFETY	TARGETS	HIT	523	2	501	504		
SAFETY	TARGETS	HIT	526	2	501	504		
SAFETY	TARGETS	HIT	531	1	500			
SAFETY	TARGETS	HIT	555	2	497	500		
SAFETY	TARGETS	HIT	570	1	198			
SAFETY	TARGETS	HIT	597	1	516			
SAFETY	TARGETS	HIT	615	1	127			
SAFETY	TARGETS	HIT	619	3	497	500	502	
SAFETY	TARGETS	HIT	623	1	502			
SAFETY	TARGETS	HIT	631	1	506			
SAFETY	TARGETS	HIT	636	1	516			
SAFETY	TARGETS	HIT	640	1	197			
SAFETY	TARGETS	HIT	661	2	497	500		
SAFETY	TARGETS	HIT	700	2	501	504		
SAFETY	TARGETS	HIT	731	1	129			
SAFETY	TARGETS	HIT	740	1	516			
SAFETY	TARGETS	HIT	763	2	99	99		

Table C2-1. Example Computer Printout - Targets Struck During Each Trial (Continued).

SAFETY TARGETS HIT	776	4	99	99	99	99		
SAFETY TARGETS HIT	793	1	516					
SAFETY TARGETS HIT	820	1	502					
SAFETY TARGETS HIT	825	1	505					
SAFETY TARGETS HIT	833	1	506					
SAFETY TARGETS HIT	888	5	99	99	99	220	220	
SAFETY TARGETS HIT	891	2	497	501				
SAFETY TARGETS HIT	921	2	501	504				
SAFETY TARGETS HIT	963	2	498	501				
SAFETY TARGETS HIT	976	1	502					
SAFETY TARGETS HIT	994	1	176					
SAFETY TARGETS HIT	1001	1	429					
SAFETY TARGETS HIT	1008	1	500					
SAFETY TARGETS HIT	1043	2	502	502				
SAFETY TARGETS HIT	1061	4	501	504	129	129		
SAFETY TARGETS HIT	1071	2	501	504				
SAFETY TARGETS HIT	1074	1	516					
SAFETY TARGETS HIT	1087	1	507					
SAFETY TARGETS HIT	1102	1	129					
SAFETY TARGETS HIT	1105	2	501	504				
SAFETY TARGETS HIT	1160	1	516					
SAFETY TARGETS HIT	1161	2	497	500				
SAFETY TARGETS HIT	1177	1	502					
SAFETY TARGETS HIT	1178	2	501	504				
SAFETY TARGETS HIT	1237	1	501					
SAFETY TARGETS HIT	1245	2	501	504				
SAFETY TARGETS HIT	1250	1	498					
SAFETY TARGETS HIT	1260	2	497	500				
SAFETY TARGETS HIT	1281	2	497	501				
SAFETY TARGETS HIT	1315	1	500					
SAFETY TARGETS HIT	1352	3	498	501	504			
SAFETY TARGETS HIT	1366	1	213					
SAFETY TARGETS HIT	1370	1	176					
SAFETY TARGETS HIT	1384	1	232					
SAFETY TARGETS HIT	1400	1	135					
SAFETY TARGETS HIT	1404	2	497	500				
SAFETY TARGETS HIT	1406	2	501	504				
SAFETY TARGETS HIT	1411	2	99	232				
SAFETY TARGETS HIT	1472	1	516					
SAFETY TARGETS HIT	1519	1	129					
SAFETY TARGETS HIT	1523	1	197					
SAFETY TARGETS HIT	1546	1	516					
SAFETY TARGETS HIT	1551	1	232					
SAFETY TARGETS HIT	1553	1	85					
SAFETY TARGETS HIT	1555	3	498	501	504			
SAFETY TARGETS HIT	1564	3	498	501	504			
SAFETY TARGETS HIT	1579	1	504					
SAFETY TARGETS HIT	1585	2	500	502				
SAFETY TARGETS HIT	1610	1	198					
SAFETY TARGETS HIT	1616	1	504					
SAFETY TARGETS HIT	1618	2	501	504				
SAFETY TARGETS HIT	1633	2	497	500				
SAFETY TARGETS HIT	1641	3	497	500	502			
SAFETY TARGETS HIT	1653	1	504					
SAFETY TARGETS HIT	1657	1	516					
SAFETY TARGETS HIT	1729	1	516					
SAFETY TARGETS HIT	1734	2	497	500				
SAFETY TARGETS HIT	1751	1	501					
SAFETY TARGETS HIT	1757	1	504					
SAFETY TARGETS HIT	1770	3	498	501	504			
SAFETY TARGETS HIT	1782	2	501	504				
SAFETY TARGETS HIT	1815	3	498	501	504			
SAFETY TARGETS HIT	1838	3	498	501	504			
SAFETY TARGETS HIT	1858	2	501	504				
SAFETY TARGETS HIT	1876	1	233					
SAFETY TARGETS HIT	1904	3	498	501	504			
SAFETY TARGETS HIT	1966	1	129					
SAFETY TARGETS HIT	1972	3	498	501	504			
SAFETY TARGETS HIT	1973	1	517					
SAFETY TARGETS HIT	1996	2	501	504				
SAFETY TARGETS HIT	1997	1	127					

Table C2-2. Example Computer Printout - Summary of Target Results.

RESULTS OF 2000 TRIALS FOR DISC 16

DISC	=	16
IOS	=	2
IAREA	=	1
THE1	=	100.0
THE2	=	285.0
TRIALS	=	2000
HITS	=	1381
PENETRATIONS	=	209
RICHOCHETS	=	1172
PENETRATIONS THROUGH ROOF	=	0
CONTAINMENT PENETRATIONS	=	0
CONTAINMENT RICHOCHETS	=	46

2000 SIMULATED BREAKUPS OF DISC RESULT IN THE' FOLLOWING:

FRAGMENTS IN TRAIN A	=	0
FRAGMENTS IN TRAIN B	=	0
FRAGMENTS IN TRAIN C	=	209
NUMBER OF PENETRATING SAFETY COMPROMISES	=	128
NUMBER OF TRAIN C COMPROMISES	=	128
PROBABILITY OF SAFETY COMP PER DISC FAILURE	=	6.40E-02
PROBABILITY PER YEAR OF SAFETY COMPROMISE	=	1.04E-07

SUMMARY OF TARGET RESULTS:

ROOM	NUMBER	PENETRATIONS	HITS	RICHOCHETS	PEN PROB	DISC FAILPROB	TOT PROB
3	85	1	7	6	0.0005	1.63E-06	8.15E-10
5	99	5	11	0	0.0025	1.63E-06	4.08E-09
6	100	0	1	1	0.0000	1.63E-06	0.00E+00
7	101	0	16	16	0.0000	1.63E-06	0.00E+00
8	102	0	1	1	0.0000	1.63E-06	0.00E+00
9	127	2	4	2	0.0010	1.63E-06	1.63E-09
10	129	9	34	22	0.0045	1.63E-06	7.34E-09
11	130	0	13	13	0.0000	1.63E-06	0.00E+00
12	135	1	2	1	0.0005	1.63E-06	8.15E-10
13	156	2	5	3	0.0010	1.63E-06	1.63E-09
14	176	2	8	6	0.0010	1.63E-06	1.63E-09
15	184	0	8	8	0.0000	1.63E-06	0.00E+00
16	185	0	7	7	0.0000	1.63E-06	0.00E+00
17	197	3	12	9	0.0015	1.63E-06	2.45E-09
18	198	2	8	6	0.0010	1.63E-06	1.63E-09
25	213	1	1	0	0.0005	1.63E-06	8.15E-10
28	220	1	2	0	0.0005	1.63E-06	8.15E-10
29	226	1	11	10	0.0005	1.63E-06	8.15E-10
30	227	0	22	22	0.0000	1.63E-06	0.00E+00

Table C2-2. Example Computer Printout - Summary of Target Results (Continued).

31	232	7	8	1	0.0035	1.63E-06	5.71E-09
32	233	1	1	0	0.0005	1.63E-06	8.15E-10
66	314	0	3	3	0.0000	1.63E-06	0.00E+00
77	363	0	4	4	0.0000	1.63E-06	0.00E+00
78	365	0	2	2	0.0000	1.63E-06	0.00E+00
79	366	0	1	1	0.0000	1.63E-06	0.00E+00
80	373	0	4	4	0.0000	1.63E-06	0.00E+00
81	377	0	5	5	0.0000	1.63E-06	0.00E+00
82	378	0	1	1	0.0000	1.63E-06	0.00E+00
83	382	0	1	1	0.0000	1.63E-06	0.00E+00
84	386	0	10	10	0.0000	1.63E-06	0.00E+00
85	391	0	3	3	0.0000	1.63E-06	0.00E+00
90	422	1	4	3	0.0005	1.63E-06	8.15E-10
97	429	2	2	0	0.0010	1.63E-06	1.63E-09
115	448	0	3	3	0.0000	1.63E-06	0.00E+00
122	478	0	3	3	0.0000	1.63E-06	0.00E+00
123	479	0	5	5	0.0000	1.63E-06	0.00E+00
125	481	0	2	2	0.0000	1.63E-06	0.00E+00
134	497	14	14	0	0.0070	1.63E-06	1.14E-08
135	498	14	14	0	0.0070	1.63E-06	1.14E-08
136	500	22	22	0	0.0110	1.63E-06	1.79E-08
137	501	36	36	0	0.0180	1.63E-06	2.93E-08
138	502	16	17	0	0.0080	1.63E-06	1.30E-08
139	504	33	33	0	0.0165	1.63E-06	2.69E-08
140	505	3	53	50	0.0015	1.63E-06	2.45E-09
141	506	2	42	40	0.0010	1.63E-06	1.63E-09
142	507	1	42	41	0.0005	1.63E-06	8.15E-10
143	508	0	33	33	0.0000	1.63E-06	0.00E+00
144	509	0	36	36	0.0000	1.63E-06	0.00E+00
145	510	1	45	44	0.0005	1.63E-06	8.15E-10
146	516	13	751	738	0.0065	1.63E-06	1.06E-08
147	517	2	8	6	0.0010	1.63E-06	1.63E-09

APPENDIX C-3 - INDIAN POINT 3 PLANT LAYOUT

Figures C3-1 through C3-10 are computer generated plant layout drawings showing the various compartments located at the indicated elevations (in feet). Safety-related areas are indicated by cross-hatching. The three LP turbines have an axis in the x-direction indicated by the line with arrows at each end. The containment is modeled as a circle of dashes.

Not all boundaries correspond exactly with the actual boundaries of the compartments in the actual plant. Approximations have been made for convenience and they are made conservatively (i.e., the area is at least as large or larger than the area of the compartment in the actual plant).

Each compartment in the model is shown on at least one figure. Rooms are identified by the identification number used by the MISIP code (see Table C1-1). However, the computer draws the room number proportional in size to the size of the room. Therefore, some room numbers may be difficult to read. In some cases, for rooms where safety compromises occurred or other important rooms, the hard to read portions of the plot are described on the side. Also, these rooms can be identified by consulting Table C1-1 and comparing the X, Y, and Z coordinates of the unknown room with those of known rooms. In most cases the identification number of a room is close to the numbers of its neighbors.

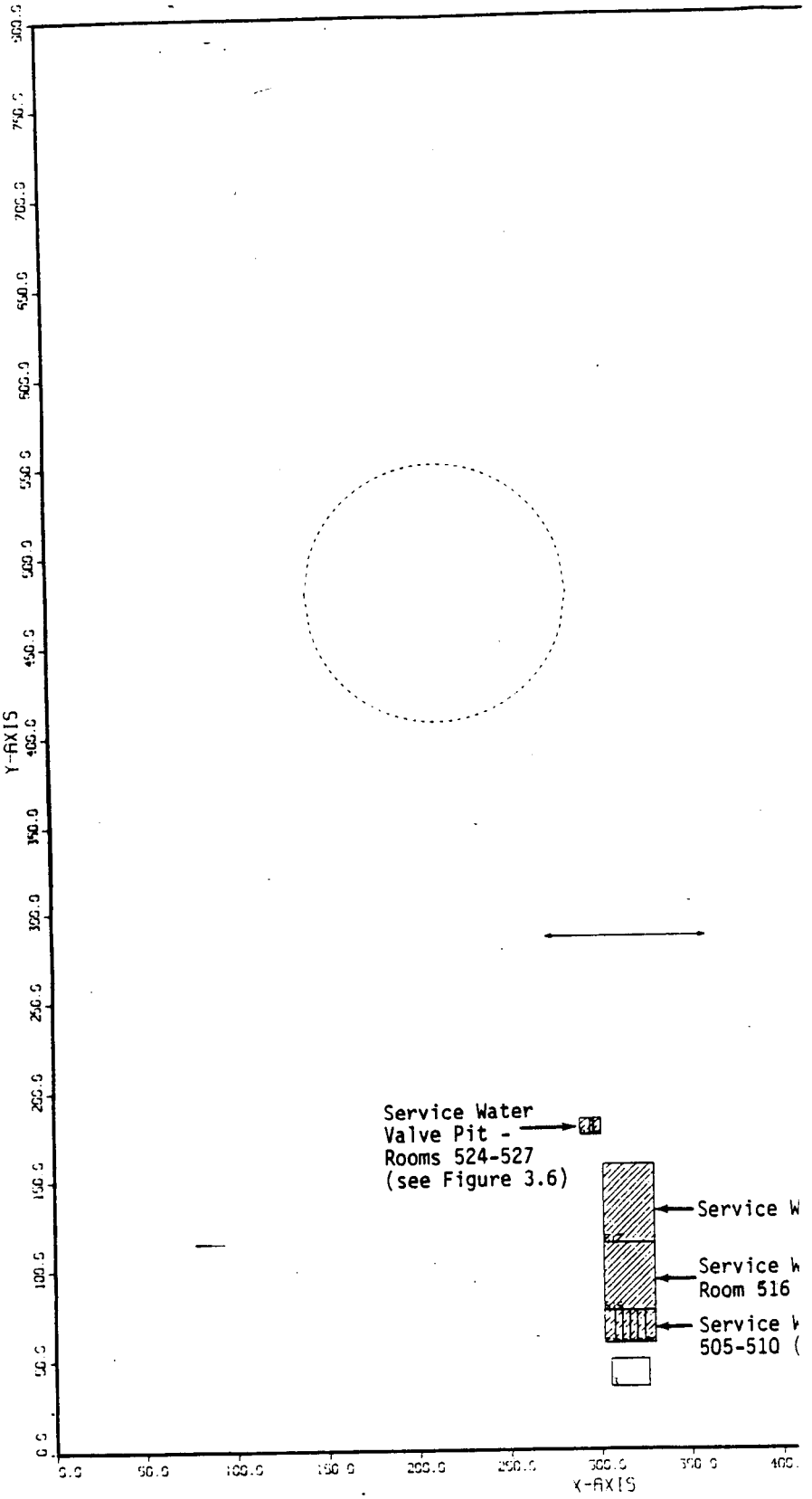

Figure C3-1. Plant Layout for Elevation

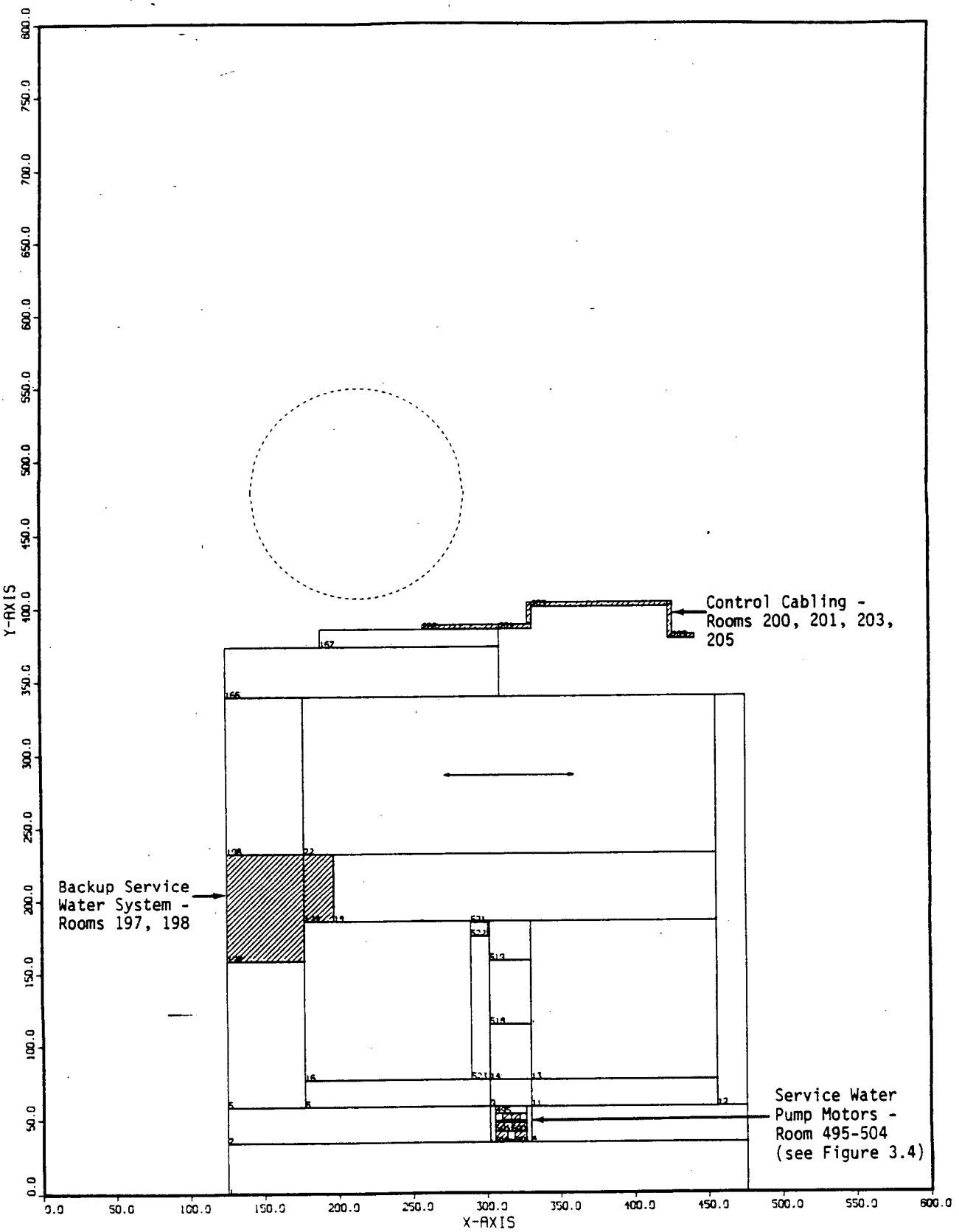

Figure C3-2. Plant Layout for Elevation = 14.

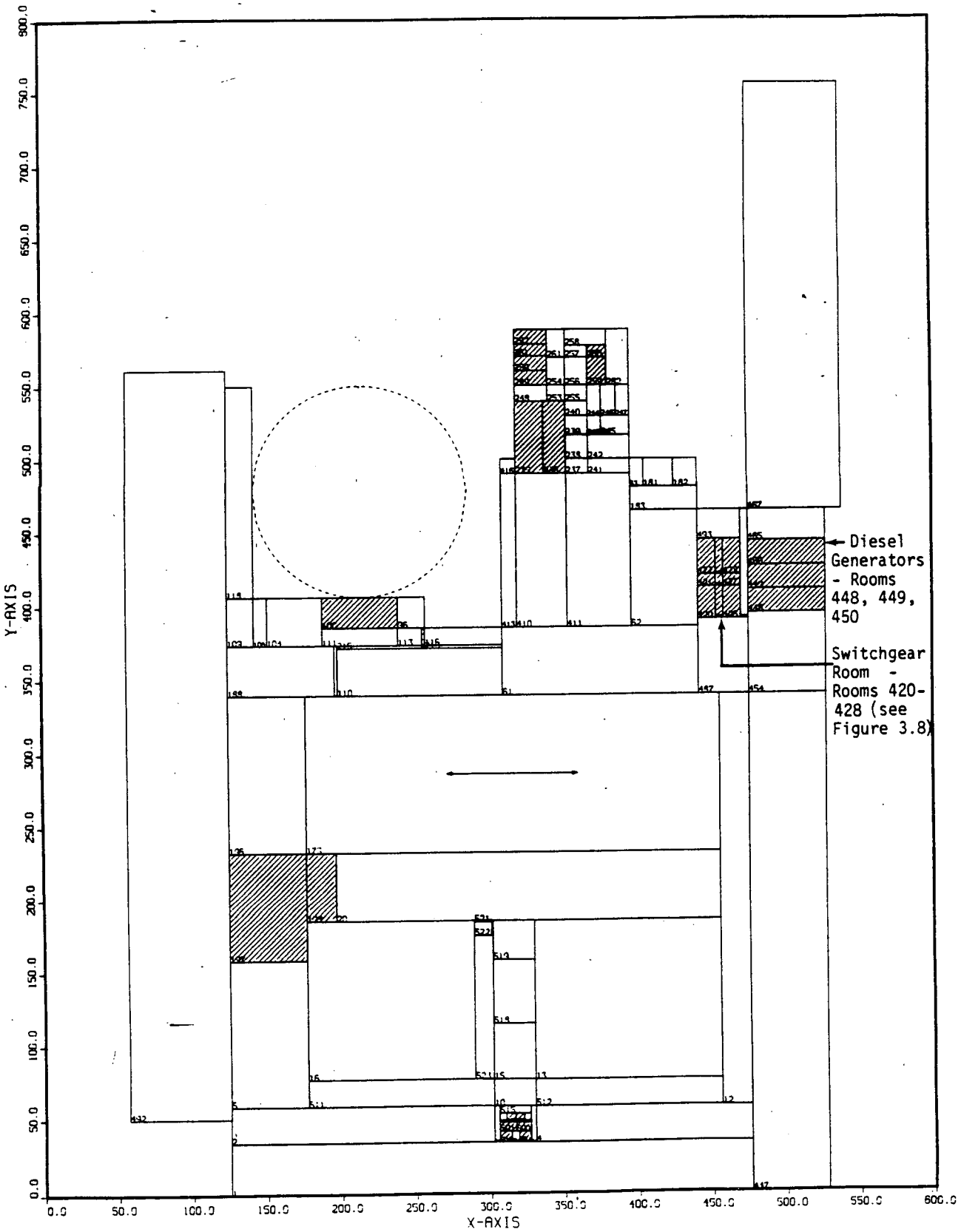

Figure C3-3. Plant Layout for Elevation = 18.

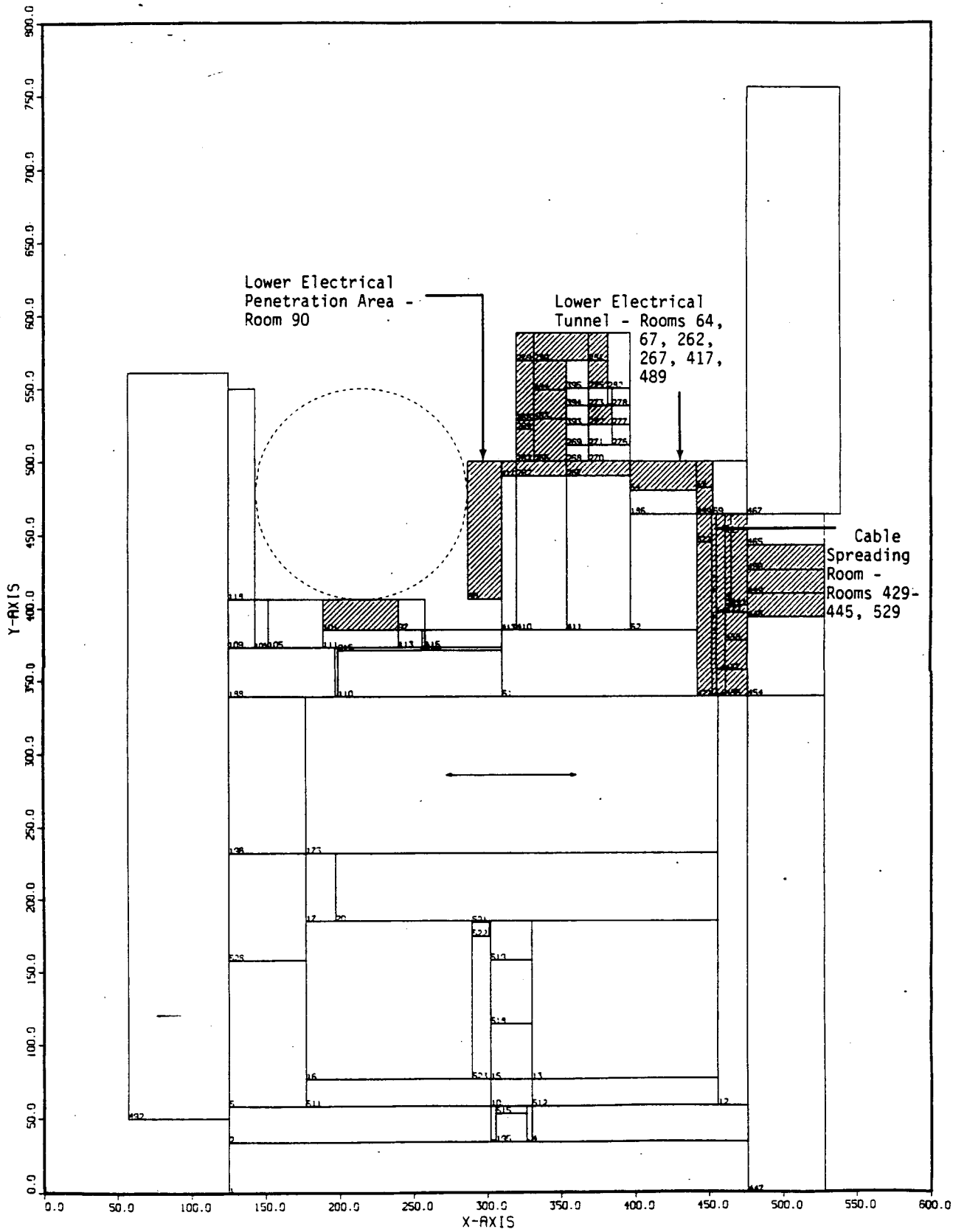

Figure C3-4. Plant Layout for Elevation = 35.

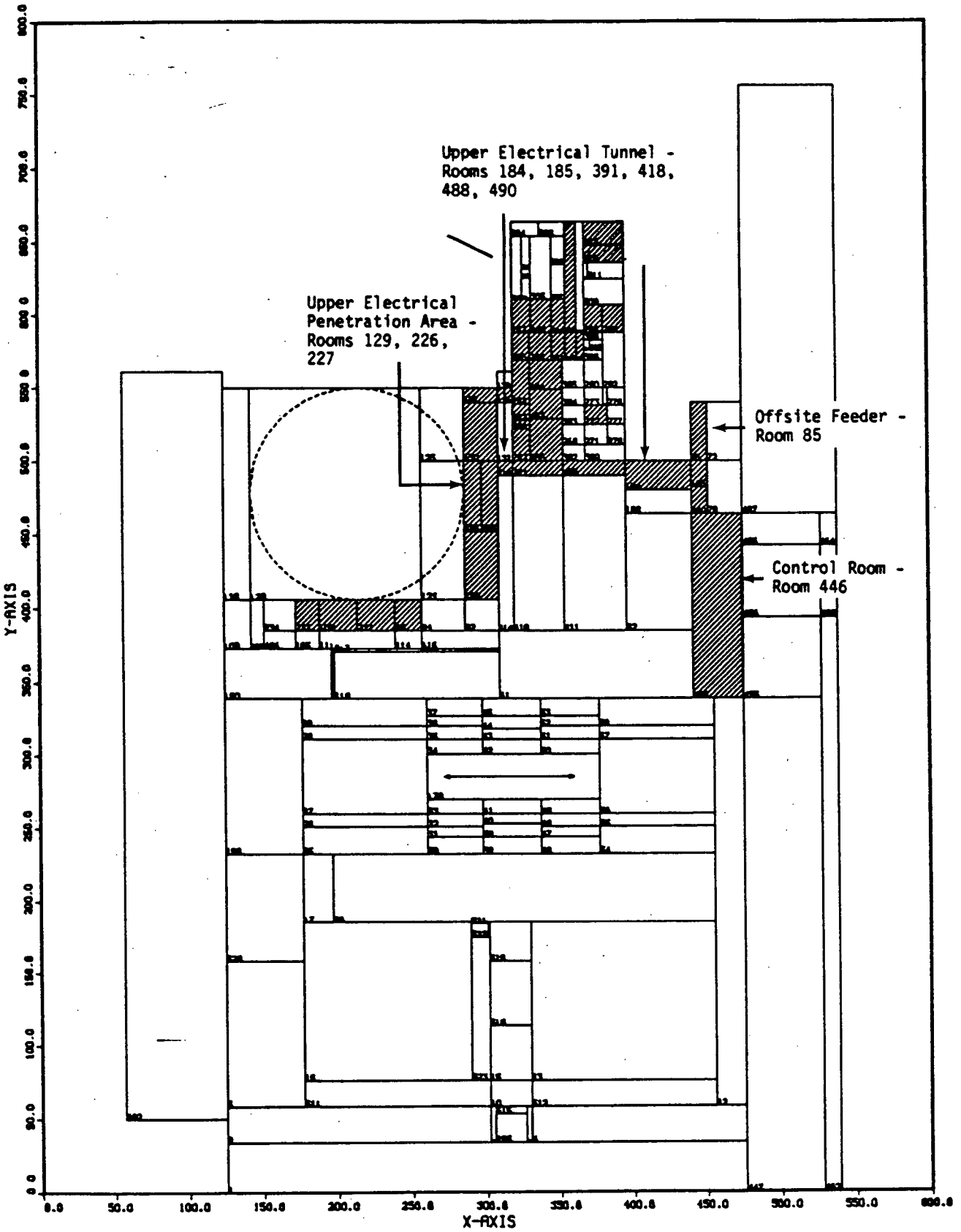

Figure C3-5. Plant Layout for Elevation = 53.

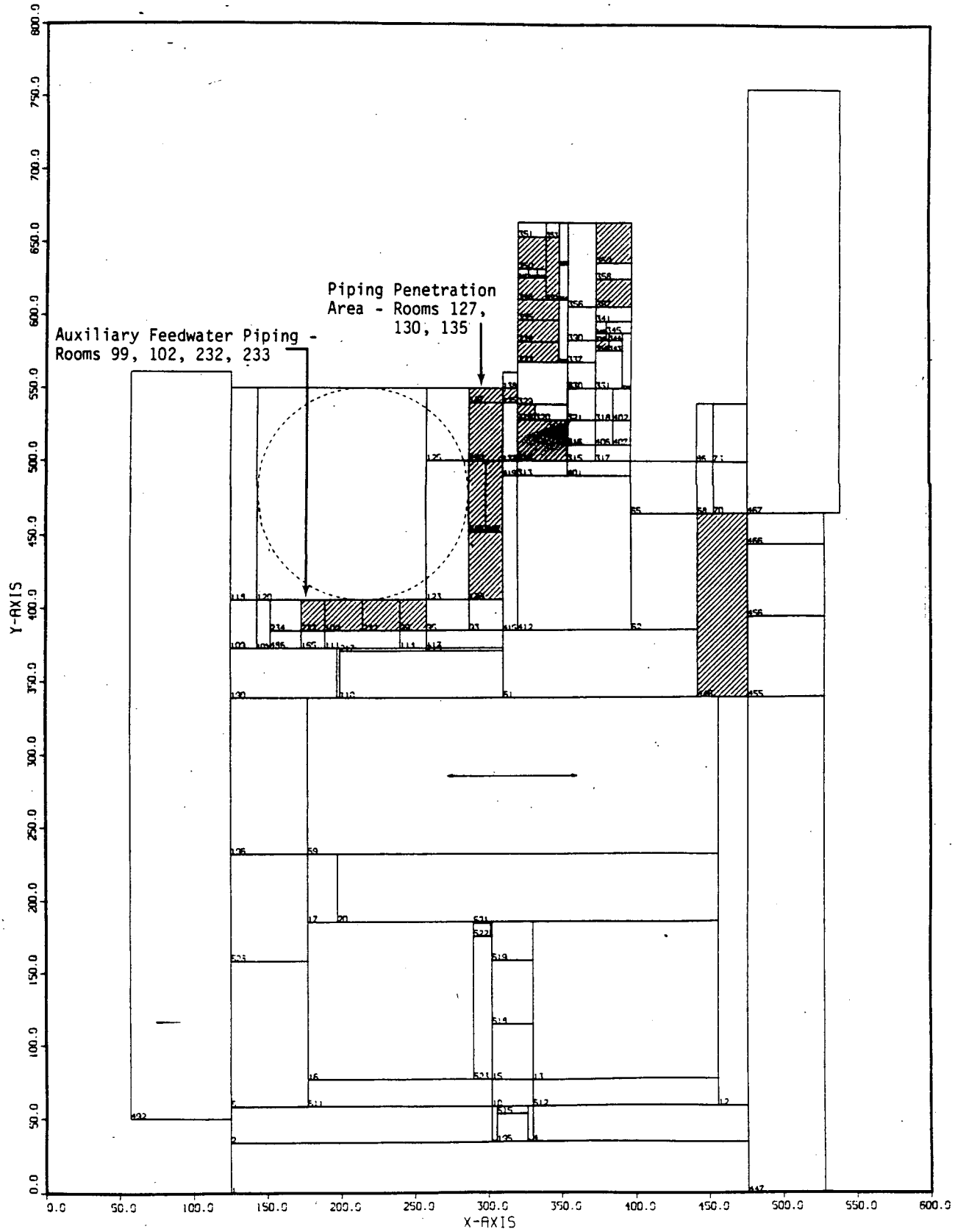

Figure C3-7. Plant Layout for Elevation = 65.

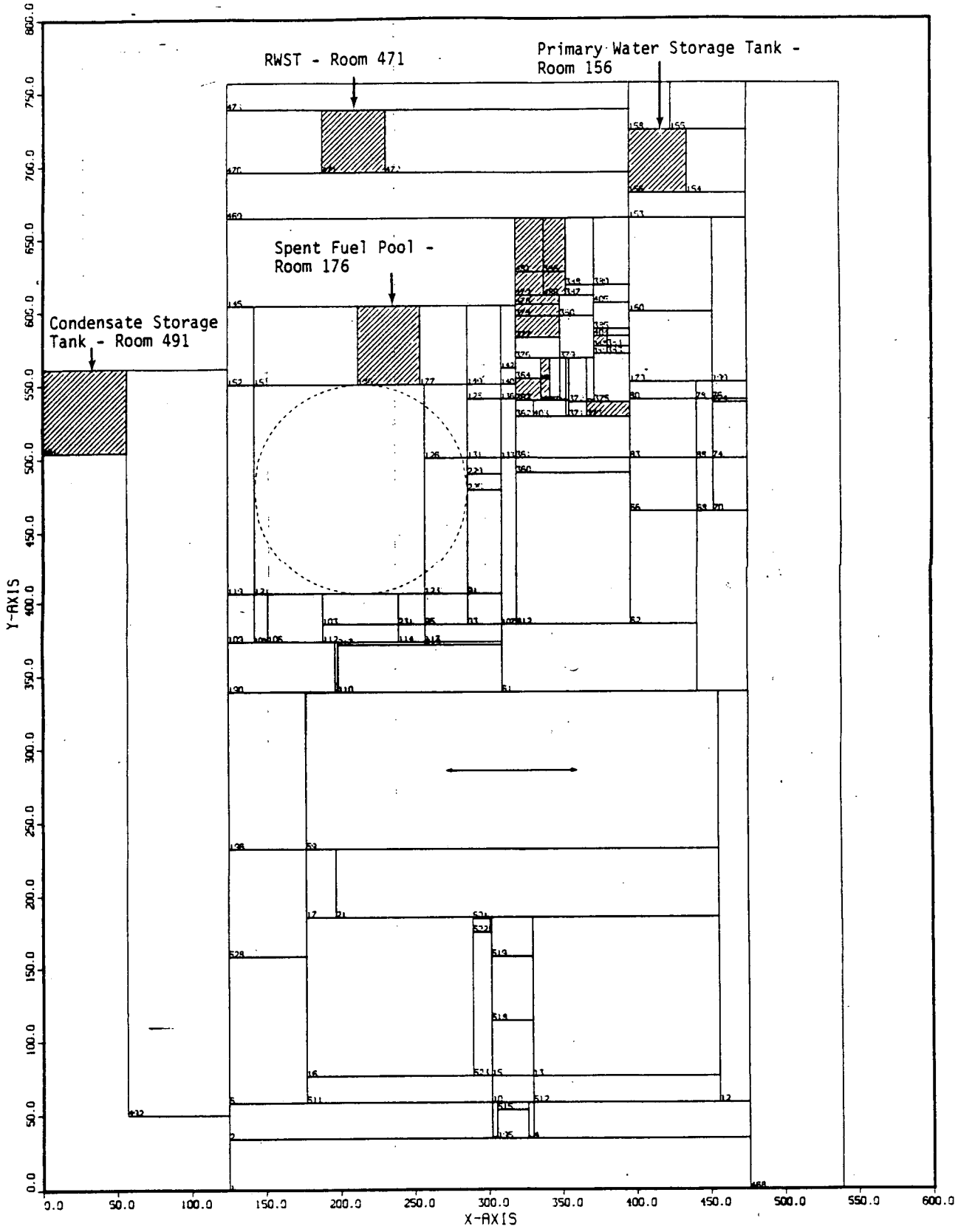

Figure C3-6. Plant Layout for Elevation = 80.

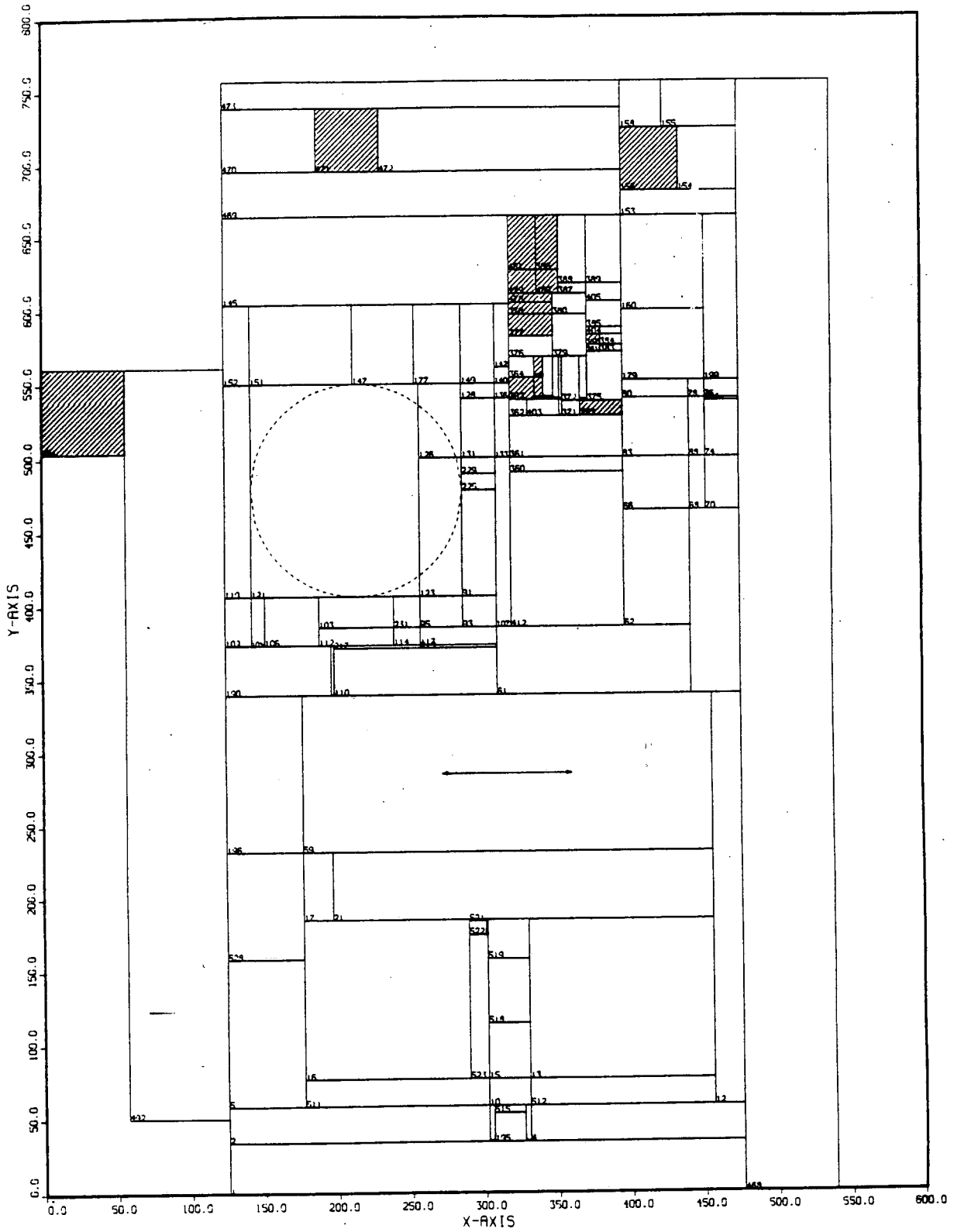

Figure C3-8. Plant Layout for Elevation = 90.

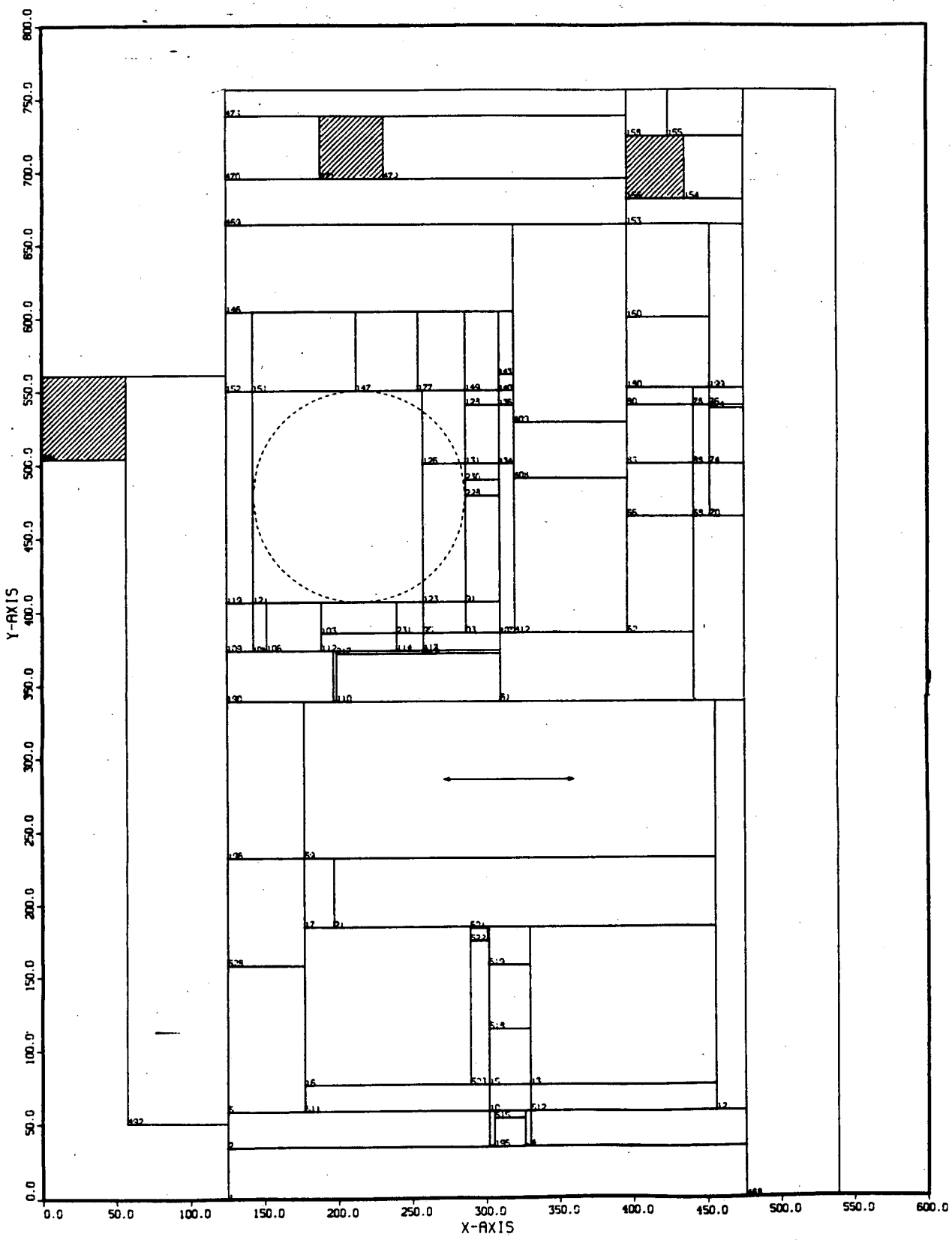

Figure C3-9. Plant Layout for Elevation = 100.

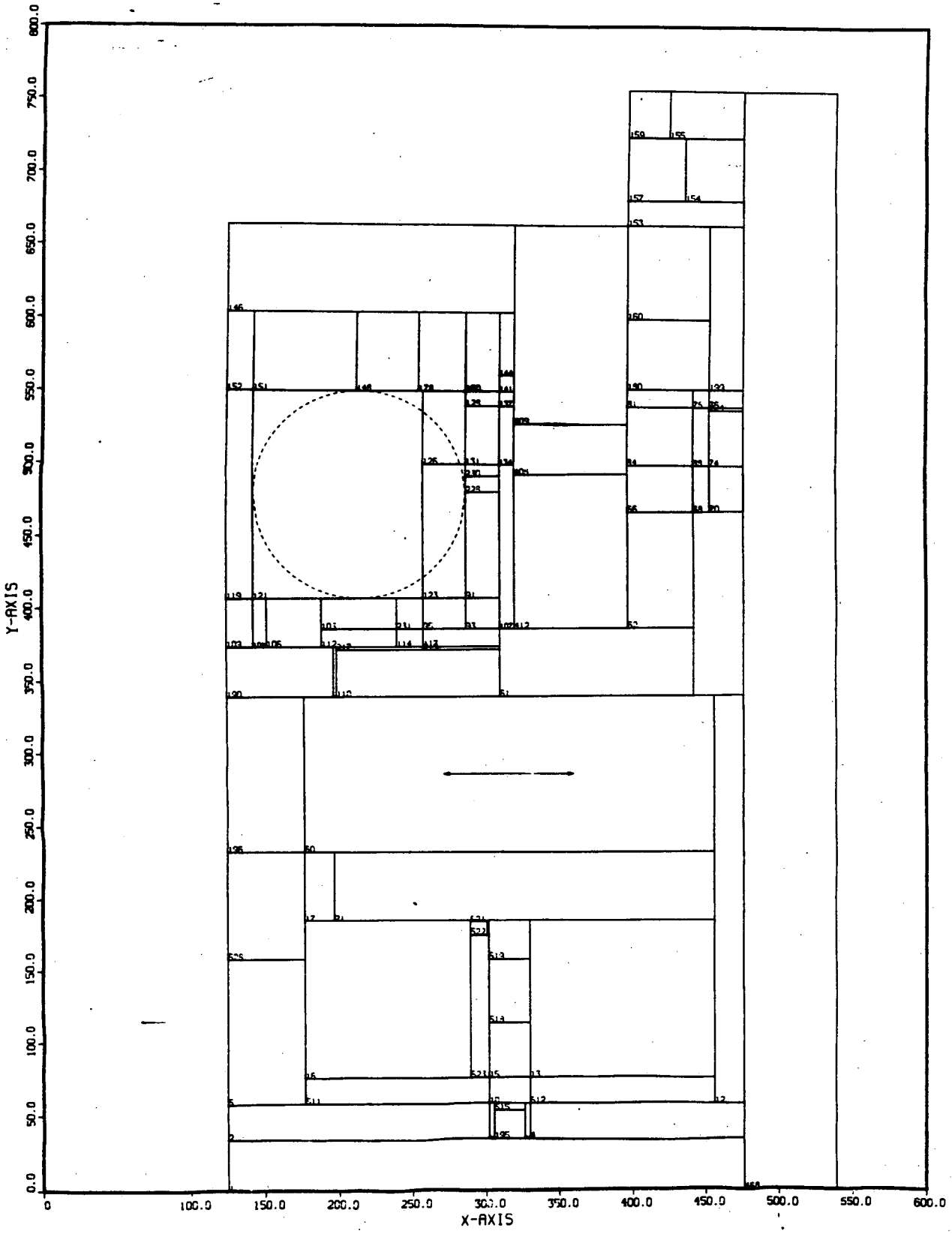

Figure C3-10. Plant Layout for Elevation = 200.

APPENDIX D - SENSITIVITY AND CONSERVATISM

D.1 PHYSICAL PARAMETERS

Three physical parameters associated with the missiles can effect the final results. These are, in order of importance:

- Velocity,
- Impact area (missile projected area), and
- Azimuthal distribution.

The first two are esentially independent of the plant modeling. The third is plant dependent. Variations in distribution of the azimuthal angle, ϕ, alter the probability of safety compromise in accordance with the location of safety-related areas relative to any given turbine wheel. Of these parameters, velocity is the most critical.

D.2 HAZARDS

The turbine missile data used, including specification of emergent velocities, is that specified by the turbine manufacturer. General Electric uses a range of velocities and Westinghouse uses discrete values. Both manufacturers base their specifications on a combination of analysis and experiment, but do not provide the specific details of their methods. Analyses have been performed for turbine missiles utilizing turbines built by both General Electric and Westinghouse. A sensitivity study on the effect of velocity on the number of strikes on safety-related regions for the Pebble Springs Plant was performed for Portland General Electric[5]. In this appendix, we extrapolate the data from the Pebble Springs Study and infer that the Westinghouse initial velocities are sufficiently conservative and that for the expected variations the results are not critically sensitive to velocity.

We start by comparing the emergent velocities of both turbines with the theoretical possible upper limits V_u, which is

$$V_u = \bar{r}W$$

where $\bar{r}$ is the radial distance from the center of the turbine axis to the mass center of the missile. Its value is[5]

$$\bar{r} = \frac{\frac{4}{3}\left(r_o^{\,3} - r_i^{\,3}\right)\sin^2\frac{\theta}{2}}{\left(r_o^{\,2} - r_i^{\,2}\right)\theta}$$

where

r_o, r_i = outer, inner radius, respectively

θ = angle of missile sector (90° for all Westinghouse disc missiles)

$$W \text{ is } (6.28)\left(\frac{\text{rpm}}{60}\right)\left(\frac{\text{percent overspeed}}{100}\right)$$

W = 343 radians/sec for Westinghouse

= radians/sec for General Electric

Figure D-1 shows emergent velocities relative to the maximum value theoretically possible for General Electric and Westinghouse turbines. Maximum theoretically possible velocities cannot be achieved because the missile must penetrate the casing and additional internal turbine structure, which degrades missile energy. Figure D-1 is a comparison of specified initial velocities for the Westinghouse turbines. A continuous, uniform range of values are used by General Electric and discrete values by Westinghouse. Figure D-2 is extrapolated from Reference 5 and is a graphical picture of the possibilities of penetration of safety areas for the Pebble Springs Plant based on General Electric velocity ranges. Superimposed on this probability curve are the discrete Westinghouse velocity values. The Westinghouse values are scaled to the average maximum of the velocity ranges given for General Electric. Figure D-2 is instructive only and certainly not a "proof of conservatism". However, it does show consistency with General Electric data and indicates that no drastic difference would occur by modest variation in the initial velocities of the Indian Point 3 missiles.

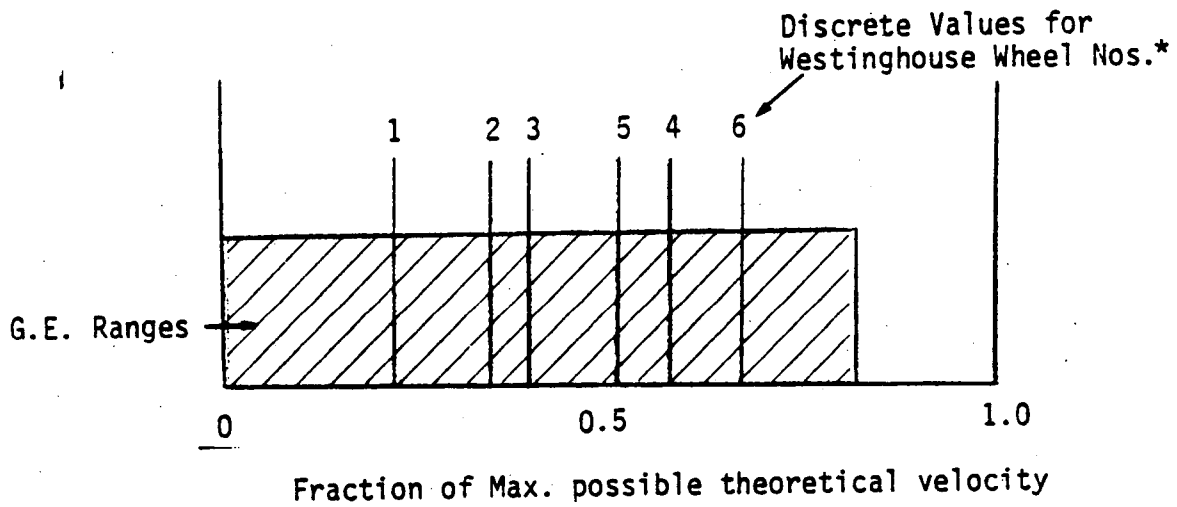

*These values are from Reference 8 and are not for IP 3. However, they are characteristic of Westinghouse discs.

Figure D-1. Comparison of G.E. and Westinghouse Initial Missile Velocities Compared to Their Maximum Theoretical Values.

$$V = V_{min} + F(V_{max} - V_{min})$$

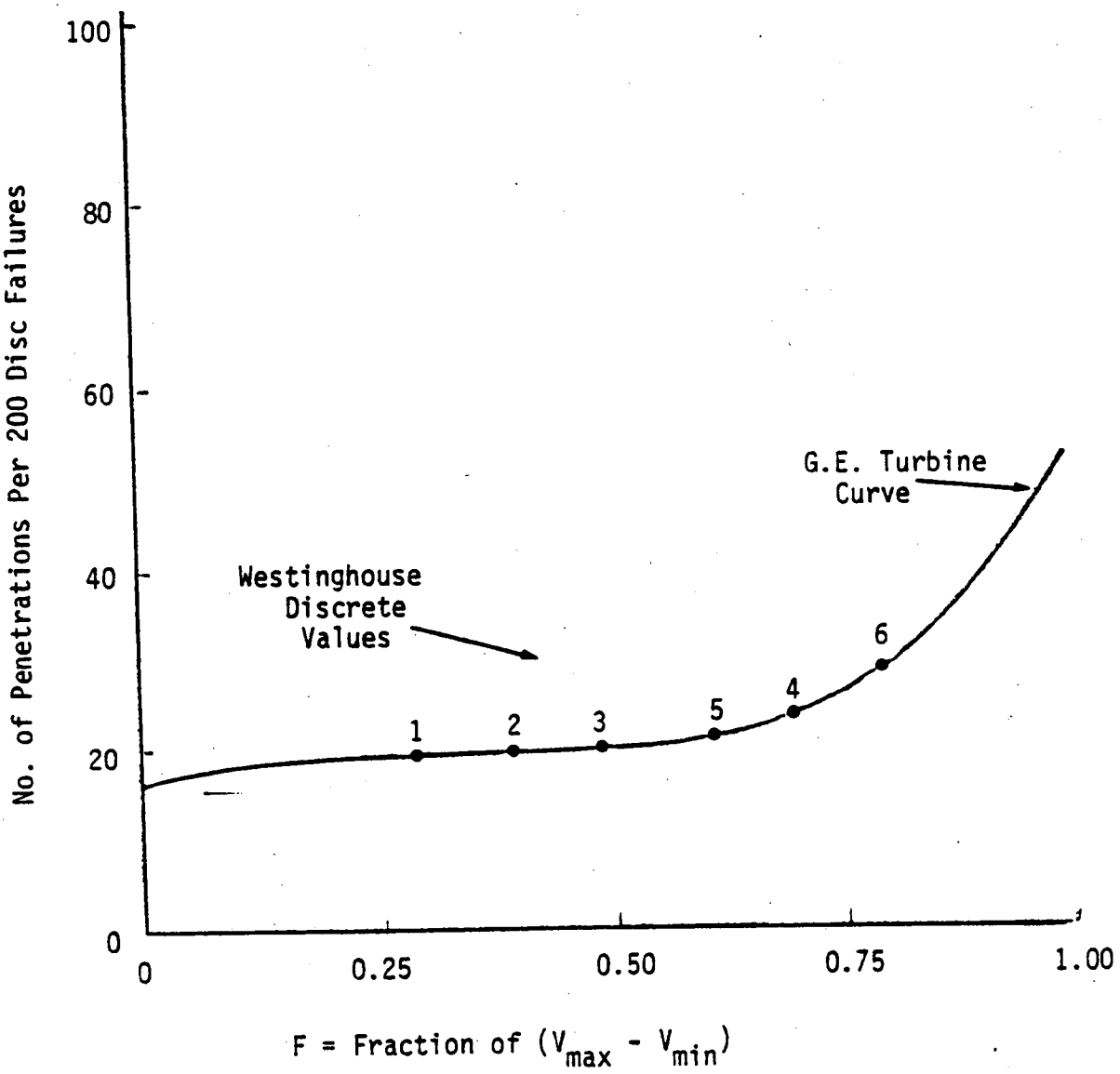

Figure D-2. Vital Areas Penetrated as a Function of Initial Velocity. (Westinghouse and G. E. Turbine Compared).

Missile shapes assumed for the Pebble Springs Plant[5] are similar to those for Indian Point 3, and the measured distribution having a smaller magnitude than the actual distribution was used. The reasons for its use were that it was much simpler to code than the true distribution and it was known to be conservative. In a test case using the actual distribution in impact area, the probability of penetration of vital areas decreased by 10 percent at destructive overspeed (180 percent) and by 24 percent at design overspeed (120 percent) over that using the approximation described above.

An additional element of conservatism utilized for the disc sectors is that the rim maximum area is used throughout rather than the flat-side maximum (the flat-side maximum is large for typical disc sectors). This assumption is indeed conservative, but extremely difficult to quantify. It can be assumed that the disc sectors maintain their original plane of rotation during the initial portions of their flights so that the rim maximum is correct. However, as successive wall interactions occur, this is no longer the case. Sensitivity studies have shown that the use of rim maximum throughout is conservative.

The effect of distribution in azimuthal range was checked for the Pebble Springs Plant. It was found that more safety-related areas were struck for azimuthal distributions which tended to spread the distribution (expand the range in ϕ). Although we have found no data reported on actual azimuthal angle distribution, it is reasonable that a distribution which tended to peak in the center is more physically reasonable than the uniform distribution. It is, therefore, reasonable that a uniform distribution tends to be conservative. Such a conclusion was the result of the Pebble Springs sensitivity study. However, it must be recognized that the sensitivity to azimuthal distribution is plant dependent.

D.3 PENETRATION/PERFORATION MODELING

Penetration/perforation models significantly effect the results. Ricochet modeling is not critical because missiles typically are rendered non-hazardous by one or, at most, two ricochet encounters.

Penetration/perforation has been calculated by the CEA-EDF formula (Reference 9). It has replaced the BRL formula which was initially chosen

based on the recommendation of the authors of BC TOP 9A*. While the BRL formula was felt to be both conservative and reasonably close to analytical and test results, the CEA-EDF formula gives a better match to the EPRI results over a full range of missile velocities.(10) Also, in a test case with the MIDAS code, CEA-EDF gave slightly more conservative results than BRL.

---

*Bechtel Topical Report "Design of Structures for Missile Impact." BC TOP 9A Revision 2, 1974.

APPENDIX E - PHOTOGRAPHIC SURVEY

Figures E-1 through E-20 are samples of photographs taken during the physical on-site survey of the Indian Point 3 plant.

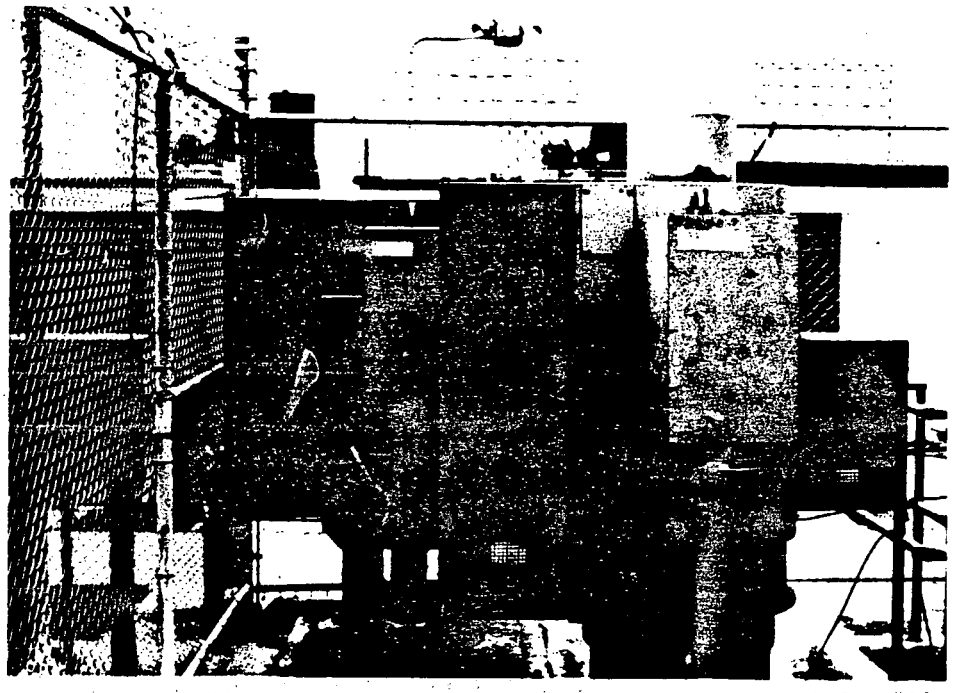

Figure E-1. Main Service Water Pump Motors #31, #32 (MISIP Targets 502,500).

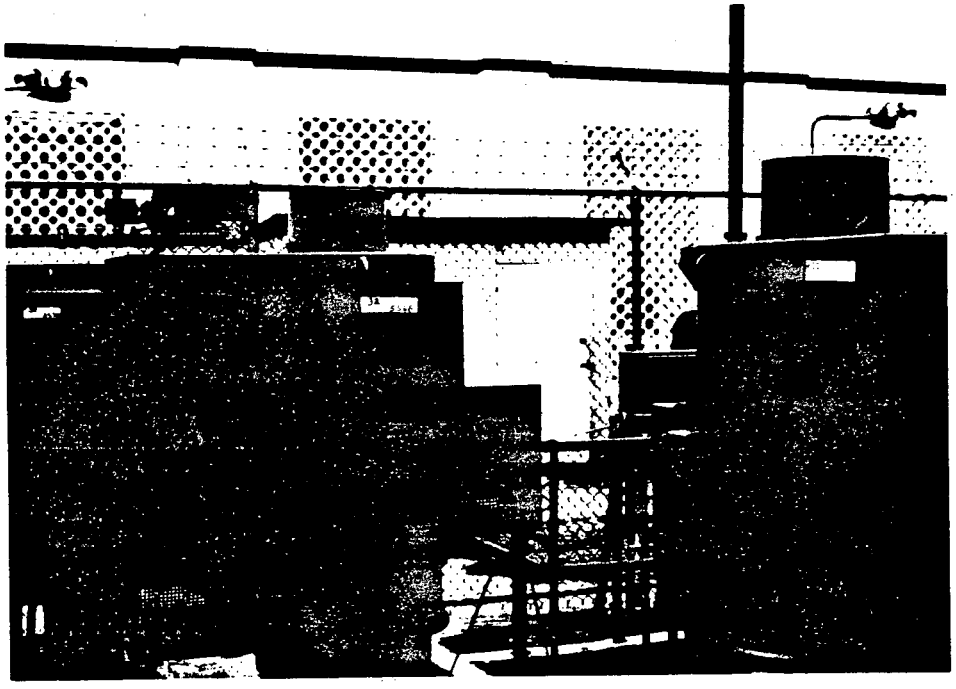

Figure E-2. Main Service Water Pump Motors #31, #32, #33 (MISIP Targets 502, 500, 497).

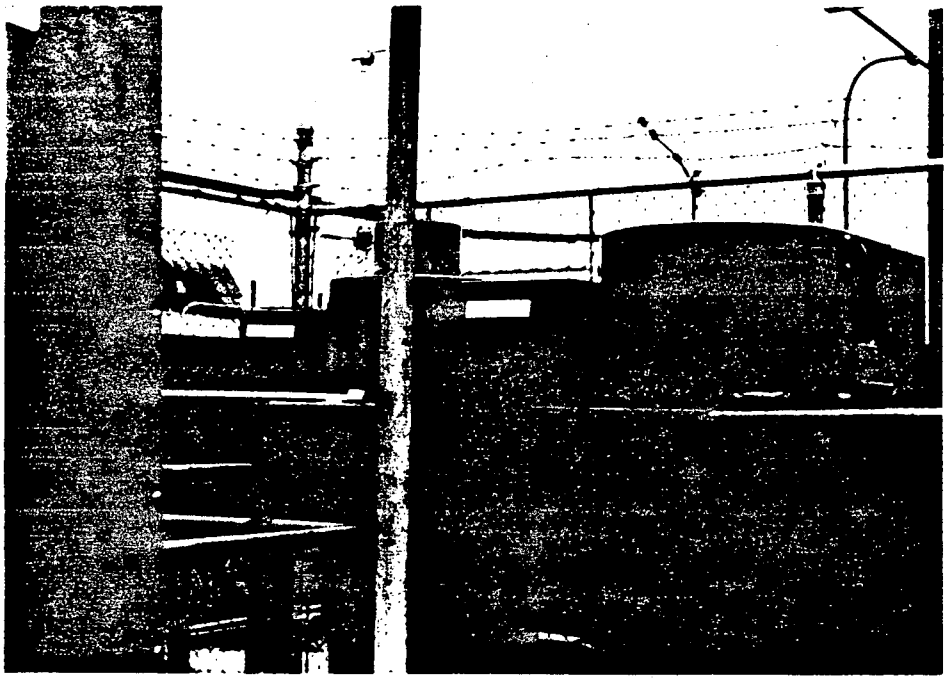

Figure E-3. Main Service Water Pump Motors #35, #36 (MISIP Targets 504, 501).

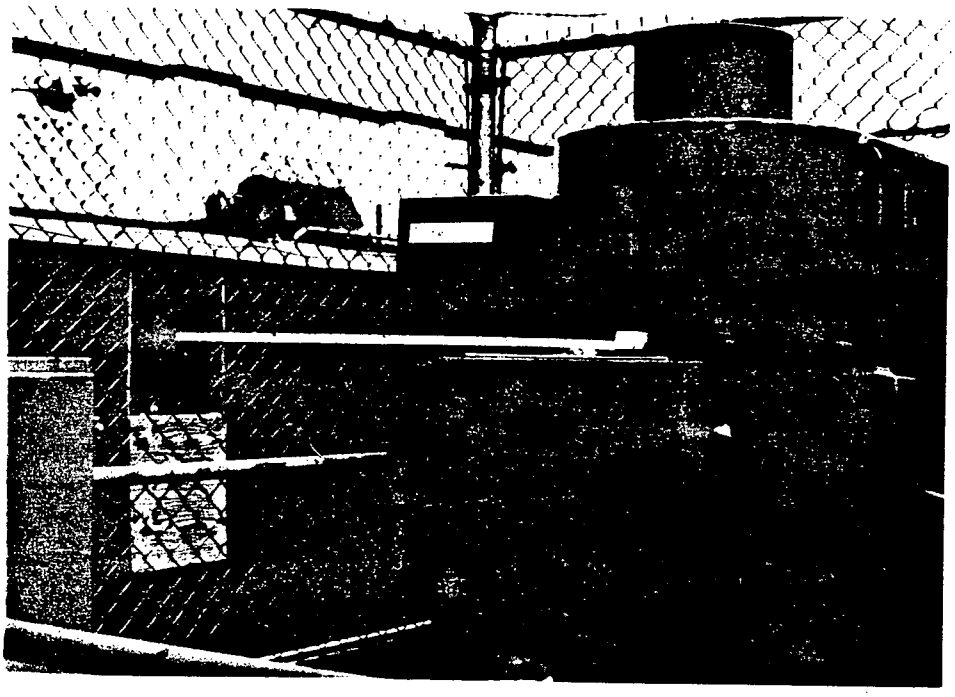

Figure E-4. Main Service Water Pump Motor #36 (MISIP Target 504).

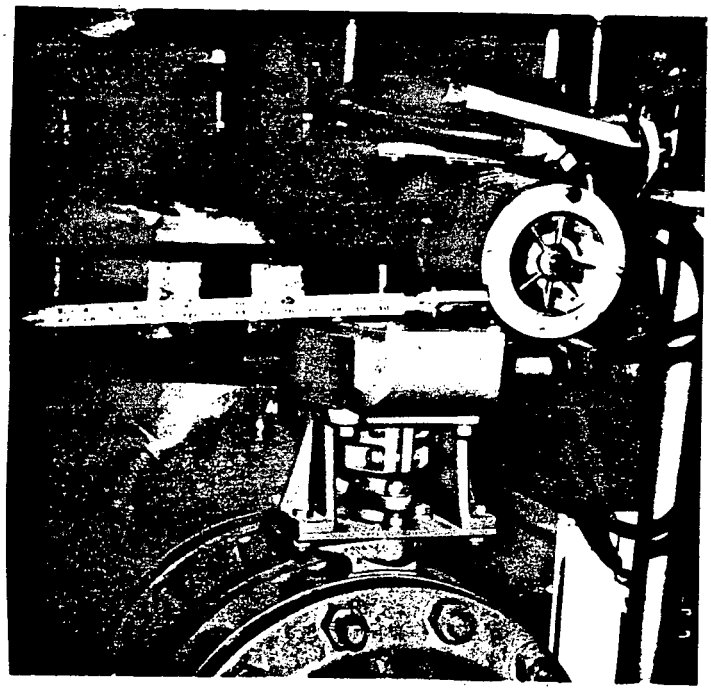

Figure E-5. Service Water Strainer.

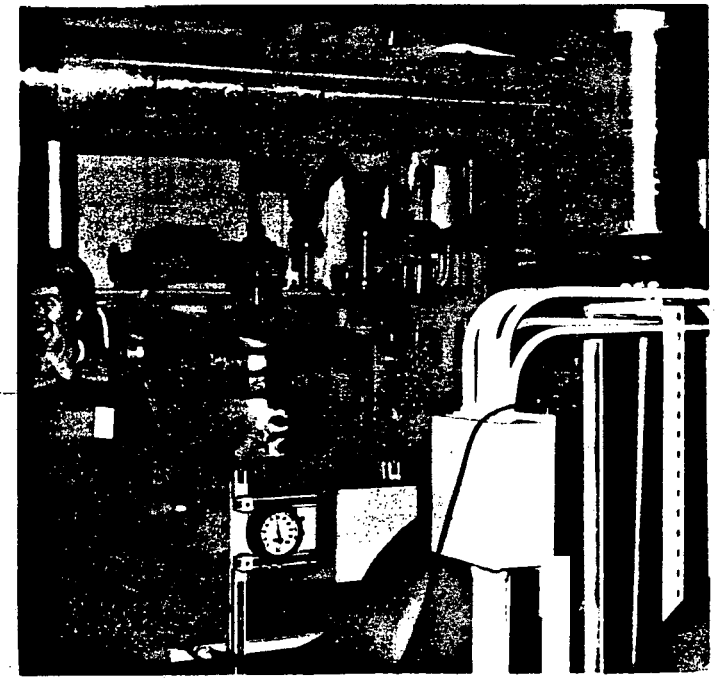

Figure E-6. Service Water Strainers #31, #32 (MISIP Targets 510, 509).

Figure E-7. View of Service Water Piping Path From Pump Motor Enclosure. Pipes are under the Road (MISIP Target 516) and the Concrete Bunker (MISIP Targe 517)

Figure E-8. View of Service Water Pump Motor Enclosure From the Service Water Valve Pit.

Figure E-9. Inside Service Water Valve Pit Showing Adjacent Essential and Non-Essential Service Water Components (MISIP Target 526).

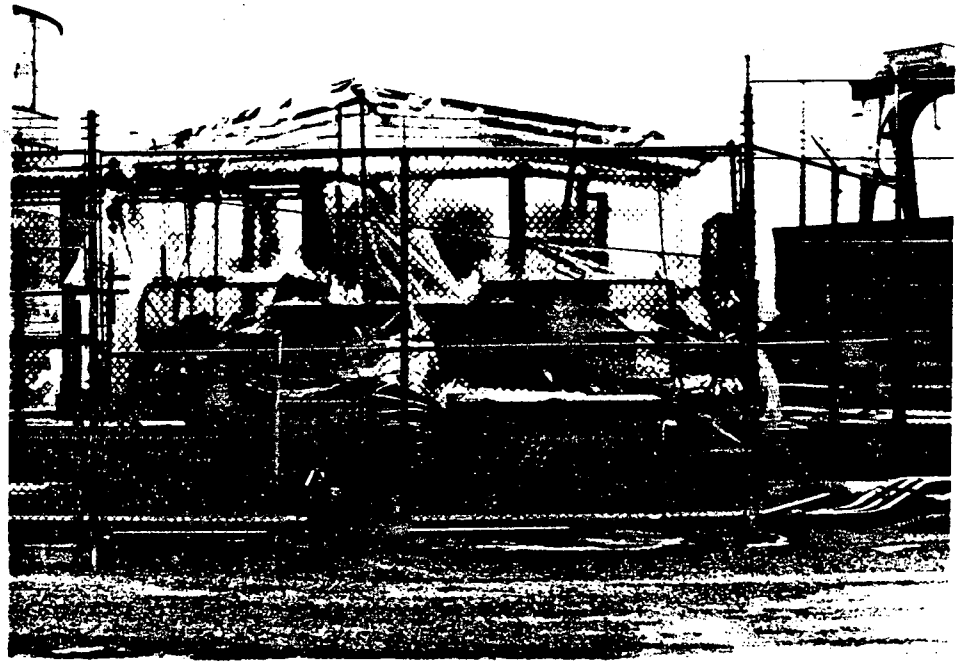

Figure E-10. Backup Service Water Pump Yard (MISIP Target 197).

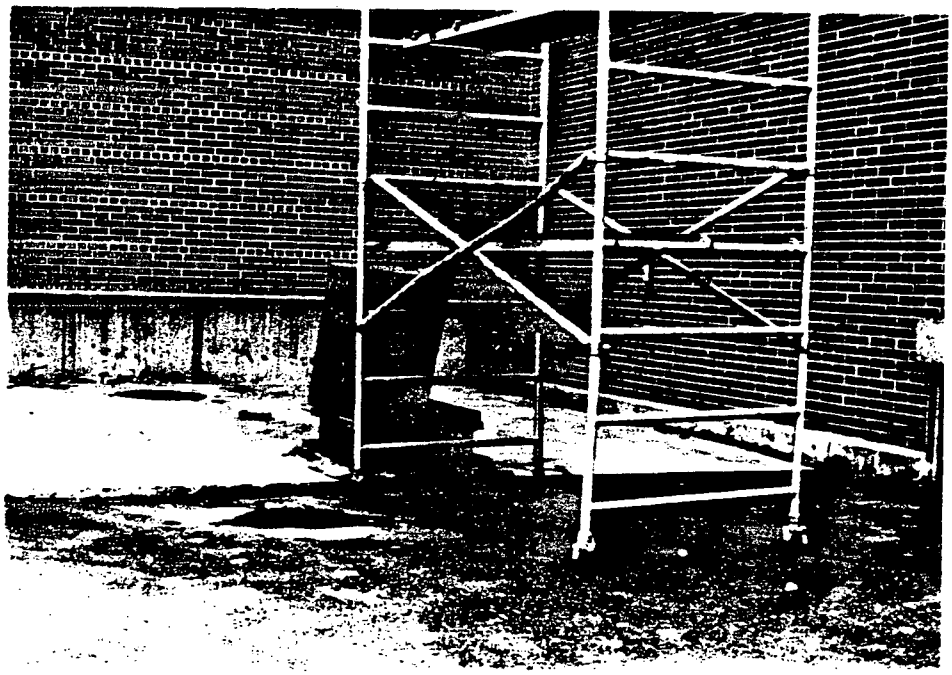

Figure E-11. Top of Backup Service Water Valve Pit (MISIP Target 198).

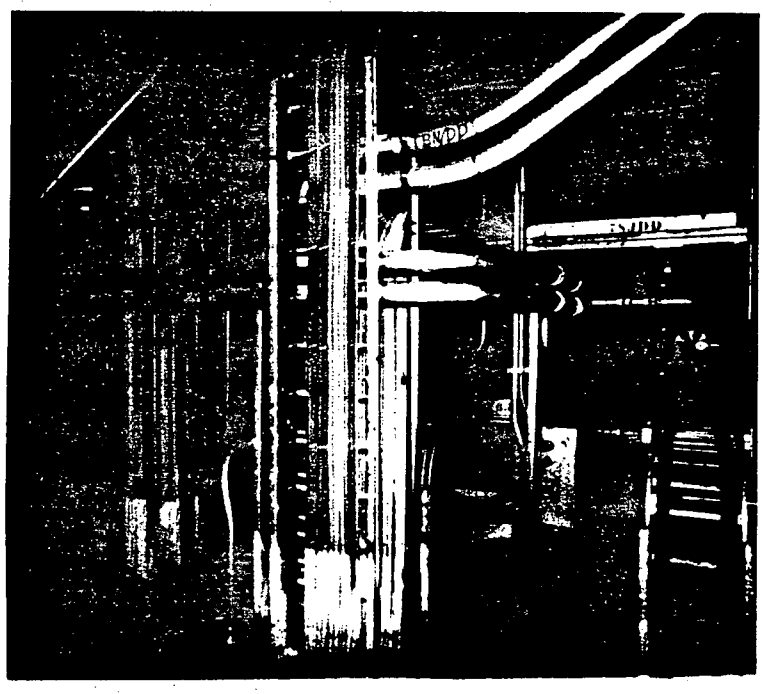

Figure E-12. Upper Electrical Penetration Area Showing Common Area Where Lower Cables Join (MISIP Target 226).

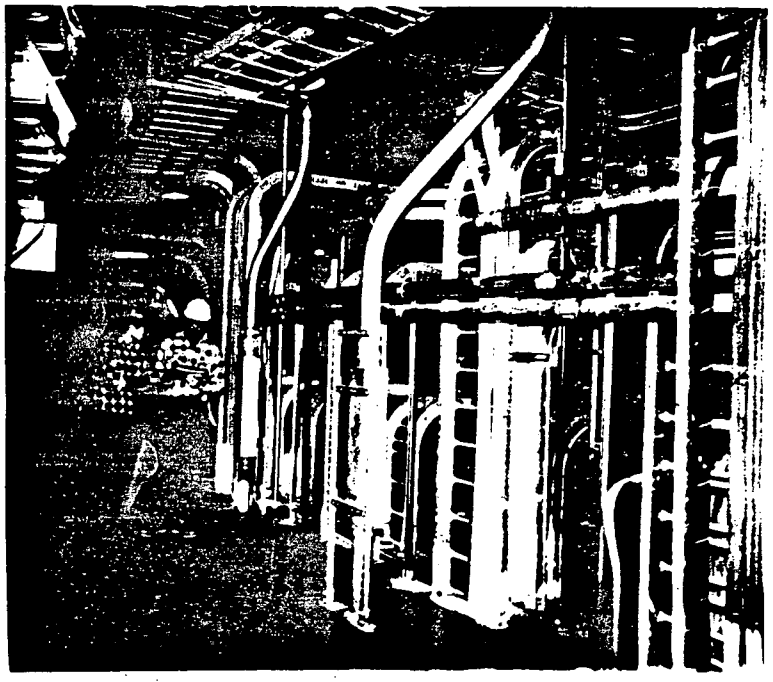

Figure E-13. Upper Electrical Penetration Area Showing Common Area Where Lower Cables Join (MISIP Target 226).

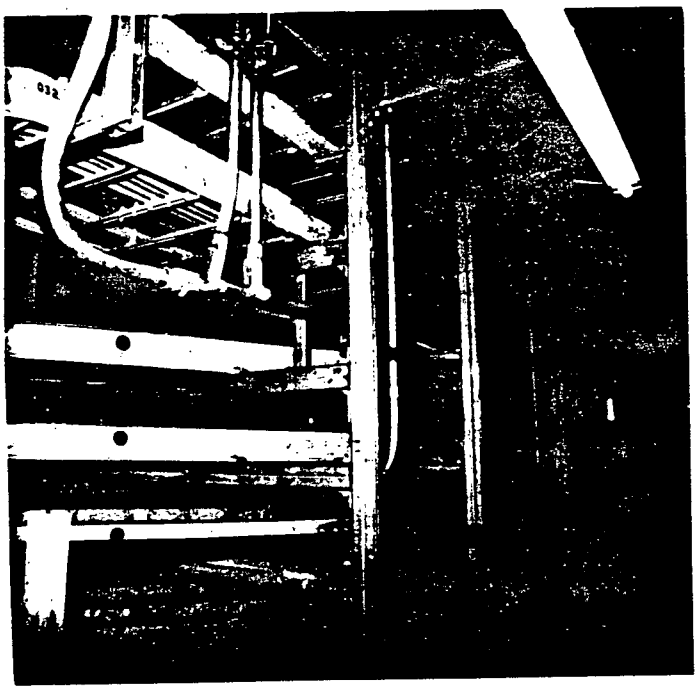

Figure E-14. Area of Cable Spreading Room Common To Both Trains (MISIP Target 529).

Figure E-15. Area of Cable Spreading Room Common To Both Trains (MISIP Target 529).

Figure E-16. Cable Spreading Room Showing All Cables Entering the Electrical Tunnels (MISIP Target 529).

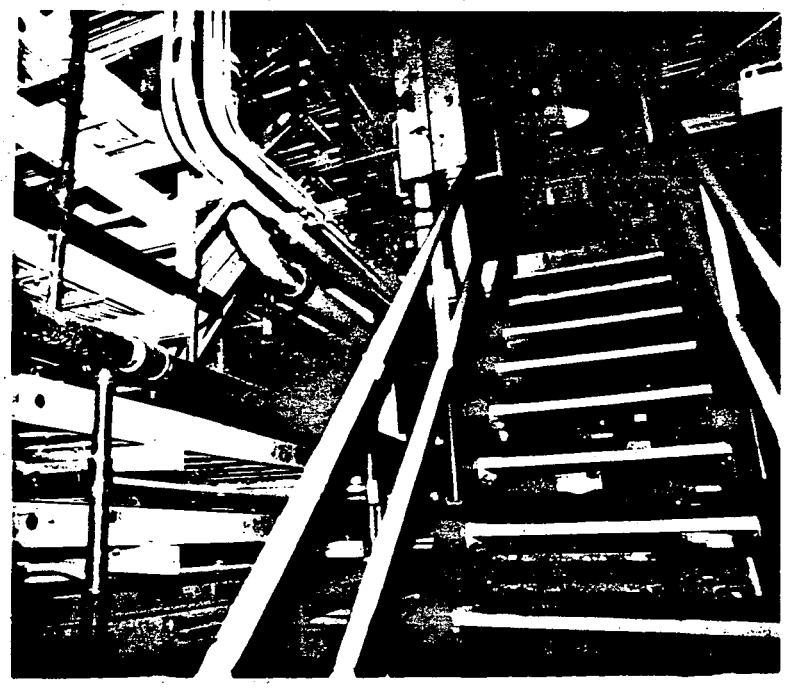

Figure E-17. Start of Electrical Tunnels Showing All Cables Together (Upper Area is MISIP Target 490, Lower Area is MISIP Target 489).

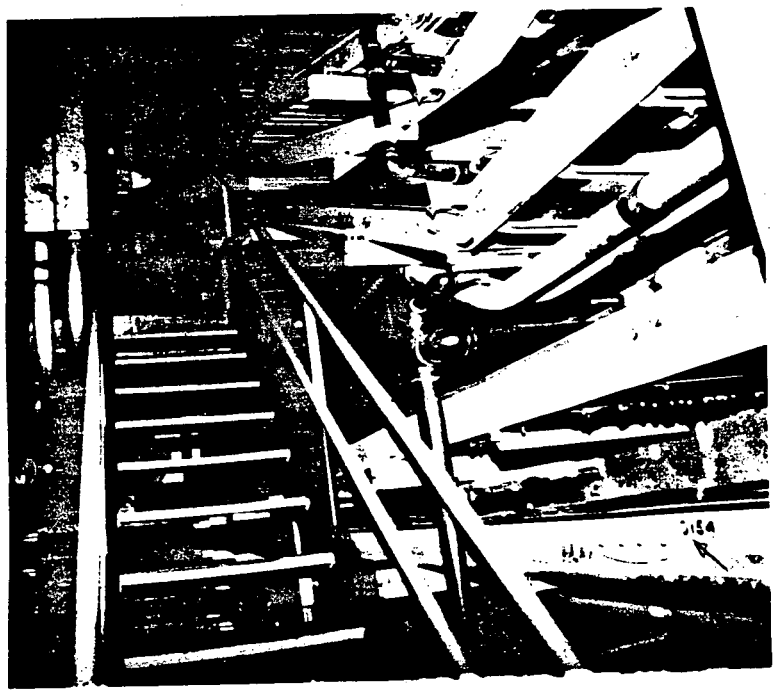

Figure E-18. Start of Electrical Tunnels Showing All Cables Together (Upper Area is MISIP Target 490, Lower Area is MISIP Target 489).

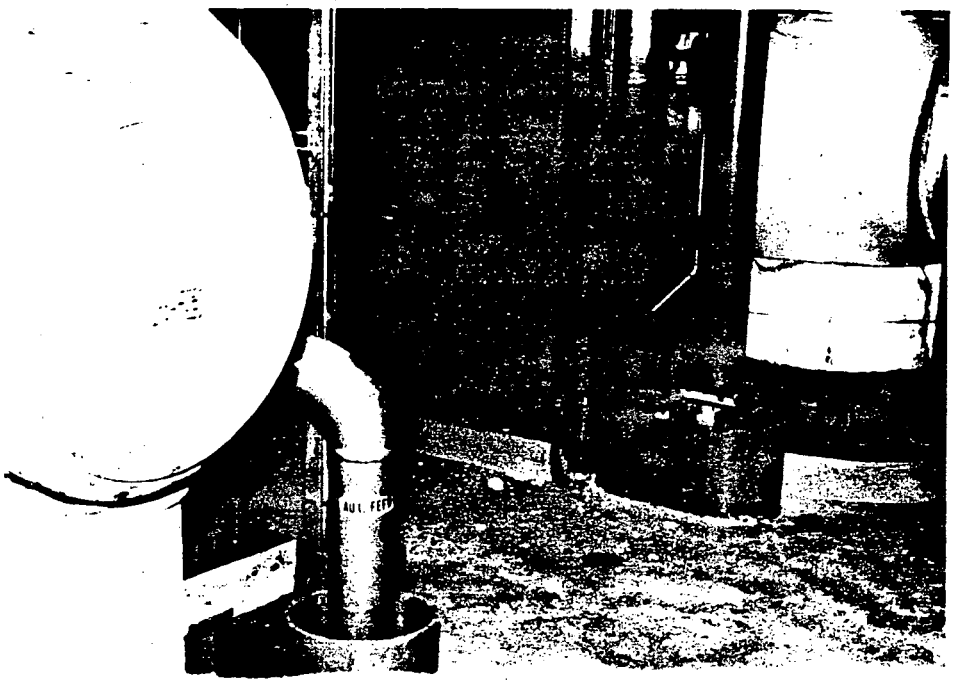

Figure E-19. Auxiliary Feedwater Piping.

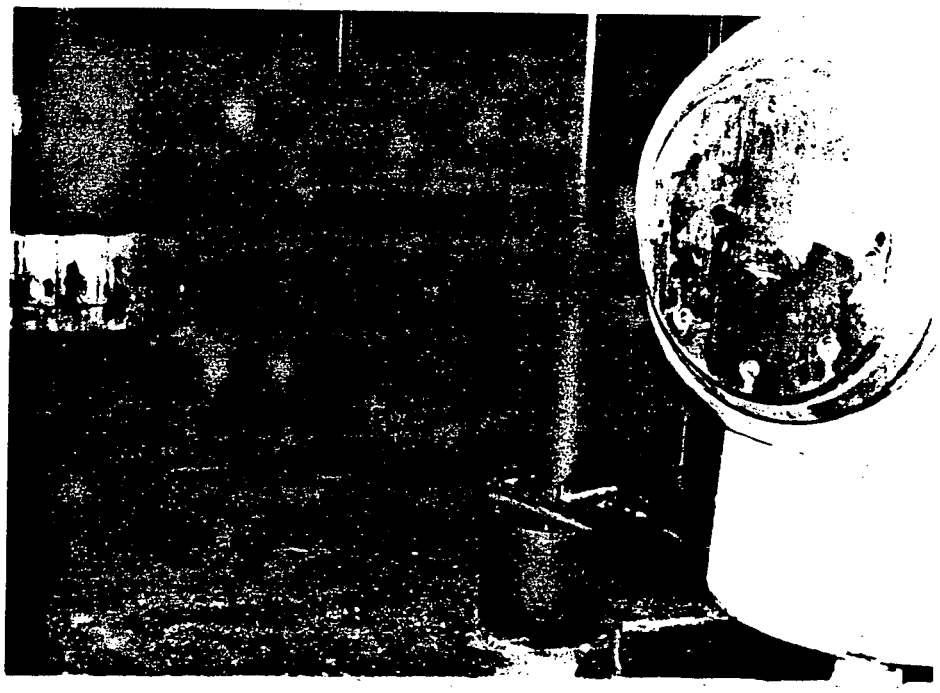

Figure E-20. Auxiliary Feedwater Piping.